CELL BIOLOGY OF THE PERIODONTAL LIGAMENT: EVOLUTIONARY ORIGIN, DEVELOPMENT, AND PROSTHETIC REPLACEMENT

A Dissertation

by

WILLIAM VERMONT STENBERG

Submitted to the Office of Graduate and Professional Studies of
Texas A&M University
in partial fulfillment of the requirements for the degree of

DOCTOR OF PHILOSOPHY

Chair of Committee,	Hu Zhao
Committee Members,	Emet D. Schneiderman
	Xianghong Luan
	Matthew J. Kesterke
Head of Department,	Larry L. Bellinger

December 2020

Major Subject: Oral Biology

ABSTRACT

The periodontal ligament of humans is a unique organ, a thin membrane of non-ossified connective tissue sandwiched between two active mineralization fronts. Factors such as oral hygiene, tobacco smoking, and pathogenic microflora are considered etiologic factors for periodontitis, but these are considered the proximate causes in evolutionary medicine. To properly approach the problems of the periodontal ligament, it must be understood why *Homo sapiens* even has one in the first place; this is a search for the ultimate cause.

The case of an extinct marine lizard, the *Globidens phosphaticus* is considered to document the sudden appearance of a periodontal ligament in the fossil record through the use of μCT radiography, thin-section histology, and isotope analysis. The results are compared to other related squamates in a phylogenetic series to document other characters that developed concurrently, and to relate these to the paleoenvironmental condition of the late Cretaceous Era. These characters are then related to some of the same characters that convergently developed in mammals due to the same environmental influences.

Analysis is then made of the nature of the occlusal wear, alveolar bone, and the root surface of the fossilized remains and it was determined the non-mineralized PDL of *G. phosphaticus* was indeed homologous to what is seen in thecodont mammalian tooth attachment tissues. To answer the question of how a tripartite attachment consisting of alveolar bone, PDL, and cementum arose from a simpler homogenous tissue,

examination was made of the μCT radiographs of extant reptiles and mammals and found that craniofacial sutures are contiguous with the tooth attachment tissues. Using a transgenic mouse model, great similarities of the unmineralized PDL and the similarly non-mineralized craniofacial sutures could be seen, the lack of ossification presumably due to an inhibition of Wnt signaling. Using a transgenic mouse overexpressing β-catenin, root deformities resembling the mosasaur root were observed.

Finally, to test the effect of direct application of occlusal force to bone without intervening PDL, dental implants consisting of titanium or zirconia were tested in a novel mouse model with sinus augmentation. In this case, superior osseous integration of titanium implants was found, despite an early delay in healing.

DEDICATION

To my late father, William Vermont Stenberg, Sr. (1932-2013). He bought me my first microscope and first chemistry set. He taught me the human circulatory system when I was in first grade. He always encouraged my love for biology. He taught me how to pray.

Although not an Aggie, his life was exemplified by the Texas A&M Aggie Motto: “Aggies do not lie, cheat or steal nor tolerate those that do”

ACKNOWLEDGEMENTS

I would like to thank my committee chair, Dr. Zhao, and my committee members, Dr. Schneiderman, Dr. Luan, and Dr. Kesterke, for their guidance and support throughout the course of this research.

My sincere appreciation goes to Dr. Kathy Svoboda and Dr. Lynne Opperman of the Department of Biomedical Sciences for their unending support and guidance, often needed on a daily basis.

From the Department of Periodontics, I give sincere thanks to Dr. Jessica Trombetta-eSilva, who introduced me to life in the laboratory and provided valuable lessons in both periodontal histology and perseverance in the face of adversity.

Thanks to Dr. Diekwisch for his assistance and instruction in photography, microscopy, and SEM.

Many thanks to Dr. Michael Polcyn and Dr. Louis Jacobs of Southern Methodist University, the world's best paleontologists, who taught me how to dig up mosasaurs in the hot Texas sun, as well as critical thinking and attention to detail.

Thanks to my labmates: Yating Yi, Dian Jing, Yuhong Wang, Yuejia Deng, Zexi Chen, Xiaofang Cao, Wenjing Luo and Yi Men.

Thanks also go to my BMS friends and colleagues, as well as the faculty and staff of the Department of Biomedical Sciences for making my time at Texas A&M University a great experience.

Thank you to my mother Beverly Stenberg for her unending encouragement. I also give my special thanks to all my children, Ashleigh, Andrew, Jensen, Parker, Jenn, Courteney, and Jared for their encouragement and sacrifices. Finally, to my wife Deborah Stenberg for her continued patience, love and support through this challenging and wonderful journey.

CONTRIBUTORS AND FUNDING SOURCES

Contributors

This work was supervised by a dissertation committee consisting of Professor Hu Zhao [advisor] of the Department of Restorative Sciences, Professor Emet Schneiderman and Professor Matthew Kesterke of the Department of Biomedical Sciences, and Professor Xianghong Luan of the Department of Periodontics.

The isotope analysis for Chapter 2 was provided Matt Clemons from Southern Methodist University.

The experiments in Chapter Three were completed with help of my labmates: Yating Yi, Dian Jing, Yuhong Wang, Yuejia Deng, Wenjing Luo and Yi Men.

The mosasaur specimens used for Chapter 2 and Chapter 3 were provided by Dr. Michael Polcyn and Dr. Louis Jacobs of Southern Methodist University.

All other work conducted for this dissertation was completed by the student independently.

Funding Sources

Graduate study was supported by a fellowship from Texas A&M. This work was also made possible in part by NIH under Grant Number R21DE027928 & 1R01DE028291. Its contents are solely the responsibility of the authors and do not necessarily represent the official views of the NIDCR.

NOMENCLATURE

μCT	Micro Computed Tomography
μm	Micrometer
BV/TV	Bone Volume/Total volume
CT	Computed Tomography
DAPI	4′,6-diamidino-2-phenylindole; a fluorescent stain
EdU	5-Ethynyl-2´-deoxyuridine; a thymidine analogue stain
Gli1+	A line of cells with specific stem cell markers
IUCAC	Institutional Animal Use and Care Committee
JIS	Japanese Industrial Standard
MSC	Mesenchymal Stem Cell
PBS	Phosphate-Buffered Saline
pCO_2	Carbon dioxide partial pressure
PDL	Periodontal ligament
PDLSC	Periodontal Ligament Stem Cells
PFA	Paraformaldehyde
ROI	Region of Interest
SEM	Scanning Electron Microscopy
SHG	Second Harmonic Generation

TABLE OF CONTENTS

Page

LIST OF FIGURES

Page

LIST OF TABLES

Page

CHAPTER I

INTRODUCTION

Teeth are one of the greatest developments beginning with the ancient arms race of prehistoric fishes in the far-off mists of geologic time, and ending with the highly effective mammalian dentition. Despite the great advantages they give us in defense and biting ability, they have left us with a legacy of pain and suffering. Our teeth, composed of rock-hard dentin and enamel, must somehow be connected to the body through an interface tissue, known as the periodontium. In mammals this attachment tissue consists of a complex of periodontal ligament, cementum, alveolar bone, gingiva, as well as other investing and supporting tissues. Unfortunately, the periodontium of humans is subject to degenerative diseases invoked by a dysbiosis of the oral bacterial flora. The prevalence of this disease in the United States is 46% in adults over age 30, and 68% of adults over age 65 (Eke et al. 2015). While minor forms of the disease are generally painless and have little impact on the person's quality of life, the effects of the disease are cumulative, and the severe forms of the disease can lead to tooth loss and oral disfigurement. The cost of treatment in the United States can be in excess of $10,000 per person, and treatment is not available in many parts of the world, resulting in widespread edentulism in less developed countries as well as in lower socioeconomic groups in the United States. Moreover, the presence of periodontal disease can be a risk factor in heart disease, diabetes and adverse pregnancy outcomes.

Treatment of periodontal diseases consists of non-surgical and surgical therapy. Nonsurgical, or root planing, can slow the progression of the disease but not eliminate or reverse the damage which has already occurred. The goal of surgical therapy is to regenerate and rebuild the lost tissue through application of bone and soft-tissue grafts, treatment which is intended to repopulate the periodontium with the same tissue types as the original structure, but is unpredictable and usually results in an unnatural repaired tissue of diminished dimensions. Even with the great advances in the use of biologics, such as enamel matrix derivative, the results of therapy are often unstable and disappointing.

Development of Mammal-like Craniofacial Characters in a Marine Reptile

The periodontal ligament as we know it first appeared early in mammalian evolution, and this mode of tooth attachment is one of the defining characters of mammals (Leblanc et al. 2016). Tooth attachment in non-mammalian vertebrates, i.e., fish, reptiles and amphibians, generally consists of a direct attachment of the tooth dentin to the jawbone without any intervening soft tissue, a condition known as ankylosis (Bertin et al. 2018). In mammals, the periodontal ligament consisting of a 200-micron thick soft tissue membrane is vital for protecting the tooth root surface from the resorbing action of the osteoclasts in the bone. This ligament is maintained through a tightly controlled system of stem cells and molecular signals to prevent ankylosis, which only occurs as a pathological condition in mammals. There is evidence that this appeared

as an early developmental stage the matured into a mineralized attachment (LeBlanc, Lamoureux, & Caldwell, 2017).

Despite great advances in paleontology and the relatively complete record of the stem-mammals, the details of the origin of the periodontal ligament are still obscure. In addition, the relationship of the periodontal ligament to other mammalian characters, such as prismatic enamel, the temporomandibular joint, endothermy, diphyodonty, and heterodonty remains obscure. The evolutionary clade most prominently associated with non-mineralized periodontal ligament, the mammals, appeared at the beginning of the Mesozoic Era, a time period characterized by the recovery from the great Permian extinction (Luo 2007). A non-mammalian that also developed a specialized periodontal attachment apparatus is the *Globidens*. The *Globidens* were a group of highly specialized mosasaurs that inhabited the deep waters of late Cretaceous oceans. *Globidens* mosasaurs were uniquely equipped to feed on a specialized diet of ammonites, muscles, and inoceramids due to their powerful jaws and robust dentition consisting of globular teeth.

Mosasaurs are secondarily marine adapted anguimorph squamates which appeared in the fossil record about 100 million years ago (Mya) and became extinct at the end if the Cretaceous, some 65 Mya (Polcyn et al. 2014). Through their first 15 million years of evolution, mosasaur jaws were equipped with simple, conical and slightly recurved teeth, similar to the typical lizard teeth of their ancestors. Blade-like teeth evolved in mosasaurs about 85 Mya and increased diversity in tooth form, including the durophagous types exemplified by *Globidens*, began at about 80 Mya

(Polcyn, Jacobs, Schulp, & Mateus, 2010). Tooth implantation also became increasingly complex through time, from pleurodont implantation in early mosasaurs (Polcyn et al. 1999) toward thecodont implantation in the most derived forms, with firm and resilient attachment to surrounding bone by mineralized periodontal ligaments (Luan et al. 2009). The resilient attachment via a periodontal ligament allowed durophagous mosasaurs to feed on hard-shelled marine organisms such as ammonites and inoceramids, substantially reducing the chance of tooth fracture from a diet of mineralized organisms. A favorite type of *Globidens* prey, the Inoceramid, was a family of oyster-like bivalves that grew to giant size during the relatively warmer climates of the Cretaceous. Their hard shells provided protection against other predators, but emerged as a novel food source for the mammal-like dentitions of *Globidens* and other durophagous mosasaurs (Martin & Fox, 2007). The availability of inoceramids as specialized food sources provided macroevolutionary pressures and opportunities for emerging squamates to positively react to changes in environment and diet. The decline of the Inoceramids due to cooling waters, parasites, and predation 1.5 million years before the end of the Cretaceous (Ozanne and Harries 2002) coincided with the disappearance of the *Globidens* mosasaurs, likely related to the loss of their highly specialized food source (Polcyn et al., 2014).

A key feature of the mosasaur attachment is the enlarged, highly vascularized cementum (Luan et al. 2009). This cementum (Wu et al. 2019; Xie et al. 2019) gives us some insight into the molecular mechanism of the reptilian-mammalian transition.

Evolution and Development of the Periodontal Ligament

In mammals, the periodontal ligament is subjected to constant stress through the forces of occlusion during mastication. As a result, it can rapidly mobilize repair and regeneration mechanisms, and does this on a constant basis through the production of new cells and new collagen fibers. In fact, it is one of the most active tissues in the body, with complete turnover every 24 hours (Berkovitz et al. 1995). This process, known as homeostasis, is necessary for the maintenance of the non-regenerating teeth of mammals which may have to last many decades (in contrast to the constantly regenerating teeth of fish and reptiles).

Homeostasis of the periodontal tissue is thought to be extensively supported by the MSCs and they are also critical in the tissue repair process after injury. Although great advances have been made in regenerative periodontal surgery, complete wound healing following therapy for an episode of periodontitis is almost impossible to achieve (Han et al. 2014). Because of the apparent essential nature of the MSC response to healing following disease, understanding the exact mechanisms involved is important in developing effective treatment for periodontal diseases.

To understand the difficulties in treating periodontal diseases, both clinicians and basic scientists need to understand not only the pathogenic microflora, the microanatomy, and the cellular response, but must also understand why the periodontal ligament is present in humans in the first place. This is part of a new branch of therapeutics known as evolutionary medicine, which seeks to identify how disease and conditions develop by looking into the past to see how conditions first developed

(Trevathan 2018). Evolution is often thought of as a long process that allows organisms to adapt to their environment, and in theory, they should become better and better adapted to the conditions within which they live. Our experience with human disease, and especially periodontal diseases, has shown us that this ability to adapt to the environment is not always present.

Periodontitis is a major public health problem, affecting nearly half of the adult population, and a major cause of tooth loss. Decades of microbiological research has determined the etiology is related to the presence of a specific group of bacteria, known as the Red Complex consisting of *Porphyromonas gingivalis*, *Prevotella intermedia*, and *Tannerella forsythus*. Despite the discovery of this complex, there is no one-to-one relationship between the presence of the bacteria and the incident disease. Recent research favors the Keystone Pathogen theory, which views the establishment of disease as a dysbiosis rather than a bacterial infection. In spite of this, periodontitis remains a human disease for the most part. Naturally occurring disease in wild populations of non-human animals is rare, and when it does occur, the magnitude of the disease is mild (De Vries et al. 2017).

The historic approach to periodontitis has been to consider first the human disease condition, and after learning all that is possible with that, impose the disease condition upon laboratory species in an attempt to understand the human disease. Indeed, much has been learned by these investigations, but an evolutionary medicine approach would consider this same condition from a different viewpoint, i.e., could this condition result from a mismatch between modern man and his environment? Is this a

failure to adapt to a changing environment, or is it some sort of mismatch between our adaptations and the twenty-first century environment? Evolutionary medicine specialist would generally use a physical anthropology approach to this problem, looking back to not only human ancestors, but also other primates for answers. These approaches have given valuable insight into the relationship between human periodontitis and systemic conditions such as Alzheimer's Disease (Hendy et al. 2018).

Although human and primate anthropology continues to give us valuable information, our investigations intend to look even farther back in annals of time, to the first appearance of the periodontal ligament, in an attempt to fully understand the nature of the processes that are being dealt with. The unmineralized PDL appeared early in the evolution of the mammalian lineage (Leblanc et al. 2016), but this investigation will consider the implications of the sudden appearance of a mammal-like unmineralized PDL in a non-mammalian clade, i.e., in a Late Cretaceous marine squamate. By examination of the prehistoric marine environment, the paleobiology of marine feeding, and the PDL anatomy of other reptilians and mammals, our goal is to determine how and why this type of PDL first appeared. This answer lies at the intersection of craniofacial suture biology (Zhao et al. 2015), MSC (Men et al. 2020a), and Wnt signaling pathways (Wu et al. 2019). This data will then be used to develop investigations with laboratory animal models to support our hypothesis, and in this way generate data that future investigators can be eventual translate back to the treatment of periodontitis in humans.

Prosthetic Restoration with Zirconia Implants and Sinus Augmentation

The history of tooth replacement through artificial dental implants may rightfully be dated back to the ancient Mayan era (Bobbio 1972), when root form artificial teeth were fabricated from carefully carved seashells. The modern era of dental implantology began in 1965 when the construction of the titanium screw implant by Per-Ingvar Branemark (1969). Today, millions of screw-type implants are placed yearly with the majority of them being of titanium or titanium alloy construction. Despite the wide application and nearly universal application, this state-of the-art prosthodontic technique is coming under increased scrutiny as the true number of therapeutic failures comes to light (Lang et al. 2019). There are many proposed etiologies proposed for the failures, including residual cement, fixture mobility, bacterial and chemical corrosion, and small phagocytosable titanium particles. A commonly reported etiologic factor is the presence of metallic breakdown products in the soft tissue surrounding the implant (Harrel et al. 2019). Some authors have proposed a non-metallic implant composed of Zirconia to prevent peri-implantitis, and these were evaluated in rats as early as 1982 (Nagai and Takeshita 1982). Even though zirconia implants were first introduced to the clinic in 2004 (Kohal and Klaus 2004), these implants still comprise only a small percentage of the total number of implants placed each year.

A common clinical situation prohibiting the use of dental implants has been the presence of thin alveolar bone in the posterior maxilla due to expansion of the maxillary sinus. This has led to the development of the sinus augmentation techniques to allow the insertion of implants in this oral region (Boyne and James 1980). These techniques have

now been used for decades and has seen considerable refinement since it was first introduced. Once such refinement has been the development of the minimally-invasive transalveolar sinus augmentation procedure (Summers 1998). Despite decades of clinical experience with these techniques, there are still many unanswered questions regarding the best method for success. It is proposed that the transalveolar sinus augmentation technique, combined with zirconia implants in the transgenic mouse model may provide further answers to the basic science behind the healing process, and provide information that was never before available.

Conclusion

The central hypothesis of this investigation was that the Wnt signaling system, along with its inhibitors and other closely related molecular mechanisms, is responsible for the maintenance of the non-mineralized state of the periodontal ligament in mammals along with the maintenance of the stem cell niche necessary for the routine maintenance of the periodontal ligament during the lifetime of the organism as well as healing in the prosthetic tooth replacement implants placed into the oral tissues. This hypothesis based on our preliminary observations of the response of the periodontal tissues to experimentally produced aberrant Wnt signaling episodes, which not only show changes in the mouse periodontium, but also show similarities to paleontological histology during the evolution of a mammal-like periodontal ligament in a reptile. The rationale for this hypothesis is that understanding the origin and control mechanisms of the cells of the periodontium, will allow controlling them for regeneration of periodontal tissues,

including increased predictability of bone and tissue grafts as well as improved outcomes in dental implant therapy.

Specific Aims

To attain the overall objectives, three specific aims were pursued:

1. Identify the characters associated with the evolution of a mammal-like craniofacial features, including the periodontal ligament, in a reptile.
2. Evaluate the evolution and the development of the periodontal ligament as a modified craniofacial suture and with the effect of changes in periodontal ligament stem cells and Wnt signaling.
3. Quantify the effect of zirconia implant placement on the microvasculature and stem cell migration of the peri-implant tissue in the maxilla and maxillary sinus region.

CHAPTER II

EVOLUTION OF MAMMAL-LIKE CRANIOFACIAL FEATURES IN MARINE REPTILES

Overview

The head of tetrapod vertebrates is evolutionarily labile, responding adeptly to changes in either environmental changes or food sources. The appearance of mammals shows that most of the adaptations are concentrated in the craniofacial region. This investigation examines the appearance of similar adaptations in an advanced squamate.

Synopsis

The definition of the class Mammalia is characterized by several key features such as the appearance of hair and lactation, but these are certainly not the only characters used for this classification. Of the many unique mammalian characters, the majority are concentrated in the craniofacial region. In this investigation a specific mosasaur is considered, a marine squamate species that was first described in 2010 (Polcyn et al. 2010). This mosasaur, *Globidens phosphaticus*, was examined by gross physical and visual methods. Following this, high-resolution microcomputed tomography (μCT), scanning electron microscopy (SEM), and thin ground section histology. Additionally, isotope analysis was performed on the tooth enamel. The data obtained from these examinations was compare with that of other mosasaurs, as well as mammals. A suite of characters uncommon in reptiles, but common in mammals was

uncovered. The sequence of the appearance of these characters along with a probable timeline was determined, indicating the rapid acquisition of mammal-like characters in a late-appearing mosasaur.

Introduction

All thermodynamic processes on earth require an energy source, and the head of living organisms, as the intake port for energetic fuel, is the key element driving the evolution of the organism. Evolution has been described as survival of the fittest in the struggle for survival. A key element of this theory is that resources are scarce, so that competition for nutrients is a fierce battle. In the early seas, this competition resulted in increasingly armored fish, which were then surpassed by fish with increased masticatory ability to crush and devour them. Not limited to just animal life, plants also became increasingly armored with spines and scales, as they were viewed as a food source for marauding metazoans. Likewise, the invertebrates, mollusks and plankton for example, also developed an armor for protection. This coating consisted of mineralized shells and plates composed mainly of calcium carbonate in the form of calcite or aragonite (Clarke et al. 2011), although some metazoans such as sponges developed skeletons composed of silica (Muller et al. 2011). A side effect of this biomineralized armor was the creation of a Carbon Cycle on the planet where the deceased carcasses of the animals settled to the bottom of the sea, where absorbed into the earth's crust, and eventually belched forth as atmospheric carbon dioxide. Through various biogeochemical processes, involving primarily carbonate and silica, a feedback loop was created that regulated the pCO_2 in

the atmosphere (Isson et al. 2020). These same biogeochemical processes are thought to be responsible for the maintenance of the pH of the world's oceans as well as maintenance of liquid water on the Earth's surface, essential for life as we know it. Although the levels of atmospheric CO_2 have ebbed and peaked over the course of geologic time, the persistence of life over the past 4 billion years is a testament to the stability of this system as well as the critical nature of these biomineralized tissues on the Earth's history.

The quest for energy, i.e., the quest for nutrients, eventually left the sea as the first tetrapods crawled out of the mud to plunder the abundant terrestrial invertebrates and flora which had moved ashore much earlier. The first terrestrial tetrapods, the amphibians, still maintained a close relationship to the shoreline, where they required abundant freshwater for their reproductive activities, but as evolution progressed the tether to the seashore was severed as the reptilians appeared on the earth's landscape. The first known reptiles are commonly considered to be the *Hylonomus* and *Paleothyris*, small land creatures about 20 centimeters long that had an appearance not unlike a modern lizard. Although the *Hylonomus* is the oldest known true reptile, modern Bayesian analytical methods have placed the Paleothyris as a basal form (Muller and Reisz 2006). Later reptilian forms included the Diapsida, which gave rise to modern lizards, snakes, crocodilians, dinosaurs, birds, and based on new evidence, even turtles (Schoch and Sues 2016). New evidence also places the precursors to mammals within the Diapsida (Ford and Benson 2020; Modesto 2020).

The true origin of Squamata (a group which includes lizards, snakes, and amphisbaenians) is somewhat problematic to determine because there is a gap of nearly 70 million years in the geologic record between the earliest recovered fossils and the calculated origin of the group (Pyron 2017). Nevertheless, light was shed on the early relationships recently with evidence from high-resolution microfocus X-ray computed tomography data of an articulated specimen of *Megachirella wachtleri*, a Middle Triassic lizard found in the Italian Alps (Simões et al. 2018). This data positioned this species as the oldest known stem squamate. As a result of this new knowledge, the origin of the squamates and most other diapsids can now be placed clearly before the Permian-Triassic extinction event, and the Triassic can be considered as a time of radiation rather than origin of these lineages. This study also places the origin of the squamates closer to the gecko lineage, not the iguanian lineage as previously supposed.

Of the extant squamates, all snakes are carnivorous. The majority of lizards are insectivorous, and only a small percentage are herbivores (King 1996). The adaptation to herbivory required not only of the digestive system modifications but also major changes in the morphology of the skull, jaw and teeth (Sues and Reisz 1998). The majority of lizard teeth are homodont with a single apex (Peyer and Zangerl 1968) reflecting an insectivorous diet, but the squamate oral apparatus has demonstrated an ability for modification based on dietary shifts. This lability is demonstrated by multiple occurrences of oral specialization appearing in different lineages at different times (Lafuma et al. 2020). While insectivory requires only the ability to hold the prey in the mouth for a sufficient time to subdue and swallow whole the captured insect, herbivory

requires a more extensive oral processing of the food stuff. The apparatus required for oral processing versus capture of prey are quite distinct (Schwenk 2000). Thus, it is determined that the acquisition of food is a strong determinant and driving force in the evolution of oral morphology.

Among the current reptiles, a number of species make their home in the sea. As all of the early squamates were terrestrial animals, this marine adaption is a secondary migration that occurred at a later time. There are approximately 11,050 species of reptiles today and an additional 2,442 subspecies, although there is some controversy among authors as the number and concept of subspecies in this group. Within the Class Reptilia, there are 195 extant species of amphisbaenians, 353 testudines (turtles), 25 crocodilians, and one species of Rhynchocephalian (tuatara). The squamates make up the largest and most diverse group with 6687 species of lizards and 3789 species of snakes (Uetz 2020). The diversity of the squamates is rivaled only by the birds, and far outnumbers the mammals. Reptiles crawled out of the aquatic environment approximately 260 million years ago, and modern reptiles had appeared by the Jurassic (150-200 million years ago). Of the 11,050 extant species of reptiles, only a small number have secondarily returned to the sea. One species of salt-water crocodile, and 7 species of sea turtle now live in the sea. Among the squamates, snakes make up the largest group of secondarily-adapted marine creatures with about 80 species and subspecies of sea snakes. Only one species of lizard lives in a marine environment, and that is the Galapagos Marine Iguana (Rasmussen et al. 2011). Although living in the sea, it is not completely adapted to marine life and must occasionally bask on land to restore

body heat. Some terrestrial animals returning to the sea, i.e., secondarily adapted marine mammals, are known to undergo rapid evolutionary changes (Thewissen 2014).

The paucity of marine squamates was not always the case. The warm climate and rising seas provided a fertile hunting ground for lizards and snakes in the brackish coastal estuaries, similar in lifestyle and habit to modern alligators. Several groups of reptiles took to the seas and adapted a completely marine lifestyle. These groups were contemporary with the dinosaurs, although no true dinosaur became adapted to the ocean environment. The primary groups of ancient marine reptiles were the Ichthyosaurs, the Plesiosaurs, and a group of squamates, the mosasaurs (Fig. 1). These groups occupied much of the niche that is now occupied by modern whales, porpoises and sharks (Callaway and Nicholls 1997). Although the mosasaurs are known to be squamates based on the anatomy of recovered fossil specimens, their exact lineage within Squamata has been controversial. The early investigators placed the mosasaur within the close relations of the monitor lizards (Cuvier 1808), but a later researcher placed the affinity closer to the snakes in a group he called Pythonomorpha (Cope 1869). A later landmark study of reptilian anatomy placed the mosasaurs clearly in the lizard group (Camp 1923), and this convention was followed for many decades following. Recent studies have reignited the controversy and placed the mosasaurs back in the snake group based on osteologic analysis (Lee and Caldwell 2000) as well as synapomorphies in the anatomy of the dentition (Lee 1997). A recent analysis of the tooth attachment tissues most basal of mosasaurs *Coniosaurus* from the Dallas, Texas region placed the mosasaurs clearly in

Figure 1 The mosasaur was a marine lizard
A lizard with many secondarily aquatic adaptations. Although a squamate and not a dinosaur, it became extinct at the same time as the dinosaurs, at the end of the Cretaceous Era, roughly 68 million years ago.

Table 1 Relationship of Mosasaurinae to other groups

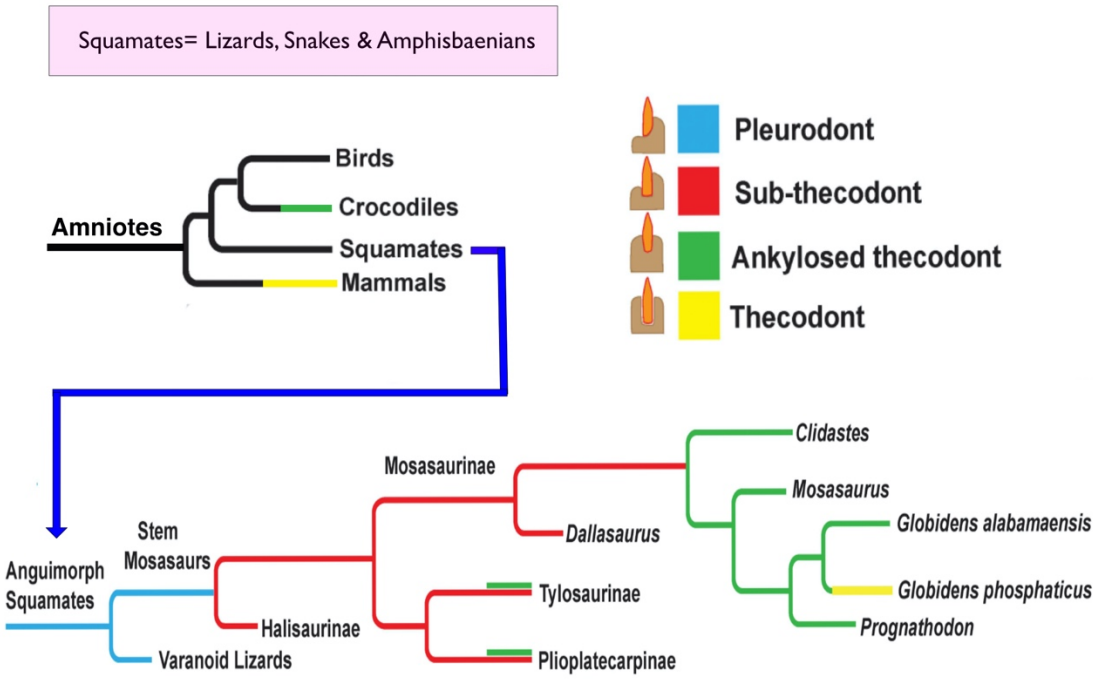

This phylogenetic tree shows the relationship of the *Globidens* to other amniotes as well as the progression of the tooth attachment schemes in the mosasaur line.

the lizard group of Varanoidea and rejected the notion of being closely related to snakes, or perhaps occupying a more basal position within Squamata (Augusta 2019) (Table 1).

This emphasis on the tooth attachment tissues of these reptilian mosasaurs underscores the importance of the homologies of these tissues to investigations into the origins of the periodontium in Mammalia. Although the reptiles and mammals had a common origin within Diapsida, the mammalian line separated during the Permian, and the Cynodonts occur in the fossil record about 260 million years ago during the Triassic of Brazil (Martinelli et al. 2016). These stem-mammals were not quite mammalian, but led to a long series of evolutionary developments culminating in the true mammals. The first true mammals appeared about 165 million years ago. A great variety of small mammals lived among the dinosaurs, but most them were the size of a shrew or a housecat (Pickrell 2019). There are important characters which must be present for an animal to be considered a true mammal, and many of these are centered in the craniofacial region. One of the most prominent features is the structure of the lower jaw. In reptiles, the lower jaw consists of a series of bones with dentary bone being the tooth-bearing structure and the articular forming the joint with the quadrate in the upper jaw. In mammals the entire lower jaw is reduced to the dentary bone, commonly called the mandible, which articulates with the squamous portion of the temporal bone in the skull. The posterior portions of the reptilian jaw became miniaturized and evolved into the sound transmitting mechanism in the inner ear of mammals. In the reptiles there are many possible tooth-bearing bones, but in mammals the tooth-bearing bone is reduced to the mandible, and maxilla/premaxilla.

As previously mentioned the teeth are valuable for the systematic diagnosis of a mammal. Because the teeth are composed of dentin and enamel, the hardest known biomineral, they are often well preserved in geologic time, and sometimes maintain their integrity for detailed histologic analysis. A key histologic feature is the presence of prismatic enamel in the mammalian dentition, and non-prismatic enamel in all reptiles with the exception of the *Uromastyx* lizard (Sander 1999). Mammals tend to do extensive oral processing of their food, and the prismatic enamel is more durable and less likely to propagate fractures. The oral processing of food also leads to specialized teeth, with mammals having molars, incisors, and canine teeth, a condition known as heterodonty, while reptile have similarly shaped teeth throughout the dentition, or homodonty. The mammalian dentition is biphyodont, meaning there are at most, two sets of teeth during the life of the animal, whereas reptiles are polyphyodonty, with many sets of teeth forming and being replaced throughout life. Mammals are usually born without teeth also, since the presence of teeth would impede nursing. A list of typical mammalian features is listed below (Kielan-Jaworowska et al. 2005):

- Prismatic tooth enamel
- Heterodont dentition
- Diphyodont dentition
- Thecodont dentition (teeth in sockets)
- Skin covered in hair
- Lactation
- Warm-blooded metabolism

- Live birth
- Occlusion of posterior teeth
- Oral processing of food
- Non-mineralized Periodontal Ligament (Gomphosis)
- High bite force for chewing
- Single bone in lower jaw
- Temporomandibular joint
- Three inner ear ossicles
- Open pulp chambers in teeth
- Hyoid/ laryngeal apparatus
- Determinant growth
- 4-chambered heart
- Small litter size
- Parental care
- Highly developed special senses
- Seven cervical vertebrae
- Sebaceous (fat secreting glands), sudoriferus (sweat), and scent glands.
- Diaphragm

This list is not exhaustive, but it does show the craniofacial bias of the mammalian adaptations. It is also not exclusive; single characters such as teeth in sockets occur in

crocodilians, and prismatic enamel occurs in *Uromastyx*. Nevertheless, the majority of these characters will be present in a mammal and absent in a reptile.

The acquisition of these characters has been studied in the stem mammals as they moved toward becoming true mammals. In this study a reptile is presented which displayed a great number of mammal-like characters and the convergent evolution between the two classes of vertebrates is explored as well as the extraordinary environment which permitted this to occur, allowing insight into their structure, function and development. This species, the *Globidens phosphaticus* of Morocco and Angola. *G. phosphaticus* may provide valuable information regarding the acquisition of mammalian characters, and may have far ranging impact.

Experimental Procedure (Materials and Methods)

Specimen procurement

The specimens of *Globidens phosphaticus* used in this study came from the fieldwork of the PaleoAngola Project and have been previously described (Polcyn et al. 2010), Briefly, this specimen was discovered from the Bench 19 coast of the Bentiaba, Namibe Province, Angola, where it was excavated and shipped to the United States (Texas) for preparation and documentation. It came from a stratum corresponding to the Maastrichtian of Angola.

Specimens examined

- *Clidastes* sp., SMU 76381
- *Clidastes liodontus*: YPM1335
- *Globidens alabamaensis*: SMU 76241, SMU 76279, SMU 76903, SMU 6527
- *Globidens phosphaticus*: (Isolated teeth for paleotemperature analysis) MGUAN PA04, PA05, PA23, PA24, PA30, PA33, PA34, PA43, PA61, PA62, PA311, PA313, and PA498
- *Globidens phosphaticus*: (Specimens used for morphological and histological analyses) MGUAN PA23 & PA24
- *Platecarpus planifrons*: SMU76516
- *Russellosaurus coheni*: SMU73056
- *Prognathodon kianda*: MGUAN PA183 and PA129
- *Latoplatecarpus willistoni*: SMU 76351
- Mus musculus used in this analysis were bred at Texas A&M University College of Dentistry. Additional Mus musculus specimens (Wild type) was purchased from Jackson Laboratories. Complies with Texas A&M University IACUC protocol number 17-0103.
- *Didelphis virginiana*: (Wild type) procured in accordance with state, local and federal laws.

Bite force analysis

The relative bite force was estimated from measurements taken of actual specimens of mandibles in the laboratory. One extant species and four extinct species

were selected to correspond to the evolutionary sequence depicted in this study. Photos were taken of the adductor fossa of each specimen using a Nikon D-80 digital camera system at a plane orthogonal to the body of the mandible using an AF-S Micro-Nikkor 105mm macro lens. Images were loaded into Adobe Photoshop CS where the following landmarks were annotated:

1. Dorsal margin of anterolateral terminus of glenoid fossa
2. Surangular-articular suture and anteromedial terminus of glenoid fossa
3. Dorsal margin of surangular at posterior margin of coronoid terminus
4. Articular dorsal margin at mid-mandibular fossa (calculated semi-landmark)
5. Dorsal margin of mandibular foramen
6. Ventral margin of mandibular foramen

The photos with landmarks were then imported into ImageJ (NIH, Bethesda, MD, USA), and each was calibrated by superimposing an in-photo scale with the line tool to obtain the unit length in pixels. Under the analyze tab, the pixel count and scale unit details were then entered in the "set scale" command dialog. The polygon selection tool was then used to connect the dots and form a polygon using the polygon selection tool. The "measure" command of the ImageJ analyze command was then used to quantify the enclosed area. The area of the medial adductor fossa was then compared with the moment arm of the mandible. This was calculated by measuring the linear distance from the jaw articulation to the mid-point of the tooth row on the dentary bone. The adductor divided by this linear distance provided a relative measure of potential jaw force.

Tooth and bone histology

Specimens were dried in warm air and embedded in Technovit 7200 VLC acrylic resin (EXACT Technologies, Oklahoma City, OK) under a vacuum, which was then polymerized at room temperature and pressure. Blocks were sawn with a diamond bandsaw and then cemented to glass slides. Samples were ground to 80µm and polished to 1200 grit using the previously described method (Luan et al. 2009). Specimens were examined under brightfield and polarized light, then photographed using a Leica DM 2700P microscope with a Nikon DSRi2 camera.

Tooth and bone SEM

Samples were embedded in acrylic resin and the resulting blocks were cemented to plastic microscope slides. Thin sections were cut with a diamond bandsaw, and the slides were then polished to approximately 100µm. These sections were examined under brightfield transmitted light microscopy, and the slide was cut with the bandsaw to preserve areas of interest. Sections were etched in EDTA for approximately 30 minutes, then rinsed in deionized water for 30 minutes. Slides were dried overnight, then sputter-coated with gold-palladium for two minutes. SEM images were obtained at the University of Texas Southwestern Medical Center Electron Microscopy Core Facility using a Zeiss Sigma VP (NL1.160F) scanning electron microscope.

Computed Tomography

Paleontological specimens were scanned at the University of Texas Austin High Resolution X-ray Computed Tomography Facility. Data was processed for visualization and analysis using Amira 6 (ThermoFisher, Waltham, MA).

Enamel isotope analysis

Silver phosphate was prepared from enamel of 11 *Globidens* teeth and additional elasmobranch teeth from Bench 19 (Strganac et al. 2015) following a previously described methodology (O'neil et al. 1994). Dentin samples were also prepared for 7 of the specimens in order to test for potential diagenesis. The silver phosphate samples were analyzed at the University of Arkansas Stable Isotope Laboratory. Of the *Globidens* samples that yielded δ18Odentin values, three displayed evidence of diagenetic alteration (PA 05, PA 43, PA 34) as evidenced by a convergence of the δ18Oenamel and δ18Odentin. As a result, these samples were deemed compromised and excluded from further analyses. A fourth sample, PA 62 deviated more than two standard deviations from the mean, and was thus considered an outlier. The body temperature estimated from this δ18Oenamel value was 6.25°C, which is well below the functional threshold of modern squamates and significantly below the known ambient water temperature at Bench 19. This sample was also suspected of diagenetic alteration and therefore not included in further analysis. The seven remaining samples yielded a mean body temperature of 20.98 °C ± (95% CI 20.48°C to 21.49°C). Body temperature calculation based on presumably unaltered samples (PA 04, PA 30, PA 498, and PA61) yielded a mean temperature of 22.12°C (95% CI 21.6°C to 22.65°C). These values were well above the ambient water temperature estimates (18°C) from both inoceramids and co-evaluated elasmobranchs (this study), suggesting that *Globidens* at Bench 19 displayed a slightly elevated body temperature compared to the surrounding environment (Strganac et al. 2015).

Results

The initial analysis of the *G. phosphaticus* specimen consisted of gross examination of the teeth and jaws. As seen in the macrophotographs, the overall condition of the teeth was good, but the jaws had suffered due to weathering and breakage. There was one remaining tooth still remaining attached; this was to the lower jaw (Fig. 2). This tooth was not firmly cemented to the bones of the lower jaw, but remained somewhat mobile within the alveolus. As can be observed in the photo, a slight gap can be seen between the root portion of the tooth and the bone. Close observation showed the tooth is being retained mechanically by undercuts in the root structure that are being impeded by crushed bone structure. The undercut can be seen to consist of a resorption cavity from the crown of a succeeding tooth which has been lost, but whose impression remains as a hemispherical concavity on the distal surface of the tooth root. The gap between the tooth and the alveolar bone represents a space that was filled with soft-tissue during the life of the mosasaur but now has disintegrated due to various taphonomic processes that have occurred in the approximately 68-million years since the death of the organisms. An approximation of the extant and the shape of this soft-tissue layer can be seen by the impression that it has left in the interior surfaces of the alveolus. It can be observed that the patterns on the surface of the alveolar bone are both longitudinal and concave. The impressions on the surface of the root are likewise longitudinal and concave. This indicates that the intervening tissue made a similar imprint on both surfaces, i.e., the exterior surface of the root did not make the imprint on

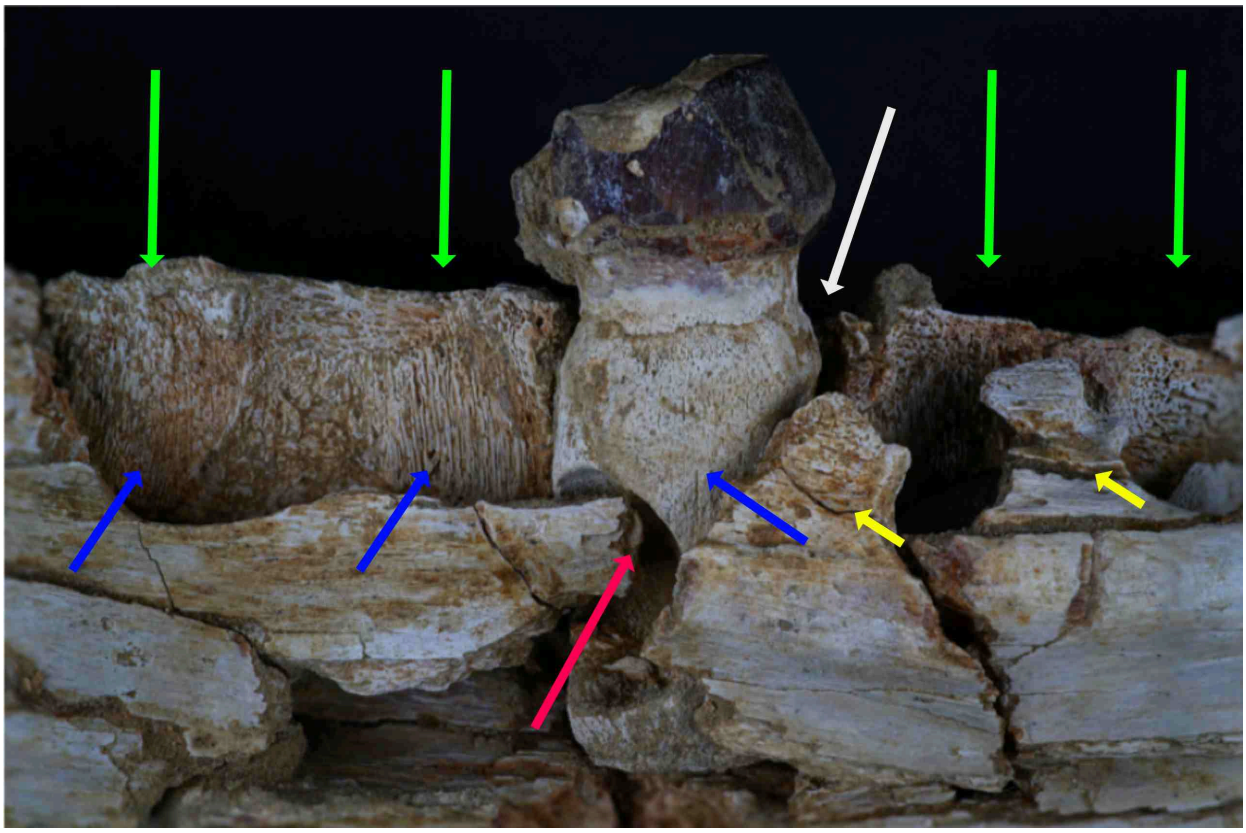

Figure 2 The crown, root and bone of the *Globidens phosphaticus* of Angola
This specimen demonstrates the one tooth remaining which was still attached to the jaw. This specimen is from the lower jaw, and a gap can be observed between the tooth and the retaining bone structure (white arrow). While all of the other teeth have been lost from the jaw resulting in empty alveoli (green arrows), this single tooth remains in place. The tooth remains mobile and it is being retained by crushed bone fragments penetrating in to undercuts on the root surface (red arrow). Distinctions can be seen in the surface texture of the tooth supporting bone (blue arrows) and the remaining structural bone of the jaw. There is also some separation of the alveolar bone from the supporting jaw bone (yellow arrows).

the inside of the alveolus. If it did, a reversed pattern would be present on one of the surfaces, which is not evident in this specimen. A further observation that can be made in this specimen is the separation between the interdental bone and the supporting bone of the lower jaw. As can be seen in the macrophotograph, the gap between these two bone types remains very small, and it can be seen that the bone fit together intimately, and the convex surfaces of one fit into the concave surfaces of the complimentary bone. This is in contrast to the tooth/alveolar bone interface as noted above.

A further evidence of the soft-tissue nature of the tooth bone interface can be seen by analysis of field photos on the excavation site in Bentiaba, Angola (Fig. 3). A key finding is that many of the teeth pictured are seen unattached. No bone can be seen attached to the surface of the tooth roots as they were found and uncovered. This point is confirmed in the original publication of this specimen (Polcyn et al. 2010). The jaws have been crushed laterally, probably post-mortem due to the heavy weight of the overlying sediment during the preservation process. The upper and lower jaw bones being in close proximity to each other, and the teeth being found in close proximity to the corresponding jaw, indicates that the craniofacial bones were most likely intact at the time of death and burial, and that the teeth became displaced from their sockets follow the decomposition of the soft-tissue anchoring them to the alveolar bone. These findings are consistent with a non-mineralized periodontal ligament, similar to what is found in the mammalian dentition. These filed photos also demonstrate the sandy matrix associated with the *G. phosphaticus* specimens found in Angola.

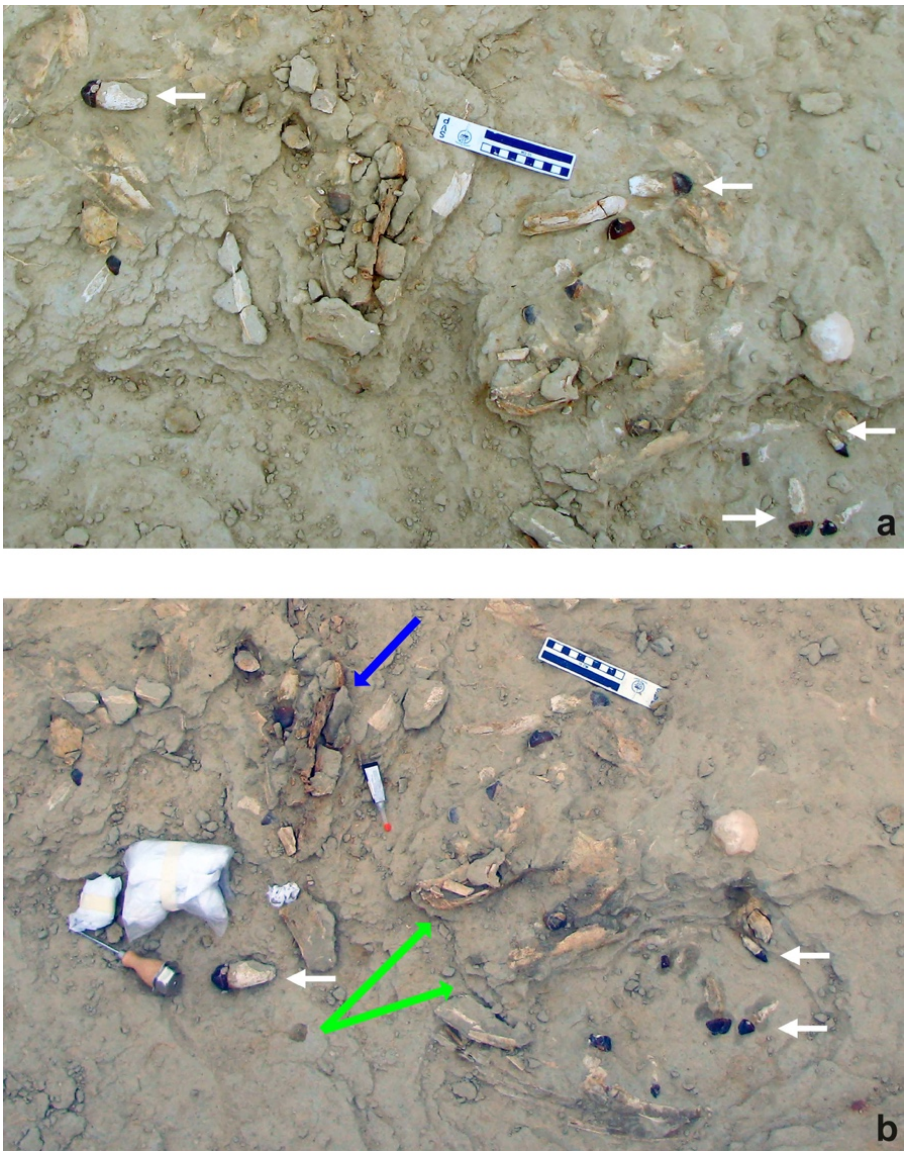

Figure 3 Field photos from Bentiaba, Angola
These two photographs demonstrate the conditions of the *Globidens phosphaticus* as it was being uncovered in the field. A) superficial uncovering of the specimen. B) Deeper excavation of the same specimen. The maxillary teeth are seen in close proximity to the remnants of the maxillary jaw (blue arrow), and the mandibular teeth are found in close proximity to the bones of the lower jaw (green arrows). A key finding is that the teeth are displaced from their sockets (white arrows).

Since these mosasaurs were feeding on inoceramids, a type of oyster living on the bottom of the Cretaceous seas along the coast of Africa, it is likely that sandy nature of this sea floor is responsible for much of the abrasion that is seen on the Angola specimens in response to the heavy occlusal forces required to break the shellfish during oral processing. The degree of occlusal wear in these Angola specimens is greater that the that seen in specimens of *G. phosphaticus* reported from other locations such as Morocco (Bardet et al. 2005).

Our hypothesis depends on the response of the oral and craniofacial tissues of *G. phosphaticus* to more intense forces than previously experienced in the mosasaur lineage. Our thought is that the bite forces gradually increased in the mosasaurine lineages as they moved into wider environmental niches in search of the abundant food sources in the late Cretaceous period. The sources of food, in this case heavily-shelled inoceramids and mollusks such as ammonites, required durophagous adaptations in order to exploit them. Further considerations of specific adaptations are predicated on showing that this species indeed had an increased bite force, and that the clade had been showing increasing adaptations to the oral processing of harder food. In order to test this hypothesis, a bite force analysis was performed which was calculated using engineering methods on the lower jaws of several species.

The results of our calculations are shown in Table 2. These results include the monitor lizard *Varanus niloticus*. This is an extant lizard with known durophagous

Table 2 Bite Force

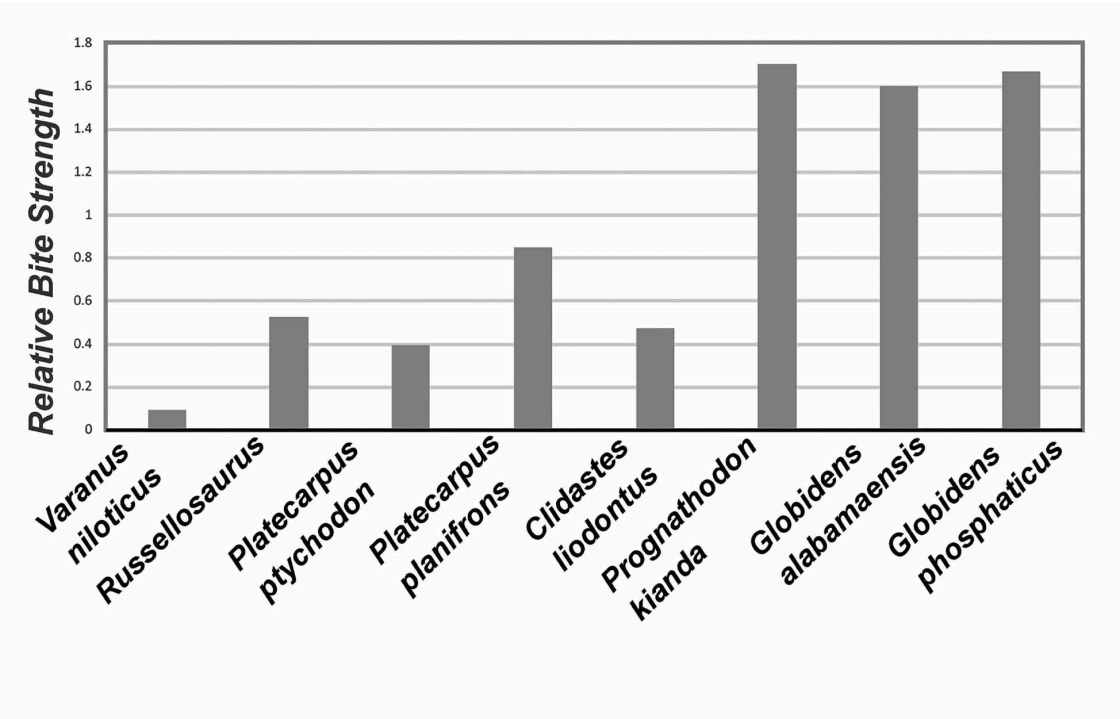

The relative bite force of eight species was calculated using the muscle attachment area of the medial adductor complex in relation to the length of the lever arm of the tooth row. One extant species (*V. niloticus*) of squamate was compared with seven extinct squamate species (the mosasaur lineage). This calculated value quantifies the robustness of the lower jaw structures and the amount of force that was able to be brought to bear upon the teeth. Although there is the trend of a progression to increasing forces, it is easy to delineate two groups. The first five with lower bite forces presumably had a diet of insects, soft vertebrates (fish and even other mosasaurs), and soft invertebrates. The last three, *P. kianda*, *G. alabamaensis*, and *G. phosphaticus*, had high bite forces for the consumption of hard-shelled invertebrates, e.g., inoceramids and ammonites.

adaptations. Juveniles of this species are generalized feeders with a diet of insects, spiders and other soft-bodied prey, but adults transition to molluscivory requiring shell-crushing abilities (Bennett 2002). These lizards possess sharp, pointed teeth as juveniles, but through ontogeny the shape of subsequent generations of teeth develop into a globe shape (D'amore 2015) reminiscent of the *Globidens* morphology. It also a terrestrial lizard, since all fully marine lizards are now extinct, but it serves as a known basis for comparison of the extinct forms. It is notable that this terrestrial lizard has the lowest calculated bite strength of all squamates tested in this evaluation. The remaining squamates include a range of the mosasaurine lineage that begins with the most basal mosasaur of the group, *Russellosaurus sp*., and then continues with *Plateplatycarpus ptychodon*, *Platecarpus planifrons*, *Clidastes liodontus*, and *Prognathodon kianda*. The final two in the tested group are the most recent mosasaurs as well as the two with the most durophagous adaptations of the tooth crown morphology, *Globidens alabamaensis* and *G. phosphaticus.* The eight species tested easily fall into three groups: the terrestrial squamates, the early marine squamates, and the late marine squamates. As previously mentioned, the only terrestrial squamate tested was the *V. niloticus*, chosen for its extant status, close phylogenetic relationship to the mosasaurine clade, as well as its durophagous diet, consisting or hard-shelled snails. It can be seen from the table that the bite force generated by this lizard falls perceptibly below the range of its marine counterparts. The next group are the early marine squamates, *Russellosaurus sp., P. ptychodon*, *P. planifrons*, and *C. liodontus*. This group all show an elevated bite strength capacity compared with *Varanus*, but there was not a clear, discernable trend within the

group, although the *P. planifrons* appeared to have an elevated capacity compared to the others in this group. Further investigation would be required to definitively confirm this with a larger number of specimens as well as correlation with the paleobiology, specifically diet and habits, of this species. The third group consists of the late marine squamates, *P. kianda*, *G. alabamaensis*, and *G. phosphaticus*. Stomach content analysis of *Globidens* of Montana has shown they had a diet consisting of hard-shelled invertebrates (Martin and Fox 2007). The teeth of the two *Globidens* species are spherical in shape (hence the name *Globidens*) and appear to be well adapted mechanically to the crushing of shells. The measurements of the two globidensine species showed the capability for high occlusal forces, as predicted from their dietary behaviors. The *P. kianda*, while having teeth of a more common single-pointed morphology, were also calculated to have the capability of generating large forces.

As diets of reptilian species diverge from the capture and swallow method of feeding, specializations of tooth morphology can occur. When differences can be seen in the anterior and posterior teeth the achieved condition is known as heterodonty. This is exemplified in the mammalian case with the development of incisors, canines, premolars and molars in the adult dentition. To a lesser extent, this type of differentiation and specialization can occur in lizards. The dental condition of the early mosasaurs such as Clidastes consists of a row of single-peaked conical teeth, with the anterior teeth very similar in form to the posterior teeth (Fig. 4a). This condition is considered homodont, and is typical of most lepidosaurs (members of Squamata and Rhynchocephalia). A later mosasaur *G. alabamaensis* can be seen to have specialized teeth with a globe shaped

morphology (Fig. 5e). In this case the anterior teeth were seen to be less globular than the posterior, indicating a degree of heterodonty. The late mosasaur *G. phosphaticus* showed even more specialization and diversity in morphology, and thus a higher degree of heterodonty than other mosasaurs. The posterior tooth crown shape has the typical globe-shaped form (Fig. 6i), but consideration of the full range of from a single individual will display a great diversity of shape (Table 3a). Each of these teeth was matched to the alveolus from which it was derived (not pictured), and it was found that the anterior teeth had a flame-shaped morphology, the mid-arch teeth had a globe-shaped form, while the most posterior teeth had a flattened mushroom-like crown shape and a thick, robust root structure. The degree of heterodonty was quantified for four mosasaurine species and compared to a typical heterodont mammal, the Virginia opossum *Didelphis virginiana*. This unique mammal is the only marsupial native to North America, and is thought to represent a basal form of dental structure. Calculations of the mesial-distal base dimensions opposed to the tooth crown height of each tooth in the arch gave a single measurement, a heterodonty index, corresponding to tooth shape regardless of overall tooth size. As expected, the heterodont mammal, *D. virginiana*, showed a great spread showing a difference in the anterior and posterior tooth shape (Table 3b). In contrast, the early mosasaurs, *Latoplatecarpus* and *Clidastes* showed tightly grouped indices of heterodonty, indicating a similarity in form of the teeth throughout the tooth row, typical of most lepidosaurs. The more derived mosasaur *G. alabamaensis* showed a higher degree of heterodonty (represented by more spread of

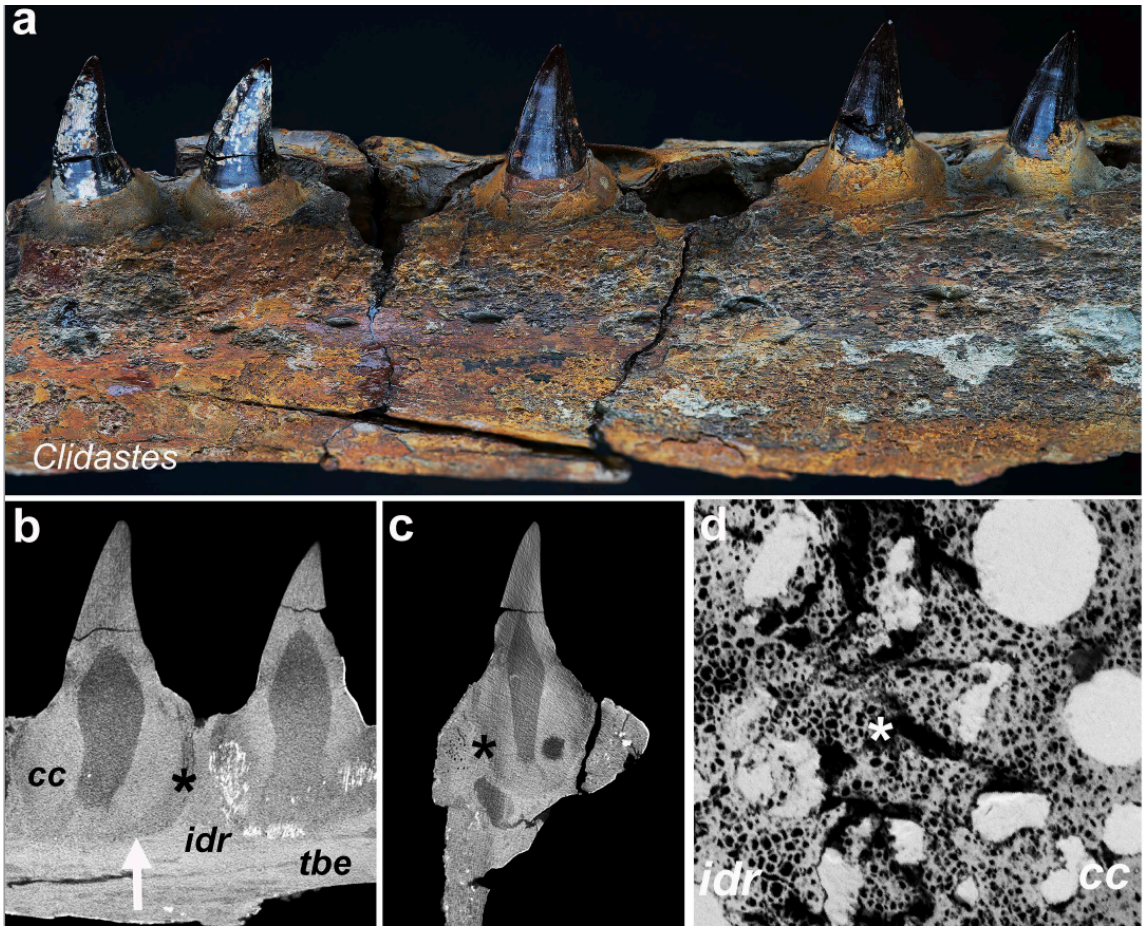

Figure 4 *Clidastes* teeth in situ, microCT, and SEM
The nature of the periodontal attachment for *Clidastes* is demonstrated. The single pointed homodont teeth indicate a generalized diet. A) The macrophotograph of Clidastes shows the teeth are surrounded by bone on all sides of the tooth sockets in a condition of thecodonty. B) MicroCT image demonstrates the nature of the periodontal attachment: cc) cellular cementum, idr) interdental ridge. Asterisk) mineralized periodontal attachment tissues. Note the broad base of connection compared to the tooth crown size.C) SEM demonstrates the mineralized ankylosis of the tooth and the surrounding bone of tooth supporting tissues.

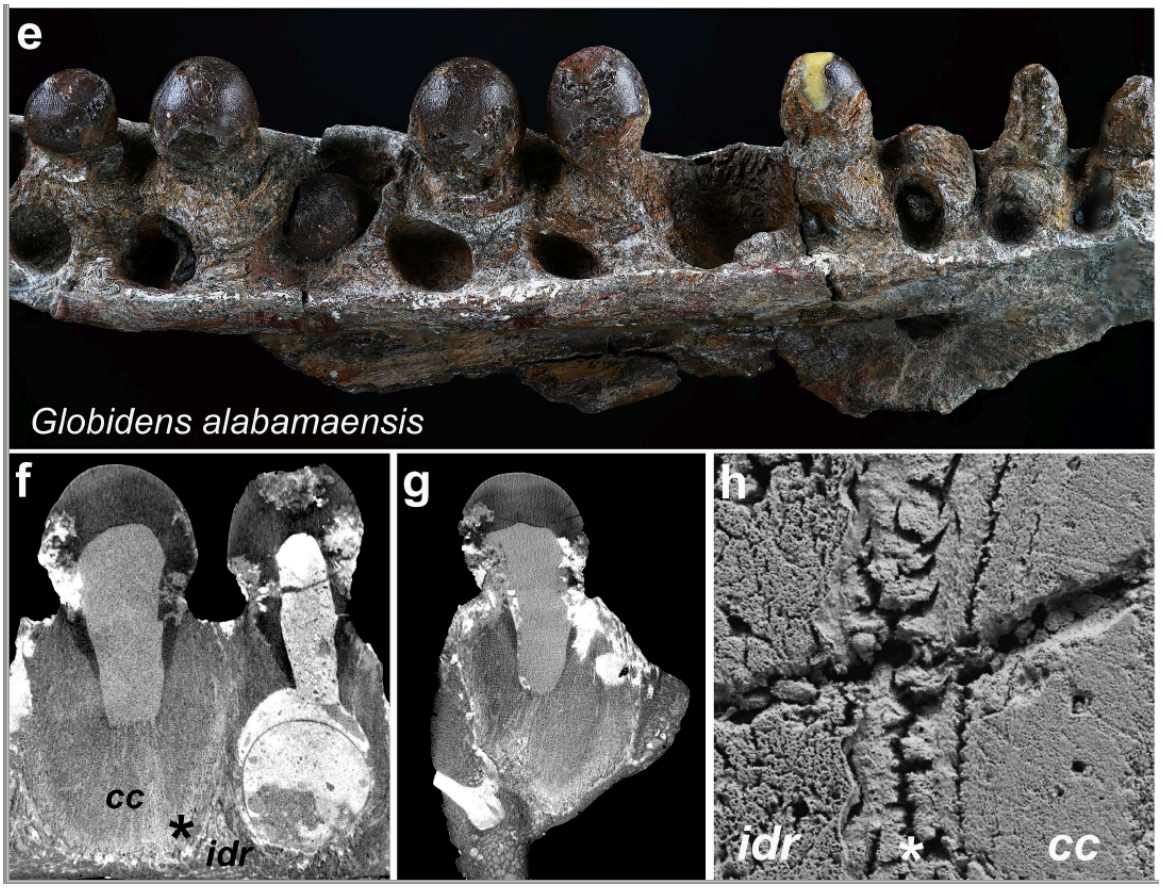

Figure 5 *Globidens alabamaensis* in situ, microCT, and SEM
The globe-shaped teeth are indicative of a hard, tough diet. E) Several missing teeth can be noted, in addition to erupting replacement teeth. F-G) MicroCT images show a broad tooth-bone attachment with an ankylosis of the tooth to the bone through a mineralized periodontal attachment (indicated by the asterisk). The forming crown of the replacement tooth can be noted on the radiograph. H) SEM imaging demonstrates the mineralized nature of the ankylotic periodontal attachment.

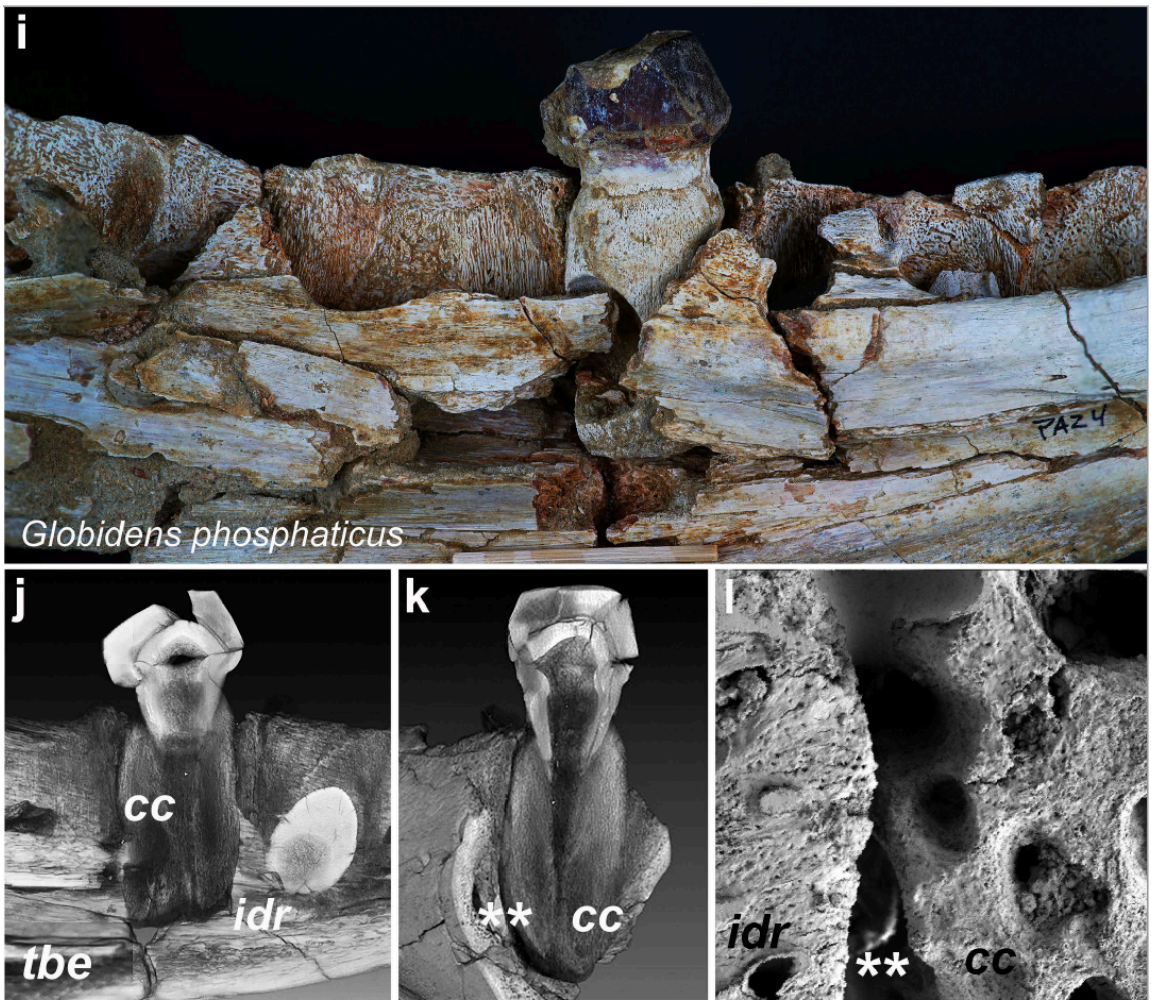

Figure 6 *Globidens phosphaticus* in situ, microCT, and SEM
The lower jaw of the *G. phosphaticus* with a single remaining tooth in the alveolus when the fossil was recovered. I) The remaining molariform tooth has a globe-like shape, indicated a durophagous diet. Severe wear can be observed on the crown apex. No mineralized periodontal attachment noted, in addition to many empty alveoli of teeth that were found in close proximity to the specimen, indicating loss post-mortem. Resorption cavities can be noted on the root surface as part of the eruption pattern of the replacement teeth. J) In the MicroCT images, abundant cellular cementum is seen with less robust dimensions compared to *Clidastes* and *G. alabamaensis*. L) In addition, no mineralized periodontal attachment can be seen in the SEM, indicating the loss of unmineralized periodontal attachment tissues post-mortem.

Table 3 Heterodonty

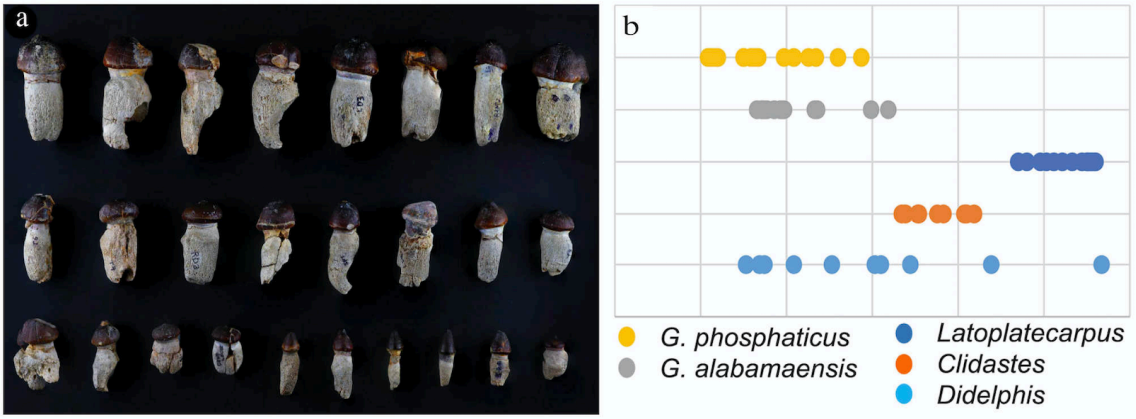

A) The teeth of *Globidens phosphaticus* consist of small pointed anterior teeth along with spherical crushing teeth in the posterior regions. B) The graphical representation of the degree of heterodonty in *G. phosphaticus* compared to other squamates as well as the mammal *Didelphis*. The greater spread in the *G. phosphaticus* (yellow) compares with the true heterodont dentition of the mammal (light blue).

the data points on the graph), due to the presence of the atypical, spherical tooth crowns needed for its durophagous diet. The latest mosasaur in the group, the end of its lineage as it went extinct at the end Mesozoic K-Pg event, was *G. phosphaticus*. This species showed the greatest degree of heterodonty of the mosasaurs examined, but still did not reach the level of the mammal, *D. virginiana*.

Enamel is the hardest substance made in the vertebrate body, composed mainly of hydroxyapatite, the same mineral as bone, but arranged in a highly organized pattern to give it great strength. In general, mammalian enamel is formed of many small subunits, known as prisms. Enamel prisms do occur rarely in reptiles, such as the *Uromastyx* lizard and some extinct sphenodontian relatives of the extant tuatara (Leblanc et al. 2020), but they have not been previously reported in squamates such as the mosasaurs . The prisms overlap in decussations, giving great strength and resistance to fracture. An example of this level of organization, similar in concept to multi-layer plywood, is seen in the SEM image of the mouse (Fig. 7d). The most basal mosasaur in this series, *Clidastes*, shows a low level of enamel organization. Individual enamel crystals can be distinguished, but these crystals cannot be seen to organize into prisms and decussations are not evident. This type of enamel is common in reptiles, and is does not achieve the fracture-resistance of the mammalian prismatic enamel. The next in the phylogenetic series is *G. alabamaensis*, a mosasaur found in North America. This species has durophagous adaptations to the overall tooth shape, and as expected the crystalline organization is more regular, resulting in a tougher, more durable enamel structure. The most derived mosasaur, *G. phosphaticus*, shows high levels of

organization approaching the mammalian level of prismatic structure as seen in the mouse.

Another key feature of enamel is its ability to anisotropically refract light due to its organization into long, slender crystals. The light can travel in one direction faster than in another, resulting in interference patterns as the light exits the material on the thin section. This is known as Michel-Levy Birefringence Interference (Carlton 2011) and results in various ranges of color, the first order colors being a bright rainbow spectrum, and subsequent orders being of more muted coloration. The basal mosasaur *Clidastes* shows very little birefringence, which can be seen in the muted coloration of the thin section (Fig. 7e). This is indicative of a lower level of organization, and a lower degree of material toughness. The durophagous mosasaur *G. alabamaensis* exhibits a much higher degree of birefringence (Fig. 7f), and this feature in the thin-section of *G. phosphaticus* is even more pronounced (Fig. 7g). In addition to the high level of organization shown by the polarized light interference pattern coloration, the crystal bundles of the enamel hydroxyapatite can be seen to diverge in different directions as they leave the surface of the dentin-enamel junction, similar to the pattern of decussation seen in the mammalian sample (Fig. 7h).

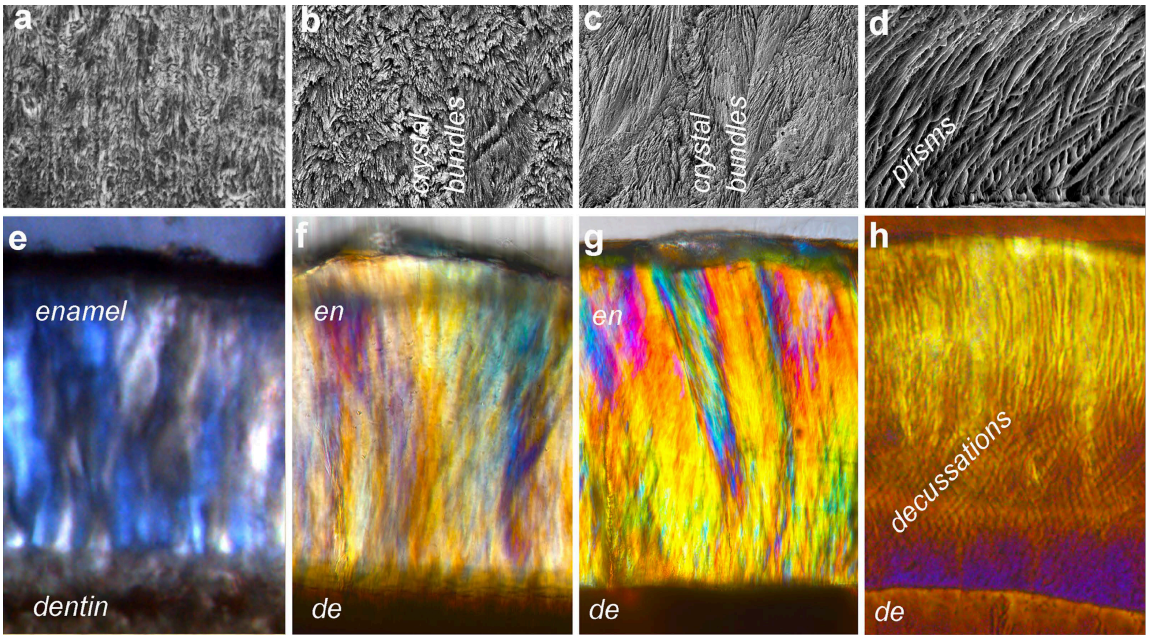

Figure 7 Enamel Structure demonstrated in SEM and light microscopy
Scanning electron microscope (SEM) images of enamel section of three species of reptile (mosasaurs) and one mammal, showing increasing levels of organization through the phylogeny. *A) Clidastes.* This section shows a relatively simple organization of the enamel. Distinct prisms are not visible and the patterns of the individual enamel bundles can be seen. B) *G. alabamaensis.* The bundles of enamel crystals are being organized in to more sophisticated structures. C) *G. phosphaticus.* This durophagous species needed a hard, fracture-resistant covering for the teeth. The enamel crystals are more highly organized, into rudimentary prisms. D) Mouse. Distinct prisms and decussation can be seen giving this enamel great toughness and fracture-resistance. Polarized light microscopy of enamel then sections of selected species. Birefringence is an indicator of high linear structure due to the presence an anisotropic structure, impeding light velocity in certain directions. This results in the emission of a rainbow spectrum of light. E) *Clidastes.* Patterns can be seen, but there is a relative lack of birefringence. F) *G. alabamaensis*. Birefringence is distinct, and overlapping divergent crystals can be seen. G) *G. phosphaticus*. Bright, first-degree interference representing birefringent enamel. Overlapping crystals, decussations, can be seen in the photomicrograph. H) Mouse (wild type). Distinct birefringence and decussations visible.

Analysis of μCT data showed distinct differences between the basal mosasaur *Clidastes* and the durophagous mosasaurs *G. alabamaensis* and *G. phosphaticus*. The most striking feature is the presence of single-pointed teeth in a condition of homodonty, indicating a generalized diet (Fig. 4a). Rather than a pleurodont attachment, consisting of a single lateral connection of the tooth to the underlying bone as seen in extant lepidomorphs such as *Varanus*, the tooth is completely surrounded by bone, a condition known as thecodonty, also seen in crocodilians and mammals. Unlike both crocodilians and mammals, the tooth is completely fused to the surrounding bone in a condition of ankylosis. Some teeth are missing in the specimen shown in the photograph. Although tooth loss can occur as part of the taphonomic processes, the ankylotic nature of the attachment likely precludes this, and the teeth are lost as part of the normal reptilian polyphyodont pattern of lifetime tooth replacement.

MicroCT images show a robust tooth root with dimensions much larger than the tooth crown in both the mesiodistal and buccolingual dimensions (Fig. 4b, 4c). The cellular cementum seen in the image displays a density very similar to that of the surrounding bone. Despite this, a distinct layer can be seen intermediate to the tooth root and the surrounding bone. This difference in mineral density is interpreted as a periodontal ligament that has mineralized as part of the normal maturation process for this species. This intermediate layer can also be demonstrated on the SEM image (Fig. 4d).

The images of *G. alabamaensis* show a distinct globe-shaped tooth crown, a sign of a durophagous diet (Fig. 5e). In addition, the cavities formed by forming and erupting

replacement teeth are clearly visible, including the crown of one replacement tooth, indicating that this mosasaur maintained the typical lepidosaur character of polyphyodonty. Similar to the teeth of *Clidastes*, the μCT of the roots show a broad dimension in comparison to the size of the tooth crown, indicating a robust attachment apparatus consistent with the extreme bite forces expected in this reptile (Fig. 5f-5g). The SEM image confirms the mineralized nature of the periodontal attachment (Fig. 5h). Close approximation of the cellular cementum and bone can be seen with an intervening layer of mineralized structure.

The macrophotograph of *G. phosphaticus* shows similarity of the tooth crown morphology of this species to the previously examined *G. alabamaensis* with globe-shaped crowns, although these are distinctive with a fine-ribbed longitudinal surface feature. A single tooth remains in the bone specimen as it was recovered (Fig. 6i). Many empty alveoli can be seen, which correspond to teeth found nearby, indicated post-mortem loss. These teeth were physically matched to their corresponding sockets in the laboratory, confirming the association. On the microCT images the dimensions of the cellular cementum portion of the root is less robust in relation to the crown dimensions in comparison to both *Clidastes* and *G. alabamaensis*, indicating changes in the physical and mechanical attributes of the tooth attachment process (Fig. 6j-6k). This is confirmed on the SEM image which shows a gap in the attachment between the tooth root and the enveloping bone, indicating loss of unmineralized attachment tissues post mortem.

Much of the change in the evolutionary development of vertebrates occurs in the head and neck region. In fact, it is often difficult or impossible to identify a specimen

without the presence of the head and neck tissues because of the similarity of many post-cranial features in closely related organisms. The opposite case is also true, that it is often possible to identify a species in great detail with the presence of but a single tooth. In addition to the changes noted in the progression of craniofacial characters previously mentioned, it is expected that other less obvious changes were occurring throughout the body. One of these is ectothermy, the ability of the marine reptile to maintain a body temperature higher than the surrounding seawater. The presence of teeth allowed us to conduct isotope analysis on the enamel to determine the body temperature of the mosasaurs in relationship to their surroundings in the late Cretaceous period. Evaluation of the Oxygen isotope levels allowed determination of a mean body temperature of 20.98 C +/- (95% CI 20.48° C to 21.49° C) (Table 4). Calculation of material from elasmobranch sharks from the same location showed a mean body temperature of 18° C. Since these sharks are poikilothermic, this reflects the mean sea temperature in this area at that time. This agrees with data from previous research on sea temperature from inoceramids found in this location, Bentiaba Angola (Strganac et al. 2015).

Table 4 Body Temperature Isotope Analysis

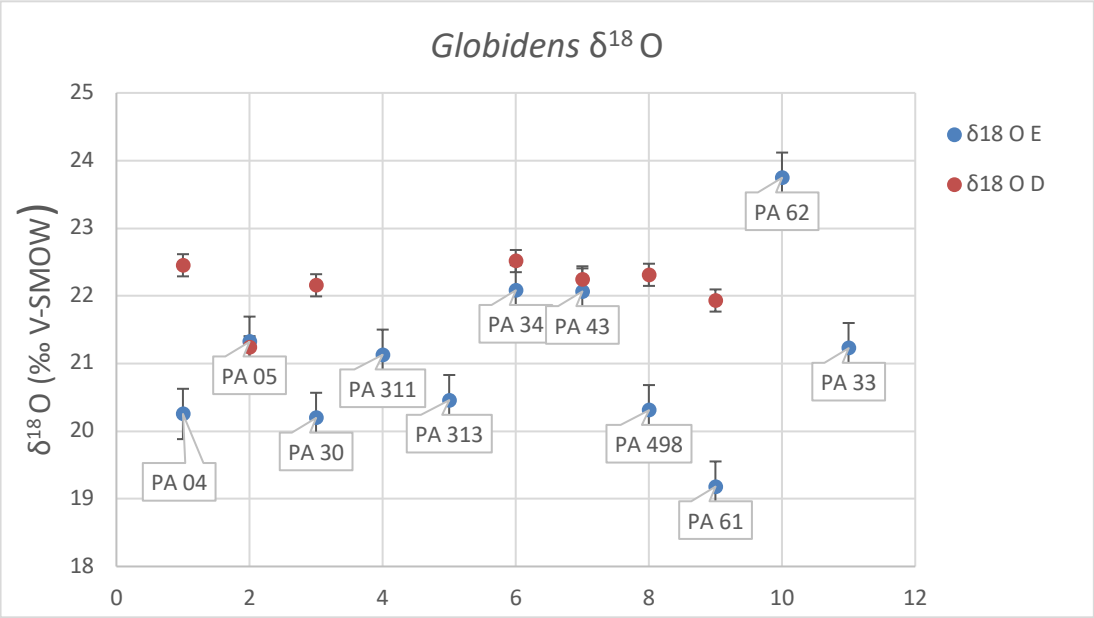

Enamel removed from the surface of *G. phosphaticus* teeth found in Bentiaba, Angola were subjected to Oxygen isotope analysis to determine the body temperature of the specimens. Each of the data points noted above represent individual tooth specimens of *G. phosphaticus*. These measurements indicated a mean body temperature of 20.98 C +/- (95% CI 20.48° C to 21.49° C). This is elevated compared to sea temperatures calculated from a known poikilothermic species, the elasmobranch shark, found at the same location as well as published calculations. This results in an ambient seawater temperature of 18°C, indicating a body temperature elevated in relationship to the environment.

Discussion

The results of our examinations reported above indicate the *Globidens phosphaticus* is not only an interesting marine reptile of the late Cretaceous, but it is also unique among mosasaurs in the acquisition of some very specialized characters. The initial transition from a land-living lizard to a fully aquatic marine reptile living in the open sea is in itself amazing, perhaps rivaled only by the derivation of whales from land living ungulates many millions of years later. The changes in physiology required for ingesting seawater and excreting excess sodium, delivering live offspring in the water, and aquatic breathing/ diving are to be expected for a fully marine species, but perhaps the craniofacial characters discussed here are a little more surprising, and show a remarkable convergence with their mammalian counterparts.

The first indication of the unique nature of the *G. phosphaticus* was the observation of the teeth dissociated from their sockets during the process of taphonomic preservation. This was noted during the initial discovery of the fossilized remains by Michael Polcyn in Angola during the 2009 fieldwork season during the first discovery of this species in this location:

"In the G. phosphaticus specimens described here, nearly all of the marginal dentition was found slightly displaced or separated from their respective sockets, suggesting that the teeth were loosely socketed and periodontal ligaments did not mineralise in life"(Polcyn et al. 2010).

This finding is very unusual as mosasaur remains are usually found with their teeth intact in the jaws, as can be seen in a report of the closely related *G. alabamaensis*

found in Texas (Bell et al. 2012). In addition, the firm boney ankylosis of the mosasaur teeth has been noted on both a gross and histological level (Luan et al. 2009). In that report, the tripartite construction of the periodontal attachment anatomy is described, with the mineralized connection between the cementum and alveolar being described as a mineralized periodontal ligament. This anticipated the homologies between this tissue structure and the mammalian periodontal ligament. This finding in *G. phosphaticus* is then one piece of evidence pointing to a convergent evolution of reptilian and mammalian vertebrates (Fig. 8).

The importance of the sudden appearance of an unmineralized periodontal ligament in *G. phosphaticus* is only significant if a reason for its existence can be determined. Although some evolutionary developments are mere Gouldian spandrels, this tooth attachment apparatus is such a deviation from the type of attachment throughout the lineage, that an evolutionary advantage for its existence is expected. Perhaps the reason for the concentration of evolutionary effects to the craniofacial region is the importance of this area to food acquisition, a strong driving force in evolution. Indeed, our findings support the notion that the tooth attachment was part of an adaptation to an expanding menu of seafood in the productive seas in the late Cretaceous period. Many types of mosasaurs cruised the submarine expanses, consuming fish, squid, and even other mosasaurs. The shellfish on the seafloor had escaped their predation with their development of a rock-hard shell. These shellfish

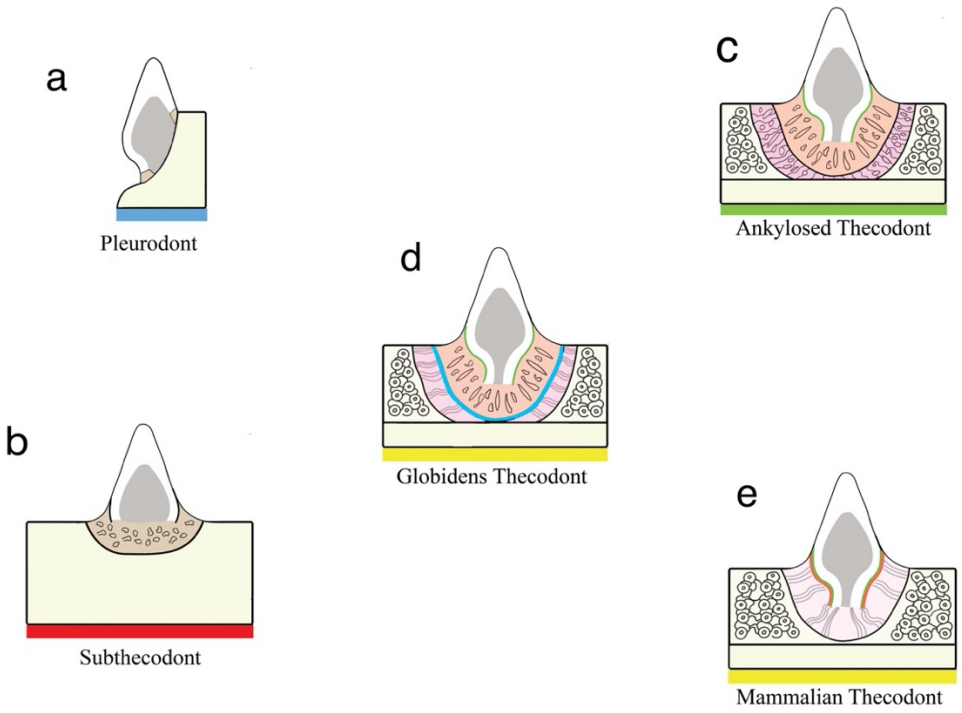

Figure 8 Attachment schematic
Modes of attachment of teeth in vertebrates. A) Pleurodont attachment is a connection of the tooth to the medial surface of the tooth-bearing bone. An example of this is the monitor lizard *Varanus niloticus*. B) Subthecodont. C) Ankylosed thecodont- seen in this paper in the case of *G. alabamaensis*. D) *Globidens* thecodont- an unmineralized connection exists between the cementum and the bone. Example: *G. phosphaticus*. E) Mammalian thecodont- The tooth sits in a boney socket separated from the bone by an unmineralized periodontal ligament. Examples: *Didelphis virginiana, Mus, Homo*.

went from protected to prey when the durophagous mosasaurs arrived on the scene. Our evidence points to increasing bite force which is interpreted to mean increased necessity for the crushing and consumption of hard-shelled mollusks (Table 2). Also noted is the presence of severe wear on the contacting surfaces of the upper and lower tooth, especially the molariform teeth in the posterior jaw where the crushing forces would be the greatest. Combined with this is the precise fit of the upper and lower worn tooth surfaces, which in mammalian species is an indication of extensive oral processing of food prior to ingestion, which is how this evidence interpreted in this reptile.

The posterior teeth most involved in the heavy crushing and oral processing of food are designed exquisitely for this task. The mid-jaw teeth are larger in all dimensions with a distinctive globe-shaped pattern, even more globe-shaped and robust in *G. phosphaticus* than in less derived *G. alabamaensis*. The anterior teeth, which were not able to develop crushing forces, are smaller and flame-shaped. Ideal for scooping mollusks out of the seafloor sand, but not for breaking the shells (Table 4). While such patterns are common, almost standard for mammals, such specialization for form is unusual in reptiles, and in the case of the mosasaur lineage is seen only in the most advanced, most derived species, which have a degree of heterodonty approached but not quite equaling the mammalian condition.

As the *G. phosphaticus* developed the capacity for heavy crushing forces, it is likely that these crushing forces were too great in magnitude for the common, thin enamel of the reptilian lineage. For these feeding strategies to be successful, strong

tough enamel, i.e., mammalian pattern enamel, would be needed. The enamel patterns of reptiles are well known. The enamel was examined from the *Varanus,* an extant lizard, and found the typical parallel crystal, non-prismatic enamel (data not reported) that is described in the literature. With increasing levels of bite force, the organization level of the enamel increased, reaching its peak with the *G. phosphaticus* (Fig. 7). Although the microstructure was not identical to mammalian enamel, it shared many of the characteristics that make it so strong. Despite the alterations noted on the SEM and histological level, which is presumed to have made it stronger, severe crown wear was noted on the teeth most subject to the most intense occlusal forces.

Many semi-aquatic reptiles, such as the alligator, and ambush predators rather than active hunters. This mode of food acquisition conserves energy by limiting unnecessary movement. It is likely that the earliest members of the mosasaur lineage conserved their method of prey capture. By the time that the *G. phosphaticus* came into the undersea world, this had changed to a process of constant food searching as they combed the sea floor looking for the inoceramids. The small size of each oyster and the energy expending in crushing each shell for a small morsel of food required a highly active lifestyle. As a fully marine organism, the only way to achieve this is by the development of internal heat. Our evidence indeed points to this, and the results of the enamel isotope analysis which demonstrate this ectothermy, agree with other reported results on closely related species, giving us further insight into the lifestyle of the *G. phosphaticus.*

It is obvious that the diet of terrestrial reptiles is affected by their stage of life. Reptiles must eat soon after hatching, and their small size limits their prey to small-bodied organisms, often insects or other small invertebrates. For this reason, the oral apparatus does not require great strength at the early stage of life. Most genera of lizards are polyphyodont, producing many generations of teeth over their lifetime, each succeeding generation slightly larger than the previous version to accommodate the ever-increasing jaw size until the full adult body size is accomplished. The generations of teeth often develop slight changes in morphology with succeeding generations to accommodate the changing diet of the reptile. Even durophagous species will develop changes throughout ontogeny, with the juvenile forms being more similar to the generalized reptile dental morphology rather than the specialized durophagous tooth shapes. Based on findings in *G. alabamaensis* (Polcyn and Bell 2005), it is expected that the closely-related, fully-marine squamates had similar ontogenic changes in dental morphology as they approached adulthood and began an adult diet. This is not possible to confirm at this time, but it is a topic for further investigation as more fossil remains are recovered, especially neonatal or young juvenile specimens.

Conclusion

Although the possibility of the unmineralized periodontal ligament was realized by Polcyn upon discovery of the *G. phosphaticus* in Angola, the importance of this fact finding is fully appreciated only in the context of the other mammal convergent characters in this unique mosasaur (Table 5). In this study the analysis of several craniofacial tissues was used to demonstrate a group of mammal-like characters that evolved in the mosasaurine lineage over a short period of time culminating in the what is seen in one of the last surviving members of the line, *G. phosphaticus*.

Table 5 Mammal-like characters

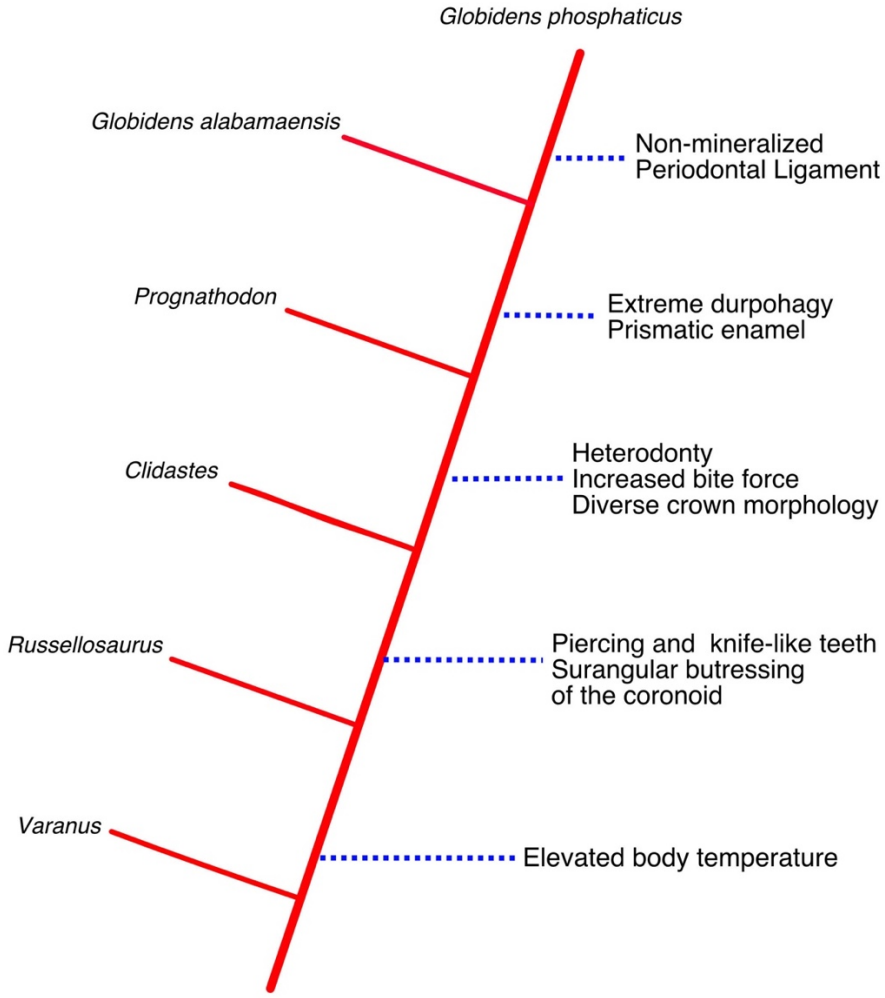

The progressive addition of mammal-like characters appearing in the mosasaur lineage.

CHAPTER III

DEVELOPMENT OF THE PERIODONTAL LIGAMENT: THE EFFECTS OF ENVIRONMENTAL FORCES ON THE TOOTH ATTACHMENT TISSUES

Overview

The periodontal ligament is an intermediary tissue between the tooth and jawbone, and as such receives a great deal of physical force during the process of biting and mastication. Different biting and chewing forces will interact with the biochemical processes in the alveolar bone, periodontal ligament, and the cementum. Over time, these forces will create and evolutionary drift resulting in distinct morphologies in different clades.

Synopsis

Bone, as the primary supporting skeletal tissue of the vertebrate body, is responsible for preventing collapse of the organism in the presence of Earth's gravity. Fully aquatic organisms, such as the Chondrichthyes, or cartilaginous sharks, survive without bone due to the buoyancy of the surrounding water, but this would be difficult in terrestrial animals with a need for overland locomotion, especially as they increase in body mass. Another major stress inducing force is located in the vertebrate craniofacial region where strong muscles connect the jaws to and anchor in the skull. Here our observations of *Globidens phosphaticus* are continued, looking at the specializations in bone and tooth-supporting tissues needed for oral food processing, and relate these

features to other species, *Iguana iguana*, *Varanus niloticus*, *Didelphis virginiana*, mouse, and human. With the use of μCT, ground thin-section histology, conventional H&E histology, and transgenic mouse models, an attempt is made to unravel the complex biochemical processes involved in the development of the mammalian periodontal ligament. The first evolutionary appearance of the PDL occurs in close proximity to the craniofacial sutures, and appears to adopt the sutures' cells and mechanisms for a similar purpose, only with a bone-tooth interface rather than a bone-bone interface. Evidence is shown that this is, in part, related to the spatial and temporal expression of the Wnt/β-catenin system, and that morphologic changes to the tooth-bearing tissues are dependent on force induced changes to conserved biomolecular systems.

Introduction

The modeling and evolution of the vertebrate skeleton is the result of mineralized supporting structures developing in the milieu of externally applied forces. The ability of bone tissues to develop along lines of physical stress has long been understood, and it is known as Wolff's Law (Frost 1994). The mechanotransduction of bone supporting cells, i.e., osteoblasts, osteoclasts, osteocytes, can result in physical adaptations to the bone architecture resulting in a better ability to resist deformation under stress. The first vertebrates were aquatic, and the first vertebrate skeleton were primarily adapted to resist the strong muscular forces developed during lateral flexion during swimming motions, in fact the notochord of pre-vertebrates actually was a functional precursor to

the later vertebral column. As animals moved from water to land, the functional demands of the skeleton changed as a result of gravitational forces acting on the body. This placed strong demands on the axial skeleton, which was required to support the weight of the organism during locomotion. An additional requirement was placed upon the skeleton of mammals as they developed a requirement for extensive oral processing of food. The development of specialized teeth in mammals has long been recognized, and their heterodonty is in fact a key defining character. It is key to note that these specialized teeth would be unable to accomplish their purpose without a simultaneous parallel development of the mammalian jaw to support the increased, sustained and repeated forces applied during mastication (Schneiderman 1978).

The skeleton cannot be completely rigid, or the animal would be unable to move. Various types of joints are present to allow mobility, but they are also critical to dissipating force applied to the skeleton in order to prevent overload damage, including fracture. Various types of joints are present throughout the vertebral and axial skeleton, but in the craniofacial region these are limited to one moveable joint consisting of the jaw articulation, and many fibrous joints consisting of sutures as well as the gomphoses of the periodontium. The jaw articulation in reptiles consist of a synovial joint between the quadrate bone on the skull and the articular on the mandible. The reptilian jaw consists of 5-6 separate bones joined by fibrous sutures. Although the teeth are rigidly held in place by a mineralized attachment in a process of ankylosis, the forces generated on the teeth can be adequately dissipated through the mandibular sutures to prevent osseous overload.

The quadrate-articular joint is placed far back on the head, and in this position in encroaches on the further evolutionary development of brain expansion, hearing apparatus, and masticatory ability which is found in the appearance of mammals. To accomplish these evolutionary processes, the posterior reptilian jaw bones over time become separated from the chewing apparatus and repurposed into the hearing apparatus of mammals. Once this has occurred, mammals are left with a single dentary bone in the mandible, i.e., no fibrous sutures for force dissipation. The mammals have solved this problem with the maintenance of a non-mineralized tooth attachment joint, the gomphosis also known as the periodontal ligament (PDL). The PDL is thought to be capable of absorbing mechanical shock and dissipating the strong forces generated during occlusion (Noble 1969) as well as allowing for tooth movement to maintain precise, post-eruption occlusal relationships between the upper and lower jaws (Osborn 1984). In fact, the PDL and cementum are plesiomorphic for all Amniota (Leblanc and Reisz 2013). Although this structure appears briefly in the early developmental stages of reptiles, it does not persist; it rapidly mineralizes to form an ankylosis. Often the boundaries between tooth and bone become blurred, resulting in a homogenous mineralized tissue (Jenkins and Shaw 2020). Thus, the persistence of the non-mineralized tooth attachment can be considered a neotenic feature in mammals (Leblanc et al. 2017b).

Because reptiles are generally polyphyodont, they are in a constant state of tooth development, eruption and maturation. After the tooth forms an ankylosis with the jawbone, the PDL which was essential for eruption, all but disappears. Osteoclastic

resorption, which is part of bone remodeling, is detrimental to the long-term integrity of the tooth root surface as it slowly gets remodeled and replaced by bone. This is not a problem for the reptiles which are constantly replacing teeth, but could be detrimental to mammals. Because mammals are generally diphyodont and have at most two sets of teeth, the teeth erupt in the juvenile and then remain in place throughout maturation and adulthood. For mammals, it is essential that the tooth root is insulated from the remodeling at the bone mineralization front. The failure of tooth attachment to mineralize as well as the maintenance of the unmineralized state after initial eruption is under the control of several genes which allow the PDL to remain in the juvenile condition.

Much of the development of the craniofacial structures is under the control of genes known as Wnt. Originally discovered as the *wingless* gene in *Drosophila*, is was later appreciated that 19 varieties exist in mammals. Heavily involved in the development of polarity, the Wnt gene, as part of the Wnt/β-catenin system, control the transcription of a downstream gene Runx2, which controls the mineralization of the tooth attachment apparatus by inhibiting the transformation of undifferentiated mesenchymal cells in PDL into osteoblasts. In addition, the Wnt system is involved in the control of another gene Twist1, which has been shown to prevent mineralization in the PDL in humans (Komaki et al. 2007).

The purpose of this study was to examine terrestrial reptiles, secondarily aquatic reptiles, and mammals to consider to determine the origin of the unmineralized

periodontal ligament as the forces of mastication were increased due to the need for extensive oral food processing.

Experimental Procedure

Computed Tomography

Paleontological and extant specimens were scanned at the University of Texas High Resolution X-ray Computed Tomography Facility. Data was processed for visualization and analysis using ImageJ (NIH, Bethesda, MD) and Imaris 9.0 (Oxford Instruments, Concord, MA).

MicroCT

After fixing in 4% paraformaldehyde for 24 hours, μCT imaging was performed at Texas A&M University College of Dentistry on the μCT-35 system (Scanco Medical; Voltage = 70 kV, high resolution 7.0 μm). The files were converted from .ISO to TIF using ImageJ (NIH, Bethesda, MD). For 3D reconstruction and quantification, we used Imaris (Oxford Instruments, Concord, MA).

Light microscopy

Specimens were dried in warm air and embedded in Technovit 7200 VLC acrylic resin (EXACT Technologies, Oklahoma City, OK) under a vacuum, which was then polymerized at room temperature and pressure. Blocks were sawn with a diamond bandsaw and then cemented to glass slides. Samples were ground to 80μm and polished to 1200 grit using the previously described method (Luan et al. 2009). Specimens were examined under brightfield and polarized light, then photographed using either a Zeiss

Axiomat microscope (Carl Zeiss AG, Oberkochen, Germany) or a Meiji EMS-7 (Meiji Techno, Saitama, Japan) with an Infinity1 camera (Teledyne Lumenera, Ottawa, ON).

SEM

Specimens were embedded in acrylic resin (Technovit) under vacuum, and then polished to 1200 grit. Specimens were etched in EDTA for 30 minutes, rinsed with deionized water for thirty minutes, then allowed to dry overnight. Sputter-coating was performed with gold-palladium for 2 minutes, and specimens were imaged at the SEM facility at Texas A&M University College of Dentistry.

Mice

All protocols for the experimental use of mice were approved by the Institutional Animal Use and Care Committee (IUCAC) of Texas A&M University College of Dentistry protocol number 17-0103. Gli1-Cre^{ERT2} (JAX#007913) and Ai14 tdTomato reporter (JAX#007908) were purchased from the Jackson Laboratories. *Ctnnb1$^{fl(ex3)}$* (Harada et al. 1999) were housed Texas A&M College of Dentistry. For all *in vivo* studies, sex and age matched mice from the same litters were used. No significant differences were noted between male and female mice. All mice used were adults, 5-8 weeks of age.

Tamoxifen Administration

Tamoxifen was diluted in corn oil at a concentration of 20mg/ml and frozen at -20C until needed. This solution was injected intraperitoneally for two consecutive days for induction. The dosage used was 1.5mg/10g based on body weight.

Tissue Clearing

The PEGASOS Method was used for tissue clearing as previously described (Jing et al. 2018). Briefly, the mice were perfused and mandibles were dissected free and fixed in 4% PFA. The mandibles were then decalcified in 10% EDTA at 37°C for seven days. Decolorization was completed with 25% Quadrol (Sigma-Aldrich 122262) at 37°C for 2 days. Delipidation was then carried out in a graded series of tert-butanol aqueous solutions (Sigma-Aldrich 360538), and dehydration was carried out with tB-PEG solution composed of tert-butanol, PEGMMA500 (Sigma-Aldrich 409529) and Quadrol. For final tissue clearing, samples were placed in a BB-PEG solution containing 72% benzyl benzoate (Sigma-Aldrich 409529), PEGMMA500 and Quadrol. Three-dimensional imaging was performed using a Zeiss LSM780 2-photon microscope (Carl Zeiss AB, Oberkochen, Germany). Three-dimensional image reconstruction was performed with Imaris 9.0 (Oxford Instruments, Concord, MA).

Results

The considerable oral occlusal forces required for the extensive mastication of hard foods is the driving force for much of the dentofacial evolution in the appearance of the mammalian form. These types of forces, developed as the mosasaur *G. phosophaticus* moved into a new environment to exploit hard-shelled prey, are reflected in the morphology of the teeth. The amount of heterodonty, discussed in the previous chapter, can be seen in looking over the diversity of tooth shapes from a single

Figure 9 Occluding teeth on *Globidens phosphaticus.*
The teeth of *Globidens phosphaticus* showed definite signs of occlusal wear from repeated, heavy grinding forces. A) The upper and lower teeth have been digitally approximated to show the complimentary nature of the wear on mating surfaces. When these surfaces were brought together in the laboratory, it could be seen that the surfaces matched exactly. As can be seen in the macrophotograph, the wear pattern shows attrition due to not only to crushing impact in a vertical direction, but also to various non-axial movements with an abrasive substrate, consistent with the sandy consistency of the geologic conditions in the Bentiaba region in the late Maastrichtian Stage when the mosasaur fed on mollusks on the ocean floor. B) The wear was not evenly distributed on all teeth. Teeth with severe wear could be identified, and their positions in the upper and lower jaws identified. The wear patterns could be matched to the wear patterns of their corresponding tooth in the opposite jaw in all cases. The teeth with the greatest amount of occlusal wear occurred in the mid-arch region wear occlusal forces would be the largest. These teeth were also determined to be of larger size than the more anterior and posterior teeth in the same arch as seen in the photo.

individual (Fig. 9). In addition to the large, bulbous, crushing tooth crowns, a large, anchoring tooth root is evident. These roots are supported on all sides, i.e., thecodont, greatly increasing the amount of tooth attachment tissues present for support of the tooth during non-axial loading compared with the partial perimeter attachments such as acrodont, pleurodont and sub-thecodont found in other reptiles. In this photo, a large amount of wear can be seen on the tooth crowns. The wear on these teeth is due to the abrasive, sandy ocean floor substrate that was present in the area where feeding took place. This degree is not evident in teeth from the same species taken from non-sandy locations such as the Kem-Kem beds of Morocco. Nevertheless, these wear patterns indicated repeated occlusal patterns indicative of extensive oral processing of food, not only axial crushing. The wear patterns on upper and lower complimentary teeth show precisely fitting patterns. When these teeth are hand-articulated in the lab, the fit is exact. While not indicative of mammalian-type occlusion, there is evidence for non-axial movements, i.e., chewing of food. The most severe tooth crown wear was evident in the mid-arch region, where it is expected the forces and repetition would be the greatest.

The greater occlusal forces present in *G. phosphaticus* required a method of force distribution to prevent damage to the tooth and jaw tissue. The large root surface area previously mentioned was one such method. This root enlargement had been a method for coping with ever-increasing forces up through the mosasaurian lineage. In addition, the tooth roots were a honeycomb of cemental trabeculae, brittle in the fossil specimen, but in life were likely very pliable allowing a certain degree of flexibility (Fig. 10). These perforating channels ran lengthwise through the root, and contained cells,

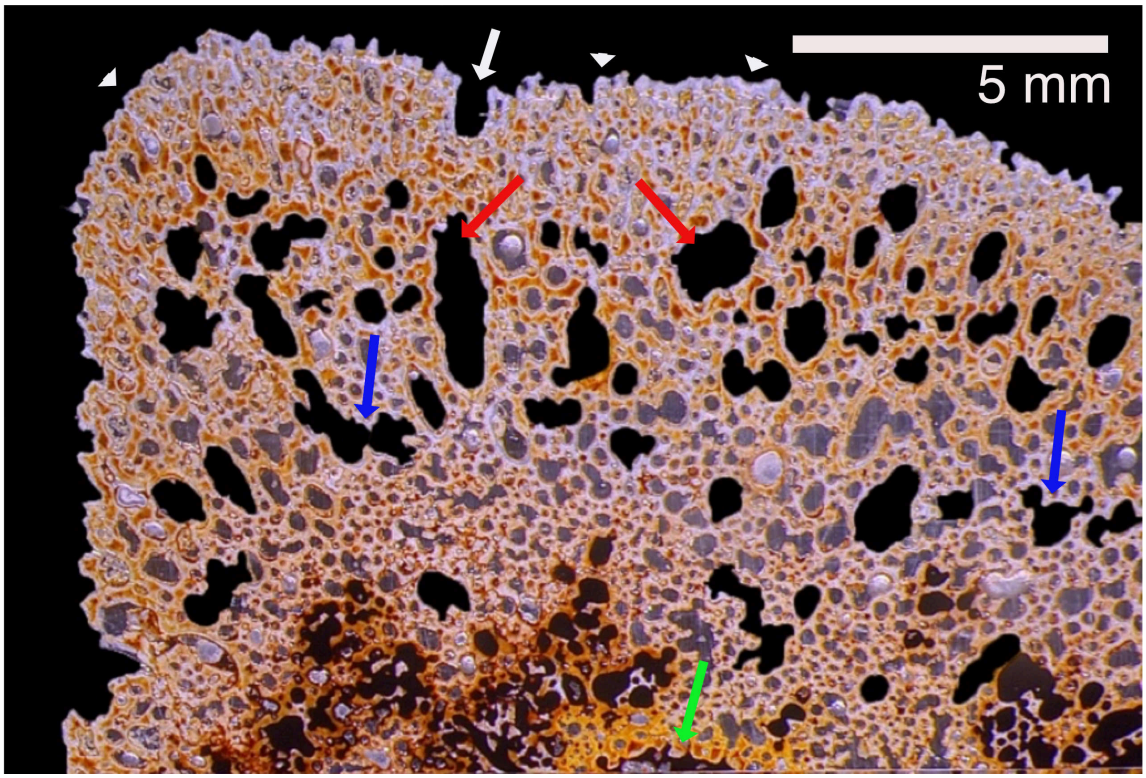

Figure 10 *Globidens phosphaticus* root in thin section
The roots of the *Globidens phosphaticus* teeth are perforated by longitudinal holes throughout their length. The porosity of the tooth roots is generally on the same scale as the porosity of the adjacent bone. A large central chamber is present in the center of each root, corresponding to the root canal in mammalian teeth (green arrow). Many of the longitudinal canals are large, often exceeding several millimeters in diameter (red arrows). There is evidence of the canals enlarging and coalescing after root formation (blue arrows). The outer surface does not show evidence of ankylosis to the alveolar bone as commonly seen in closely related mosasaurs. Instead there is a thin layer of a distinct mineralized tissue, which appears clear and glass-like on thin ground sections (white arrowheads) the exact homologies to mammalian mineralized tissues are unclear. Vessels from the surrounding periodontal ligament soft tissue are often seen invading the hard tissue of the tooth root surface (white arrow).

connective tissue, nerves and blood vessels when the mosasaur was alive. The exact proportions of these contents have yet to be determined, since there are no exact homologies to extant organisms. Some branching patterns reminiscent of blood vessel patterns can be seen in some of the larger channels, and channels can be seen entering from the periodontal ligament space. The central channel appears homologous to the root canal of mammals, and likely carried a combination of tissue types.

The distinct feature of the *G. phosphaticus* root that is not seen in less derived mosasaurs is the undulating outer surface that is not ankylosed to the enveloping bone. On a macro scale, there are impressions appearing to be blood vessels that are present along its surface, indicating a highly vascular soft-tissue membrane covering the root surface. As we examine this surface at higher magnification, another modification is the presence of a thin, 100-300 μm vitreous outer layer. This layer is not present in the less derived mosasaurs (Fig. 10). In all other mosasaurs, the outer tooth root layer is fused to the surrounding bone. In some cases, an intermediate mineralized tissue can be seen, representing the remnants of a vestigial periodontal ligament that has become mineralized (Luan et al. 2009). Bridges of mineralization can be seen passing from the tooth to the bone through this layer (Fig. 11). In these mosasaurs, once the PDL ossified, the connection would become less flexible, and less able to absorb shock from high levels of force. In general, the porosity of mosasaur tooth root approximates the porosity of the surrounding bone, giving these two tissues similar mechanical properties in force transfer. Any Sharpey's fibers present during the developmental process have become

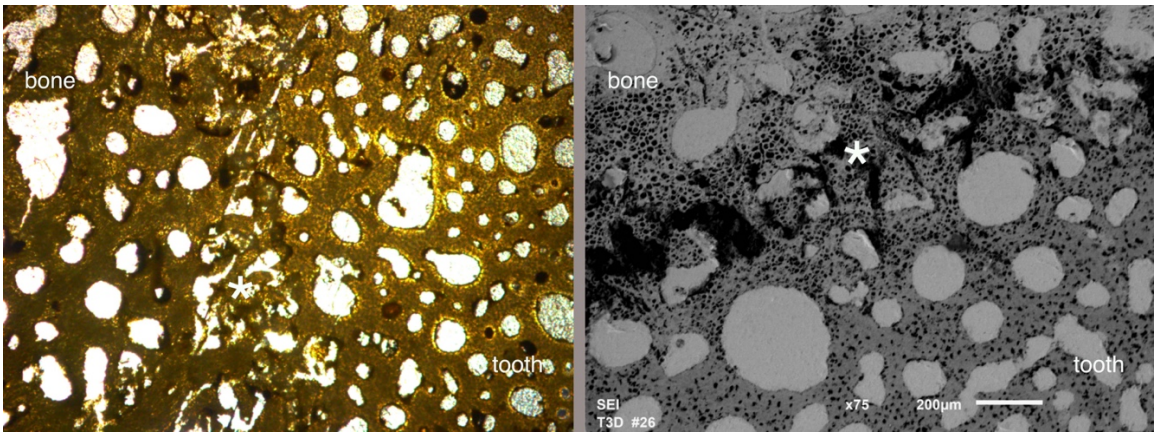

Figure 11 Clidastes root and bone
The tooth root and the enveloping bone are intimately connected in the mosasaurs as seen in this specimen of *Clidastes* sp. (Left panel) A thin section viewed with brightfield microscopy shows a tight connection between the tooth and bone. An indistinct intermediate layer can be seen (marked with and asterisk), and it appears to be of a similar mineral density to the adjacent tissue. Note that the degree of porosity of both tissues appear similar. (Right panel) SEM also demonstrates a tight connection of the root and bone with bridges of mineralization crossing between the two.

incorporated into the bone structure and are no longer evident and distinguishable structures. As the periodontal connection matures, bone remodeling can obliterate any evidence of the PDL. Through the process of ankylosis, the bone takes of the periodontal space, with bone actually invading the cementum and remodeling the cementum into a mixed tissue (Fig. 12). This bone-cementum fusion can be clearly seen in *G. alabamaensis* using polarized light microscopy, which readily distinguishes bone from cementum through the differences in optical properties of the two tissues. Although the mineral phase of bone tissues is composed of hydroxyapatite, the differences in the non-mineral phases create an optically anisotropic condition, resulting in different colors through refraction.

The condition is quite different in the derived mosasaur *G. phosophaticus*, in which no ankylosis is present, even in specimens from mature animals. In these animals, there is no intervening mineralization in the PDL space. Although the space is now empty through taphonomic processes, in life it would have filled with a periodontal soft tissue; the exact nature of this tissue is at present impossible to determine, but likely similar to mammalian PDL in structure as well as function. Like other mosasaurs, the porosity of the root is similar to the bone, and at high magnification, the vitreous outer layer of tertiary cementum can be seen to be generally devoid of vascular channels, unlike the great bulk of the cementum. Exceptions occur, and small channels can be seen passing through this layer without branching (Fig. 12e). These appear to be channels for blood vessels passing from the PDL to the tooth. Such small vessels also be seen in mammalian (and even human) enamel, which is for the most part avascular. The nature

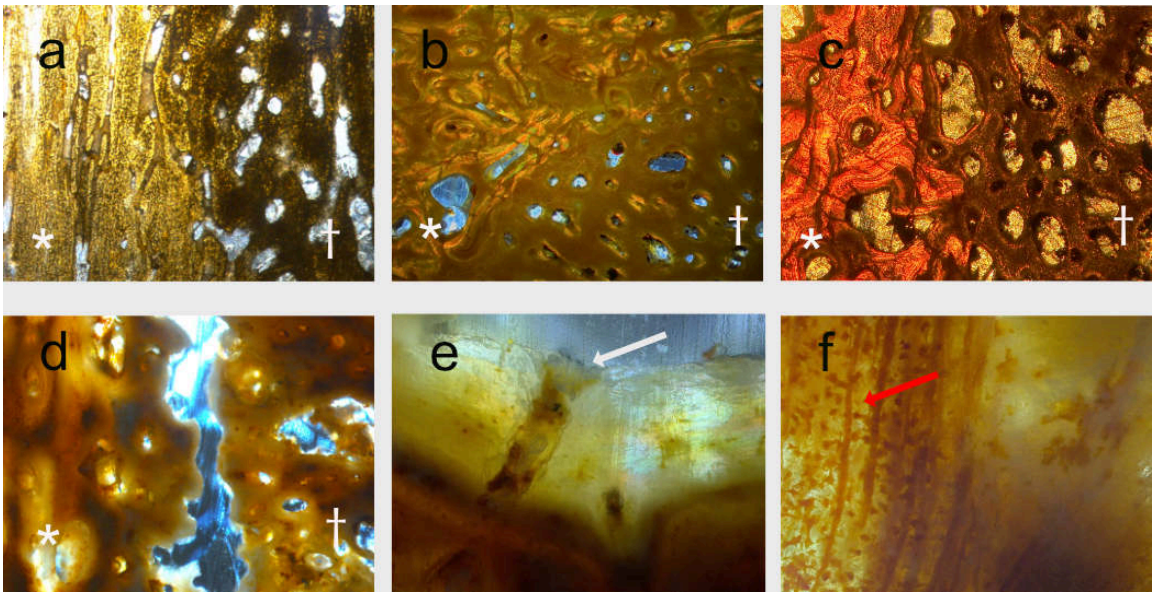

Figure 12 Attachment types in derived mosasaurs.
The images show features of the tooth attachment tissues of mosasaurs with thin-section, polarized light microscopy. The top row is A) *Prognathodon* sp. and B-C) *G. alabamaensis,* and the lower row is *G. phosphaticus*. The (*) denotes the bone portion of the specimen, and the (†) indicates the tooth root. A) The bone/root junction is fully mineralized and becomes indistinct as the two tissues come into contact. B) Bone cells and cementum cells can be distinguished by their polarized light properties due differences in the anisotropy of the mineral and organic portions of the materials. C) Bone cells can be seen within the cementum and vice versa. D) In *G. phosphaticus*, there is no intervening tissue between the tooth root and bone. Although soft tissue was present in this space during the life of the mosasaur, it has not survived the taphonomic processes and appears as an empty space on histologic thin sections. E) the outer vitreous layer, the tertiary cementum, appears clear in light microscopy. It is readily distinguished from the underlying cellular/vascular cementum, and appears to be devoid of cells and vessels. Some vessels do occur (white arrow), but the merely pass through this thin layer without branching, similar to accessory canals penetrating cementum in human teeth. The channels of the roots run longitudinally, have many parallel runs, and areas connected to rows of lacunae (red arrow) within the cementum by many fine branches, shown in this rehydrated sample.

of the longitudinal channels can be deduced from analysis of rehydrated samples viewed with transmitted light at low magnification with a stereomicroscope. The channels can be seen to pass from the coronal to the root apical direction with few branches. Very fine channels connect to long chains of lacunae which are evenly spaced along the channel. Assuming homology to mammalian tissues, the longitudinal structures contained blood vessels and the lacunae were home to cellular components.

Vessels within the root range from small, less than 100 μm, to rather large, approximating 1,000 μm (Fig. 13). The majority of longitudinal channels are in the small range, but the thickness of the cemental wall, i.e., the distance between adjacent channels remains remarkably consistent at about 200 μm, giving an appearance similar to trabecular bone. When viewed with SEM, the distinct impressions of blood vessels on the outer tertiary cementum layer are evident. When viewed at higher magnification with SEM, the wavy surface is evident. When etched with a weak solution of EDTA, this outer layer is more resistant to etching and appears to have a higher mineral content than the bulk of the cementum in the root (Fig. 14). The optical properties when viewed with light microscopy would also support that this is a highly organized mineral layer (Fig. 15). The anisotropic properties of this material give it a level of birefringence suggestive of a highly organized crystalline structure. This tertiary cementum layer would have precipitated from the PDL during life, although the biochemical processes leading to its formation are unclear. Thin bands of a similar appearing mineral structure occur around some of the blood vessels. These are sometimes seen around blood vessels in mammalian bone (Weinmann and Sicher 1955). Sharpey's fibers can be seen to be

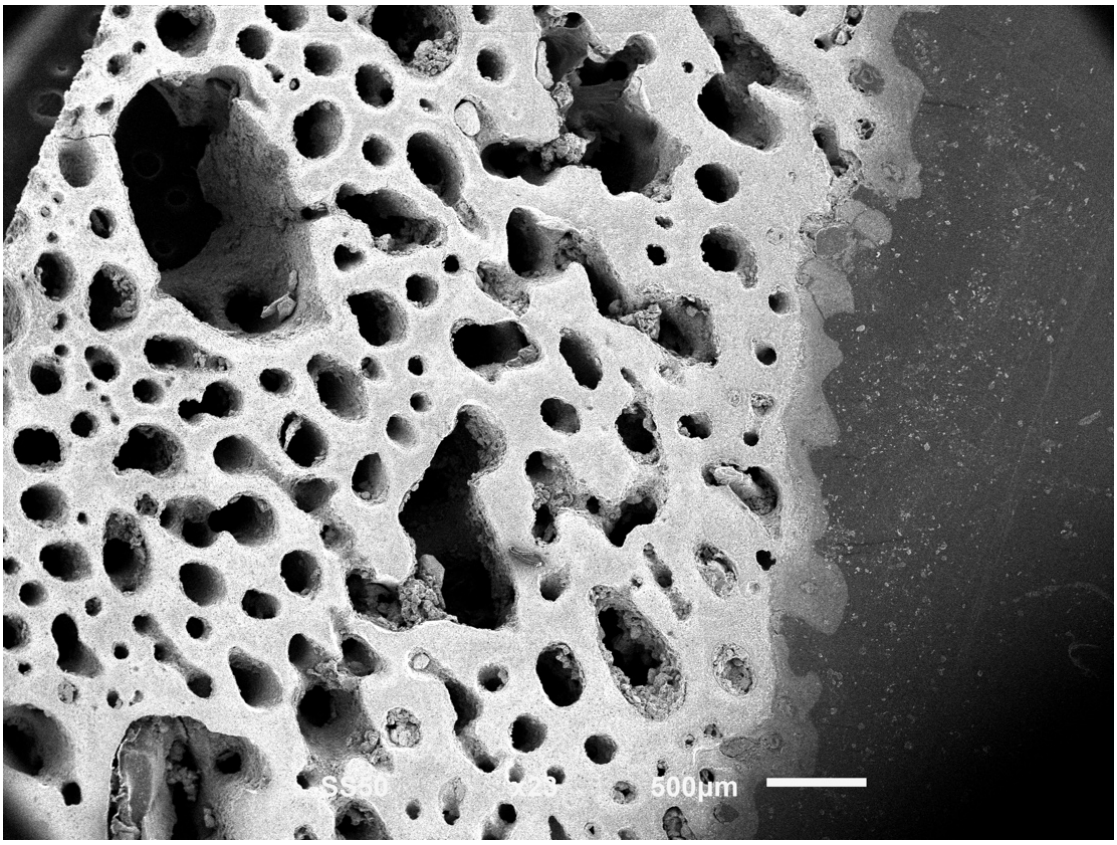

Figure 13 The root of *G. phosphaticus*
A coronal section of the tooth. Note the abundant vascular/cellular channels throughout the cementum layers. A mineralized layer is seen on the exterior surface of the root, which varies in appearance from the bulk of the root structure (white arrow). This layer would have been in contact with the periodontal ligament in life. Although vessels can be seen crossing the thin, outer layer (white arrowhead), this layer is for the most part avascular and acellular.

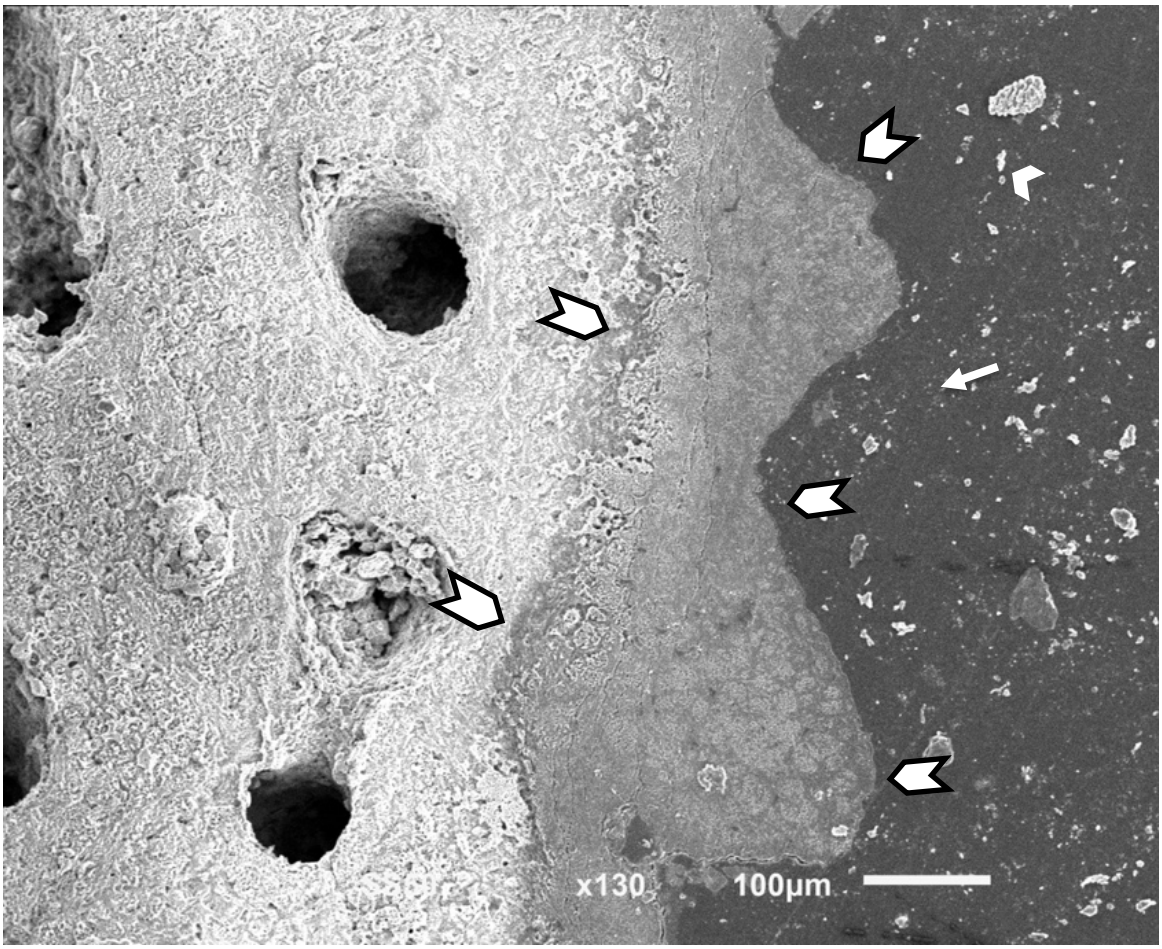

Figure 14 The outer layer of *G. phosphaticus* root
An SEM image of a cross section of the root of *G. phosphaticus*. The porosity of the cellular/vascular portion of the root is clearly seen on the left side of the image with numerous pores visible, each of approximately 100 µm in diameter. The white arrowheads delineate an outer layer that is not visible on the other species of mosasaur, nor on other reptile tooth roots. This layer is generally acellular and avascular, although small vessels do penetrate its surface. This section has been etched prior to imaging, and this layer of tertiary cementum appears to be more resistant to etching than the underlying cellular/vascular cementum. This layer has formed between the non-mineralized periodontal ligament and the underlying cementum.

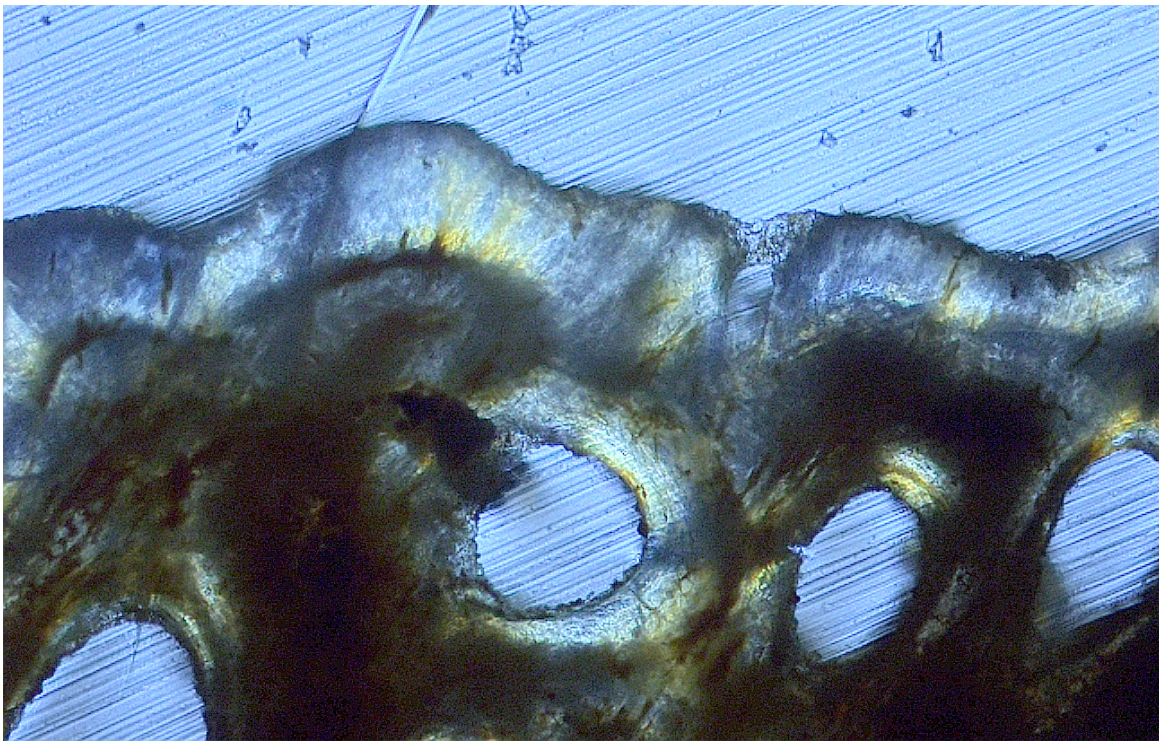

Figure 15 The *Globidens phosphaticus* root
Note that the outer layer of the root surface is avascular. This thin layer, approximately 100-300 μm thick, appears glass-like in light microscopic section. It is clearly distinguishable from the underlying cellular/vascular cementum. The organic content of the underlying cementum is not seen, with the exception of small tufts of intrusion. A similar appearing layer is present around some of the channels in the interior of the root, presumably around what were blood vessels in the tooth root during life.

crossing the tertiary cementum layer, indicating that the fibers were present first and the mineralization occurred around them, entombing them within it.

In mammals, the PDL is a thin, non-mineralized membrane the separates the alveolar bone from the tooth root. At both the inside and outside surfaces of the PDL there are mineralization fronts, while the central portion of this membrane is inhibited from mineralization. On the interior surface, the cementoblasts slowly add to the hard surface of the tooth, while on the external surface bone is added through a process of apposition. The same process is seen occurring in the reptile *G. phosphaticus* (Fig. 16). Although the collagen fibers of the PDL are missing due to decomposition, the ends which were embedded in the cementum have been preserved. Specimens show cementum-embedded fibers to which further mineralization of the tertiary cementum has occurred, leaving the fibers visible within this vitreous layer. Similar fibers can be seen in the bone-PDL interface, which represent the opposite end of the now absent intra-PDL fibers. The fibers can be seen with their origin within the surface of the alveolar bone, but around these fibers many layers of lamellar bone have accumulated, representing many waves of mineralization. The period of these waves is unknown at present, but since no mineralization bridging between the root and bone occur, it can be surmised that the alveolar bone and cementum apposition occurred at a rate slow enough to maintain an unmineralized PDL. This, while all other mosasaurs saw the eventual fusion of the tooth and bone, *G. phosphaticus* was able to maintain the paedomorphic condition of the non-mineralized PDL, similar to the mammalian condition.

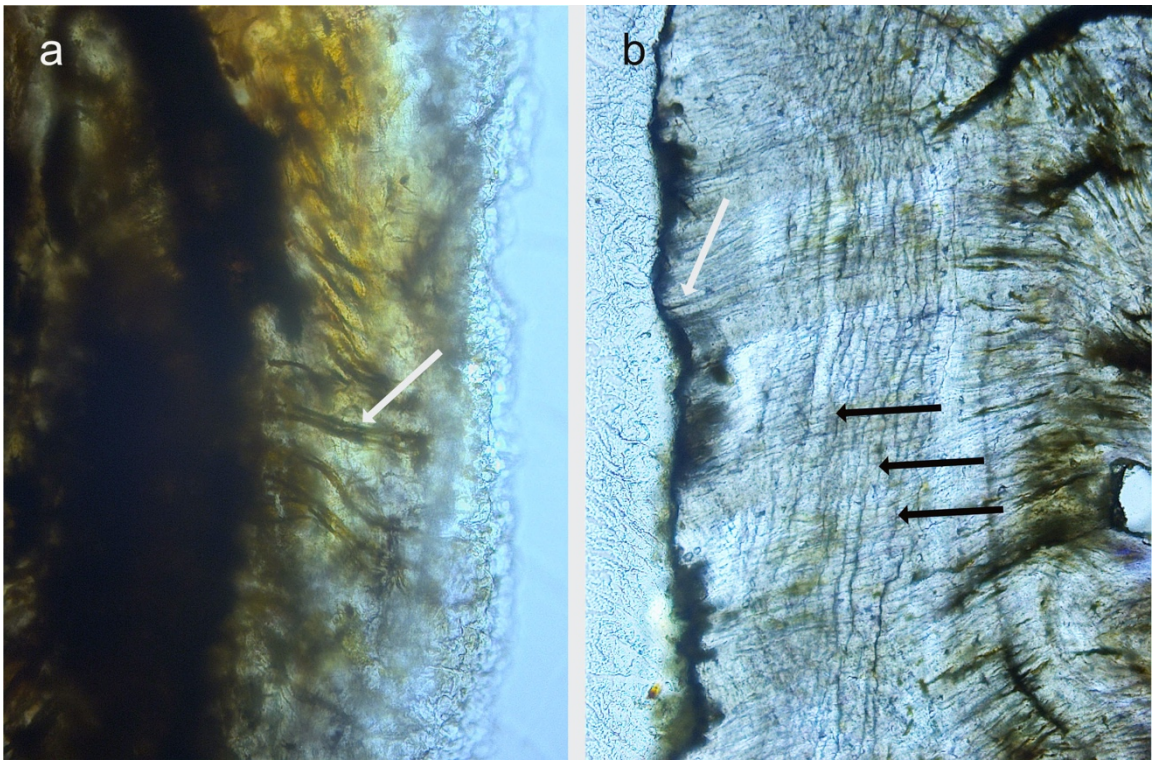

Figure 16 Bone and cementum in adjacent to PDL in *G. phosphaticus*
The outer layers of the bone and tooth root show evidence of Sharpey's fibers attaching the mineralized tissues to the PDL (white arrows). A) Polarized light: the root of *G. phosphaticus* in this thin section demonstrates fibers originating in the cellular/vascular cementum and penetrating through the outer tertiary cementum layer, indicating apposition of this layer after the tooth has become attached to the soft tissue of the PDL. The distinct vitreous appearance of this layer is easily appreciated in this unstained, thin-section, Brightfield image. B) Von Kossa Staining: the alveolar bone also has the Sharpey's fibers originating in the deeper layer of the Haversian bone. Multiple layers of bone apposition appear on the interior surface of the alveolar bone, indicating a decrease in the width of the periodontal space in this area, although there is no bridging of the soft-tissue PDL by mineralized tissue as in other mosasaur species.

The question then arises as to why the periodontal ligament is non-mineralized in mammals. The answer is again to be found by going back to the development of the non-mineralized periodontal ligament in marine reptiles. The common condition for tooth implantation in reptiles is the pleurodont attachment (Zaher and Rieppel 1999). This type of attachment consists of the tooth structure being firmly fused to the medial surface of the jaw bone by a mineralized structure known as the "bone of attachment". This gives a very rigid attachment, but flexibility and shock absorbing properties are provided by the sutures of the multi-bone lower jaw. The jaw of the *V. salvator* has pleurodont attachment for the teeth, but the varanoid lizards are known to have a degree of shock-dissipating properties provided by flexibility between the anterior and posterior jaw (Romer 1956). The skull generally provides movement between the various bones in a process known as cranial kinesis. This process is very common in teleost fish, amphibians and reptiles. In animals with requirements for strong biting forces during feeding, such as the alligator, cranial kinesis is very limited allowing more force to be applied to the jaw bones by means of adductor muscles attached to the skull. In humans, cranial kinesis is unknown. In is not surprising therefore, that these same vertebrates without out cranial kinesis, for example primates and crocodilians, have developed modifications of the periodontal ligament.

The simple pleurodont attachment is adequate for the feeding on soft foods for the common insectivorous and piscivorous diet, but may not provide adequate mechanical strength for extensive oral manipulation of food. During the many millions

of years of evolution, one of the primary themes has been adaptation to allow expansion into new ecological niches, to take advantages of new, untapped food sources. The plants and animals which are then preyed upon then up-armor with the development of shells, bark, scales, and spines to provide resistant to predation. This ever-increasing predator-prey arms race then leads to the need for a stronger tooth attachment. This is seen in marine reptiles by an increase in the medial parapet of bone; this bone providing at least a small amount of resistance to non-axial, i.e., shear forces acting through the tooth into the attachment tissues, by providing a degree of wrap-around support.

A trend through the evolution of marine reptiles is the increase in overall size as well as the increase in the size and hardness of their preferred diet. An example of this is the Texas mosasaur *G. alabamaensis*, whose durophagous adaptations have been previously discussed in this paper. At this level of adaptation to a hard diet and ability to deliver a crushing bite-force, the tooth has become encompassed by a circumferential buttress of supporting bone. Following this, the final step in this trend is the failure of the PDL to mineralize during the process of development and maturation (Fig. 17). Although this is the common condition in mammals, which perform extensive intraoral food processing with considerable non-axial loading of the teeth, this developmental variation in *G. phosphaticus* becomes very interesting in this reptilian context.

A defining character of mammals is a single mandibular bone, the dentary, while reptiles have a lower jaw consisting on many bones separated by sutures. The jaw of the alligator has many such bones separated by sutures which are sites of growth and flexibility (Fig. 18e). The sutures which can be seen plainly on μCT imaging, are

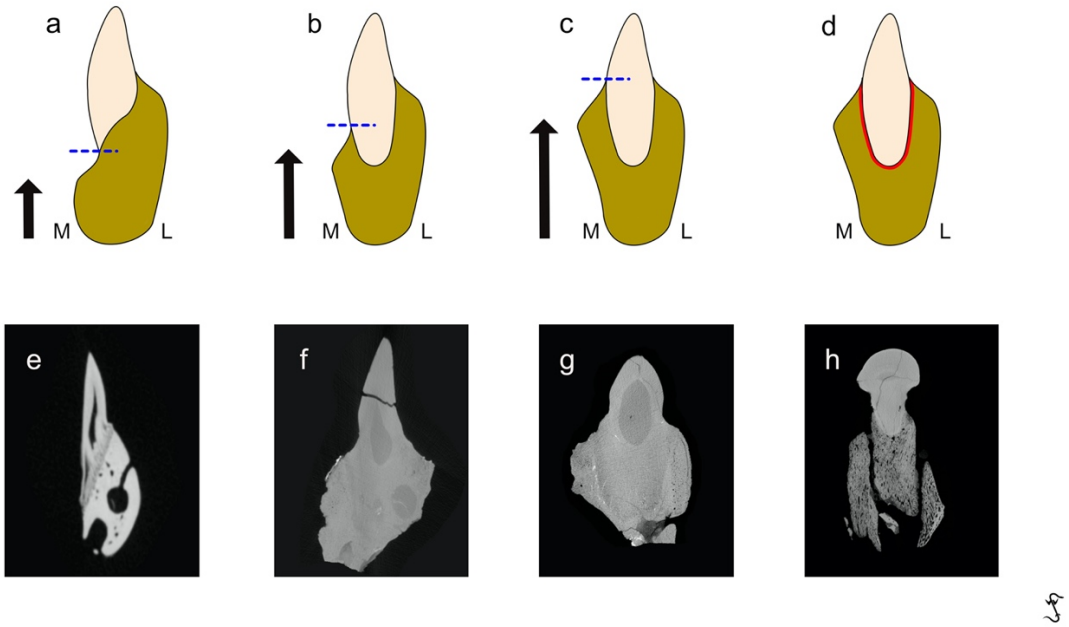

Figure 17 Evolution of the thecodont tooth implantation and non-mineralized PDL The evolution of the Mosasaurine tooth attachment tissues is described in four phases. The primitive condition of the squamate tooth attachment is characterized by the pleurodont tooth attachment. **A, E)** The pleurodont attachment is shown here in *V. salvator,* a terrestrial monitor lizard. The tooth is attached to the medial side of the bone only, and rigid, unyielding attachment tissues are required to hold the tooth in position. **B, F)** This example of *Clidastes* demonstrates attachment tissues surrounding the root apex and the formation of a medial parapet, giving more rigidity to the tooth attachment. **C, G)** With the advent of extreme durophagy, the tooth is completely surrounded by supporting bone in a thecodont condition, but remains ankylosed. Here it is demonstrated in *G. alabamaensis*. D, H) Although extremely durophagous, the complete thecodont condition of *G. phosphaticus* no longer requires the rigidity of ankylosis, and the PDL fails to mineralize during development.

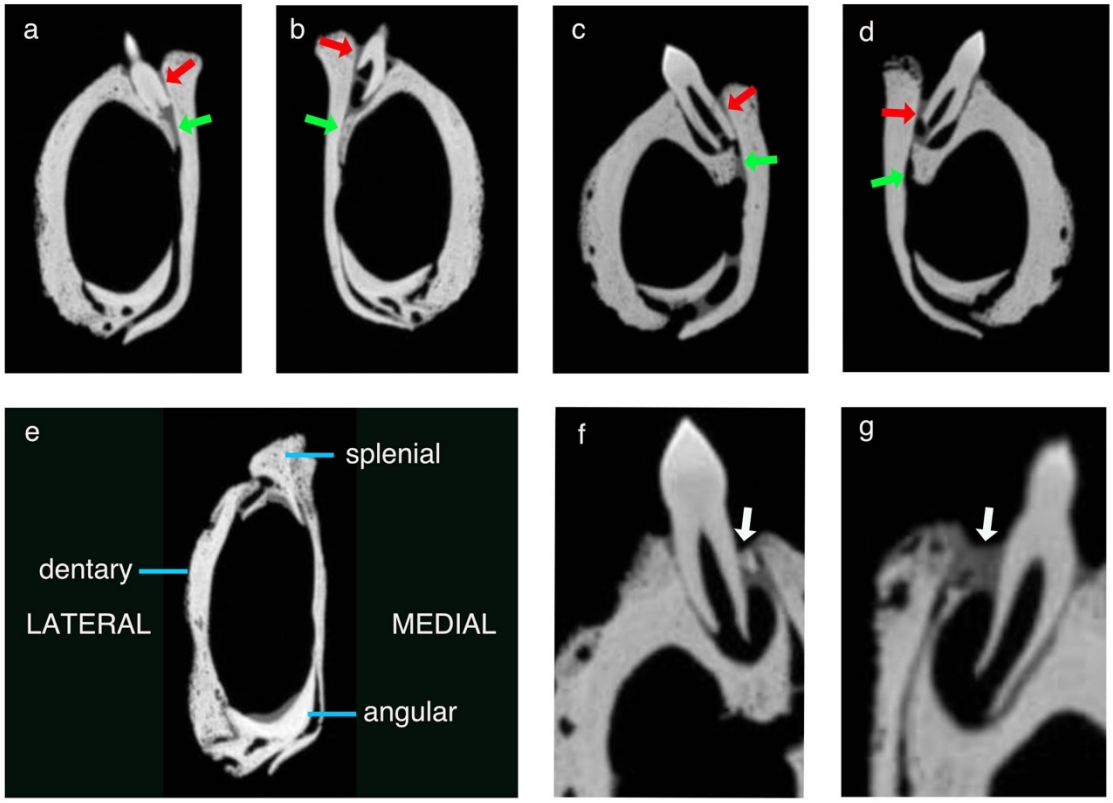

Figure 18 Alligator sutures
The sutures of the lower jaw of *Alligator mississippiensis* are continuous with the periodontal ligament. A-D) In all sections examined, the periodontal ligament (red arrows) is continuous with the suture (green arrows) between the dentary and splenial bones when examined by microCT. E) The lower jaw of the *Alligator mississippiensis* is composed of several distinct bones which are separated by sutures, unlike the condition in mammals. F-G) Some mineralization of the periodontal ligament normally occurs in alligators, whereas mineralization of the periodontal ligament in mammals invariably represents a pathological condition.

continuous with the PDL of the alligator teeth in every section imaged (Fig. 18a, 18b, 18c, 18d). The PDL of alligators develops as an unmineralized membrane, similar to the mammalian PDL, but it does not remain patent, eventually assuming a partially mineralized state (Fig. 18f, 18g), an intermediate between the common reptilian and the mammalian states.

A survey of other extant species was undertaken to determine the proximity of the mandibular sutures to the PDL. In *Varanus salvator*, *Iguana iguana*, as well as the previously examined *A. mississippiensis*, the sutures are in direct contact with the PDL (Fig. 19). It appears in all sectioned examined that the reptilian tooth attachment apparatus is adjacent to the sutures, and to the extent that the PDL of *A. mississippiensis* is unmineralized, it is actually an extension of the mandibular sutures. The μCT of the marsupial *D. virginiana* shows a patent, non-mineralized PDL and no evidence of mandibular sutures, as expected for a mammal (Fig. 19d). A survey of teeth in the upper jaws was also undertaken to determine the spatial relationship of the sutures and PDL, to determine if it correlated with the findings on the mandibular arches. On the μCT sections examined, it appears that the skull sutures are in direct contact with the tooth attachment tissues, an example of which is shown (Fig. 20). It is proposed that the non-mineralized PDL is a specialized craniofacial suture that first appeared as an extension of the mandibular and skull sutures. If the non-mineralized PDL is an extension of the craniofacial sutures, it should be possible to see some evidence for this in modern mammals, which retain this character. For this purpose, a cell lineage tracing experiment was undertaken in mice to look for a common origin for

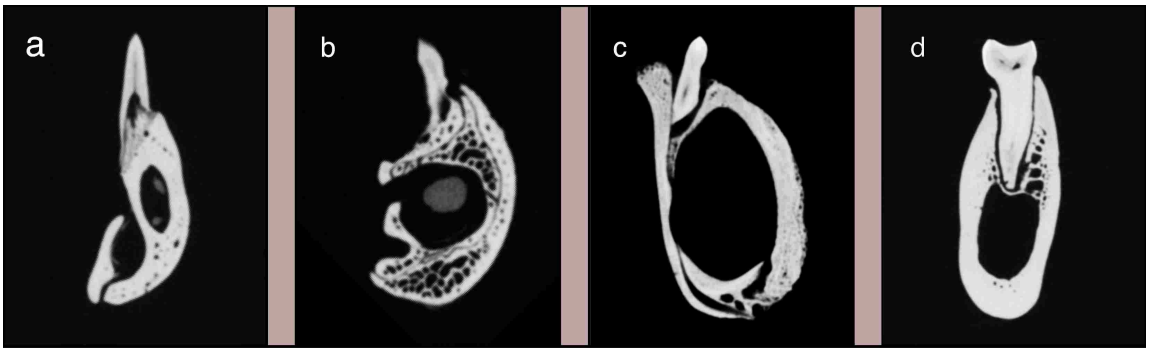

Figure 19 Mandibular sutures in vertebrates
This is a series of microCT sections demonstrating the relationship of the sutures of the lower jaw to the periodontal attachment tissues. A) *Varanus salvator*. B) *Iguana iguana*. C) *Alligator mississippiensis*. D) *Didelphis virginiana*, in this mammal, no mandibular sutures are visible, but the periodontal ligament space is clearly demonstrated.

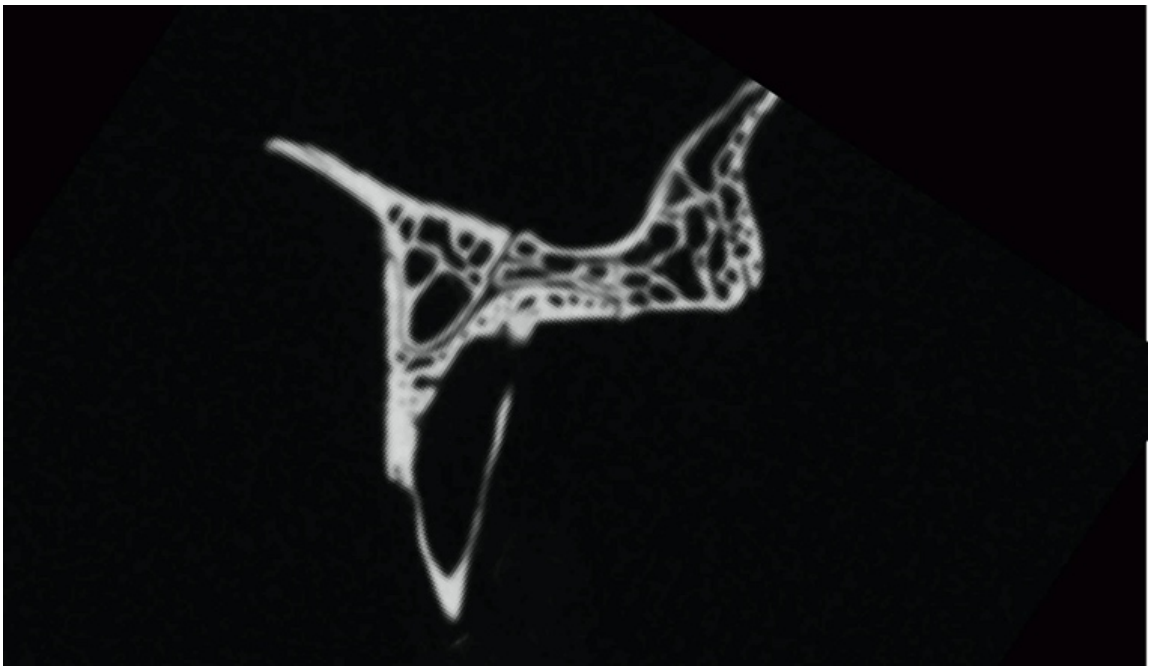

Figure 20 Upper jaw of *Iguana iguana*
This μCT image demonstrates the proximity of the maxillary sutures and the tooth attachment tissues.

the sutures and PDL. The Gli1+ cells have been shown to be a typical mesenchymal stem cells (MSC) when grown *in vitro*, but have been to be the main MSC population within the craniofacial sutures (Zhao et al. 2015). In humans, the craniofacial sutures eventually fuse with maturation in during the periods of early to middle adulthood (Badve et al. 2013; Senarath-Yapa et al. 2012), but the craniofacial sutures in mice stay patent throughout their lifetime.

To determine if the cells within the PDL and the craniofacial sutures are derived from a common development origin, a *Gli1-Cre^{ERT2};Ai14* transgenic mouse line was generated. These mice were at P60 at the time of this experiment. They were induced with tamoxifen for two days prior to processing for imaging. The tissue from the mice was harvested and processed for imaging following the PEGASOS tissue clearing protocol (Jing et al. 2018). Three-dimensional imaging was completed with confocal microscopy. Gli1+ were visualized within the soft tissue of the cranial suture of the mouse, but not within the osteocytes or bone (Fig. 21a). In, comparison, similar sections from the PDL were obtained. The distribution of Gli1+ cells within the PDL was identical, to the suture; the Gli1+ cells contributed to the soft tissue of the periodontal ligament (Fig. 21c). In these adult molars, they were not visualized within the alveolar bone osteocytes or within the cementum. In addition to the cellular make-up, the general morphology of the sutures and the PDL were of a similar dimension and morphology.

The canonical Wnt signaling pathway is thought to be essential for the activation of Gli1+ cells within growth plates of long bones and healing fracture sites (An et al. 2018; Maruyama et al. 2016; Shi et al. 2017). An attempt was made to determine if the

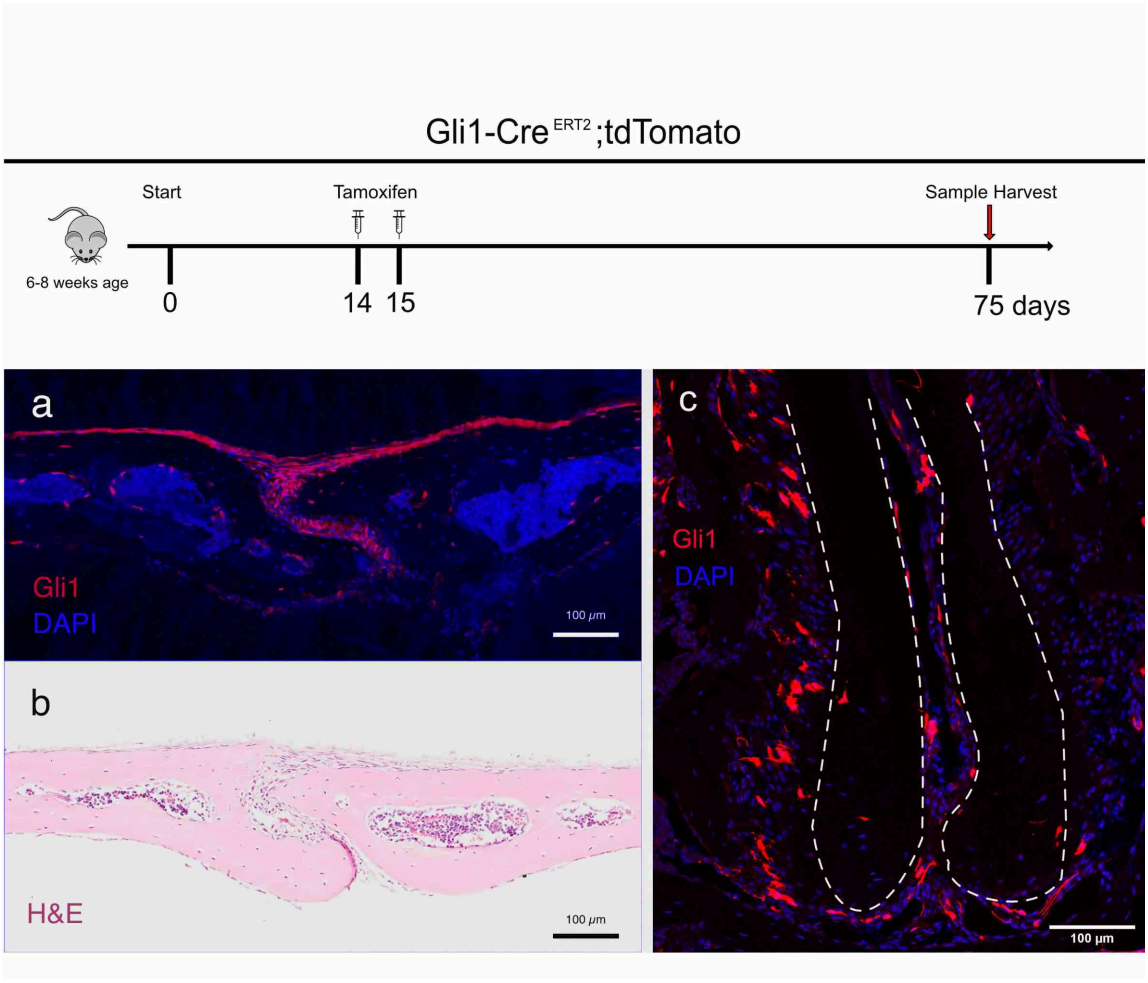

Figure 21 Skull sutures and PDL in the mouse
These images demonstrate the mid-sagittal suture in a transgenic mouse. A) Cells marked with DAPI show cell nuclei and give an indication of the number of cells present in this confocal microscopy section. The Gli1 cells are indicated which are marking the presence of stem cells in the suture, indicating that this is an actively remodeling area. B) This is a conventional histologic section taken in an area similar to the location shown in the upper image. The presence of osteocytes in lacunae is clearly seen, as in the non-mineralizing nature of the mid-sagittal suture. C) PDL cells in the mouse. The mouse, as a typical mammal, has a non-mineralized PDL. The Gli1 cells show that these cells derive from a stem-cell niche at the base of the tooth, and that this area is constantly renewing, i.e., a fast cell turnover rate. These cells are found in the PDL but not in the adjacent bone. The blue DAPI stained areas represent cell nuclei; these DAPI labeled bone cells do not derive from the Gli1 cells. The dotted white line is outlining the root surface.

root anatomy of the mosasaurine reptiles, i.e., voluminous cementum containing extensive vascular and cellular elements could possibly derive from a tissue response to an overactivation of Wnt activity in the Gli1+ periodontal ligament stem cells (PDLSC).

In an attempt to recreate this morphology in a mammalian model, *Gli1-Cre^{ERT2};Ctnnb1$^{fl(ex3)}$;Ai14* (Exon3 mutant) mice were utilized. Mice were examined two days after tamoxifen induction, and EdU incorporation. Severe periodontal tissue loss with an altered and widened PDL space associated with these mice was previously reported our laboratory (Men et al. 2020b). The mice showed increased activation of EdU on the second day, revealing an increased activation of the Gli1+ cells. On day 21, an increase in the volume of cementum was noted on confocal microscopy (Fig. 22). Of note is that the proliferating cementoblasts were all labeled Gli1+ cells, indicating that the derived from the same PDLSC line. This expansion of cementum and cementoblasts was not seen in the control mice. This expansive growth of cementum was confirmed with histology, and in addition to the greater volume, the cellular and vascular elements of the newly formed tissue were confirmed. Of note is that the alveolar bone appeared unaltered in both the control and mutant specimens.

Discussion

The PDL in mammals contains is a non-mineralized zone separating two distinct mineralization fronts. This space has one of the highest tissue turnover rates in the human body, and in fact, has many characteristics of an embryonic tissue (Berkovitz et al. 1995). In order to maintain this space in this fashion, many specialized cells, factors,

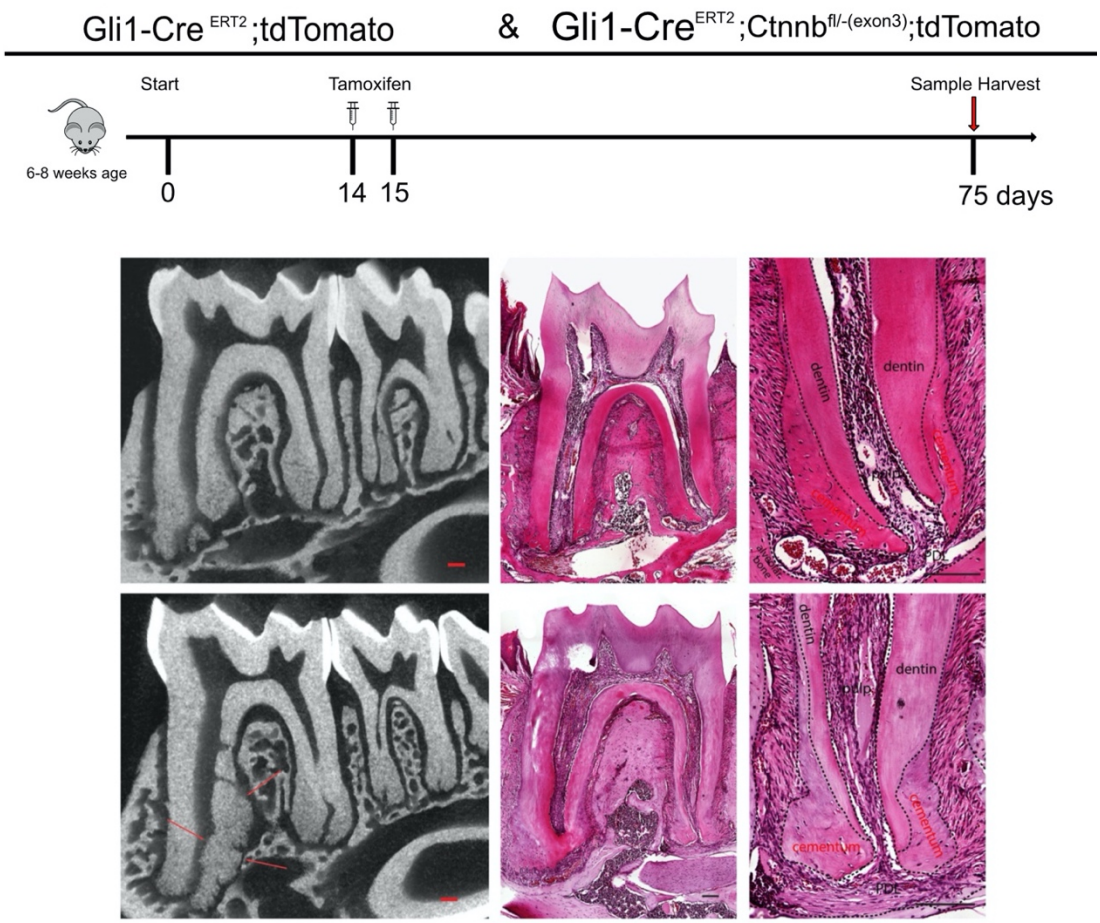

Figure 22 Constitutive activation of Wnt signaling in the mouse.
The top row of images shows the control mice. These adult mice were *Gli1-Cre^{ERT2};Ai14*. The lower row shows the experimental group, and these mice were *Gli1-Cre^{ERT2};Ctnnb1$^{fl(ex3)/+}$*. All mice were induced with tamoxifen 21 days before sacrifice, at which time the mandibles were harvested. The experimental mice show greater volumes of cementum than the control mice as a result of overactivation of Wnt.

and signaling systems need to be present and work in coordination, and this to have been an early adaptation in the mammalian lineage (Diekwisch 2016). The question then becomes: how does this complex system arise *de novo* in *G. phosphaticus,* when the less derived mosasaurs had only cementum and bone joined in ankylosis? This development has also occurred several different times in different lineages, i.e. mammals, dinosaurs, and bolosaurid parareptiles (Snyder et al. 2020), so how does this repeatedly appear in the evolutionary record in response to increased levels of occlusal force? The answer to this question may be found in the examination of the dental apparatus of the crocodilian *A. mississipiensis*. While these archosaur crocodilians have many characteristics which superficially resemble their lizard relatives, they also have some very advanced anatomic specializations, e.g., a four-chambered heart, etc., that make them a model for comparison to mammals. Of particular interest to us here is the presence of teeth in sockets, i.e., thecodont dentition and a PDL, characters which they share with mammals and dinosaurs (Leblanc et al. 2017a) and pterosaurs (and extinct dentate birds). This makes them invaluable as a living vertebrate that can give us insight into the rise of the PDL.

The crocodilians are known for their ability to develop enormous bite forces, and this has had a great effect on the evolution and development of their craniofacial apparatus (Gignac and Erickson 2016). The crocodilian PDL is partially mineralized and is an intermediate between the fully-mineralized reptilian PDL and the totally unmineralized mammalian condition (Mcintosh et al. 2002). While the unmineralized membrane of the PDL has been the subject of a great degree of dental scientific

investigation, it is by no means the only nonmineralized membrane separating two active mineralization fronts in the craniofacial region. The PDL is a gomphosis-type joint, separating cementum from bone, but craniofacial sutures form a similar joint separating one bone from another bone. The tissue of these sutures has many characteristics in common with the PDL, viz. the ability to resist osseous obliteration of the inter-bony space, and this has been determined to be the result of soluble factors, and not merely the induction of cell to cell interactions (Opperman et al. 1995).

Because most of the larger reptiles have indeterminate growth patterns, meaning that they continue to grow in size throughout life, the craniofacial skeleton likewise continues to grow throughout life. This is combined with polyphyodonty, continued tooth replacement throughout life with each successive tooth generation being slightly larger than the preceding generation. This necessitates constantly growing tooth bearing skeleton. In reptiles the teeth can be found on several different bones including the dentary, maxilla, pre-maxilla and pterygoids. The site of this intramembranous bone growth in the craniofacial skeleton is at the sutures (Opperman 2000). Besides being the site for growth, these sutures are also able to allow for some flexibility in the skeleton; in doing so the cells within the suture respond with the mechanotransduction of signaling molecules which contribute to both bone growth and patency (Alaqeel et al. 2006).

The functions of the sutures, i.e., maintaining patency, bone growth, mechanotransduction of active molecules, and flexibility are also the functions of the PDL. The similarity of the of the structures has previously been identified based on light microscopy with epoxy-embedded ground sections, the differences being the presence of

both lamellar and bundle bone in the PDL and lamellar bone only in the PDL (Pirelli et al. 1997), It is noted the cited study consisted of human biopsy samples only, and the differences could be explained by differential rates of bone deposition in the two sites. Nevertheless, the question then becomes: do these two tissues, so alike in function, have a common origin? Upon examination of the mandibular bones of the *A. mississippiensis*, it can be seen that they are clearly separated by sutures which remain patent throughout the life of the alligator, as it continues to grow. By looking at various section of the jaw of the alligator, it can be determined that the mandibular sutures are continuous with the PDL at every location imaged. Although the PDL will mineralize with the maturation of each tooth, as each tooth is lost and replaced by a successional tooth, a period of nonmineralized patency occurs, allowing for a period of bone growth from the alveolar bone. This is necessary for the jaw to enlarge to accommodate the ever-larger successional teeth.

It is proposed that PDL first arose in the pre-mammalian lineage as a modified extension of the craniofacial sutures (Fig. 23). It was confirmed through radiographic data that the craniofacial sutures are continuous with the tooth attachment tissues in many species of extant reptiles. By consideration of the anatomy of the extinct marine squamate *G. phosphaticus*, the first appearance of non-mineralized PDL in this lineage can be noted, and it can be determined that it fits the pattern here described. To provide further support for this claim, the laboratory mouse model provides a valuable resource, in order to apply molecular techniques to determine the features of the craniofacial

sutures and PDL which point to a common developmental and evolutionary origin (Fig 24). Earlier studies have determined that the Gli1+ cells are MSCs specific to the craniofacial sutures. Here it is possible to compare the PDLSC to the craniofacial suture MSC.

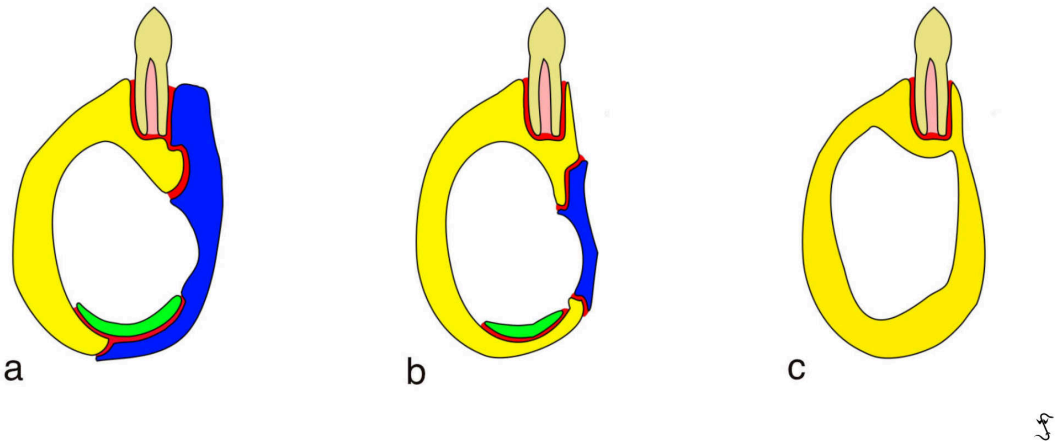

Figure 23 Schematic diagram of the evolution of the periodontal attachment tissues A) Reptiles have multiple bones in their lower jaws, which are joined by unmineralized sutures (illustrated in red). These sutures are in intimate contact with the periodontal attachment tissues. B) Hypothetical intermediate condition in which the bones have become reduced, and the sutures between the bones of the lower jaw are no longer in contact with the periodontal tissues. C) The condition of extant mammals in which the unmineralized periodontal ligament persists, but no intraboney sutures remain.

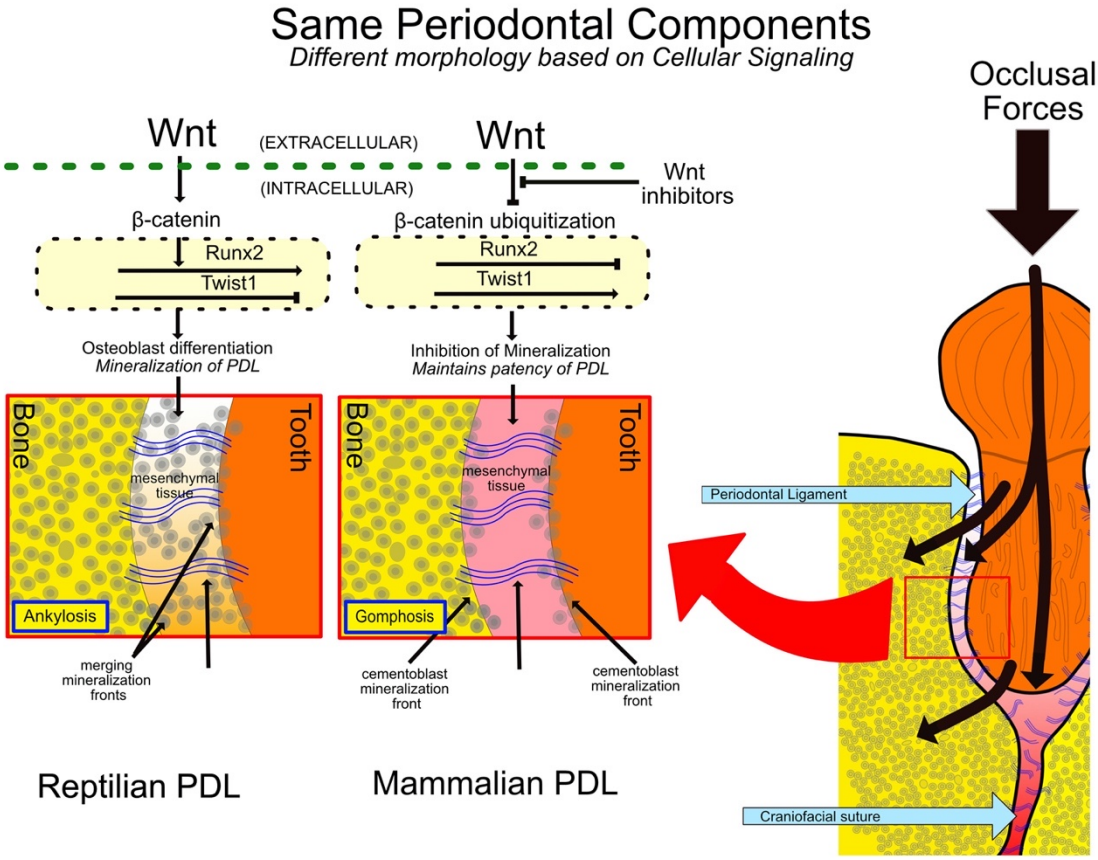

Figure 24 Comparison of Reptilian and Mammalian PDL
The patency of the mammalian PDL is maintained by inhibition of the Wnt signaling pathway. This results in the ubiquitization of β-catenin and the resulting decrease in osteoblast activation. The transcription of Twist in the PDL also contributes to is patency. The conditions within the mammalian PDL are similar to the conditions in the craniofacial sutures, which also has two mineralization fronts separated by a narrow non-mineralized zone. The mammalian and reptilian PDL are initially very similar but with maturation the reptilian PDL mineralizes to form an ankylosis.

CHAPTER IV

GLI1+ STEM CELLS RESPONSIBLE FOR EARLY HEALING OF ZIRCONIA DENTAL IMPLANTS WITH SINUS AUGMENTATION

Overview

In recent decades dental implants have become a common and accepted part of dental therapeutics in the United States and the World. Here tested in mice are new materials primarily consisting of zirconia as a replacement for the more common titanium-based implants. By evaluating bone and tissue response, it can be determined that the biocompatibility of the zirconia implants is not superior to titanium-based devices.

Synopsis

Over the past 40 years dental implants have gone from being an uncertain, experimental procedure to a routine part of restorative treatment, yet many problems are beginning to emerge from this seemingly innocuous procedure. Previous sections have detailed the emergence and functional attributes of the PDL in the mammal, yet the current design of dental implant loads occlusal forces directly into the jawbone without an intervening PDL, sometimes in great excess of tooth borne occlusal forces. Titanium particles from the implant can enter the tissue resulting in an inflammatory reaction, leading to periimplantitis and implant loss. A newer implant material, yttria-stabilized zirconia, is a ceramic that is claimed to eliminate the inflammatory reaction and promote

healing through its great biocompatibility. Using a transgenic mouse model, both zirconia and titanium implants were placed to examine both bone healing at the implant surface (osseointegration), often viewed as a criterion of success, and blood vessel proliferation at the implant surface, a sign of early healing response. The use of μCT at 1-week, 2-week, and 4-week periods showed better bone integration at the 1-week and 2-week timepoints for the Zirconia implant, but superior healing of the titanium implant at the 4-week timepoint. Blood vessel proliferation measured through 3-Dimensional fluorescently labelled mice, showed greater angiogenic response at all time points for the Zirconia group compared to the Titanium group. The results of this study provide evidence for a greater early healing response to zirconia dental implants, and suggest the further research should be performed to investigate this promising implant material.

Introduction

In the past forty years, dental implants have become commonplace in dental reconstructions, composed of either commercially pure titanium or titanium alloy which provides greater strength. They are no longer in the exclusive purview of the oral-maxillofacial surgeons, but are also commonly performed by other practitioners, i.e., periodontists, prosthodontists, and general dentists. The great success of dental implantology has led to this becoming a first-line treatment for not only the replacement of missing teeth, but also as an alternative to restoration or repair of natural teeth.

Although the modern era of implant dentistry can be traced back over a hundred years, the current paradigm of dental implant restorative dentistry began in earnest with the introduction of screw-form dental implants composed of commercially pure titanium. Earlier configurations had used a variety of implantable materials including stainless steel and Vitallium, an alloy consisting of Chromium, Cobalt and molybdenum. These materials were selected based on what was known of their biocompatibility profiles at the time. Implant design consisted of blade-form implants placed into slots prepared in the jaw, or subperiosteal implants, which consisted of a metal denture framework placed between the periosteum and alveolar bone (Adell et al. 1970). These procedures were risky, unpredictable, and often resulted in significant morbidity. For these reasons, dental implantology was considered outside of mainstream dentistry, and was often considered an experimental or unethical practice.

Nevertheless, there were pioneers in restorative dentistry who realized the potential of dental implantology and sought to bring the available science into the clinical and academic dental realm (James 1979; Kratochvil et al. 1976). Two historical factors provided a major impetus for a change in the field. The first was the changes to casualty care in the Vietnam War (1955-1975). In previous American conflicts, casualty care had been provided in field hospitals located close to the front. In Vietnam, the paradigm changed to provide rapid transportation to high-level hospitals that could provide advanced craniofacial reconstruction (Kelly et al. 1978). This approach resulted in a much lower incidence of crippling facial deformities than previous conflicts (Parsons and Thering 1972). This advanced military medical training provided a large

cadre of Army and Navy veteran clinicians, general dentists, oral-maxillofacial surgeons, and prosthodontists, returning to civilian life with the expertise, experience, and willingness to translate these advanced reconstructive services to their civilian patients (Morgan and Szmyd 1968). The second factor leading to the implant acceptance was the serendipitous discovery of osseointegration of titanium screws placed into bone. While conducted research on hematopoiesis in rabbit tibias, Brånemark found the optical chambers, constructed on a titanium screw, were difficult to remove because they were tightly adherent to the bone. Although he was not a dentist, he saw the possibilities for this method of anchorage of dental prosthesis leading first to studies in dogs (Brånemark et al. 1969) and later in humans (Branemark 1977).

Clinical placement of implants requires a substantial amount of investing bone in which to place the implant. The thickness of bone is required to be at least the length of the implant, the shortest of which in clinical use are 8-10 mm. This amount of bone is often not present in the edentulous posterior maxilla because of pneumatization of the maxillary sinus. The sinus augmentation procedure, commonly known as the "sinus lift" surgery, is commonly used as a preparatory procedure prior to the placement of dental implants in the edentulous posterior maxilla. This procedure was originally performed by US Navy oral surgeons during preparations for conventional dentures where there was not sufficient space between the maxillary ridge and the mandibular teeth for a denture. The condition results from a healing process known as pneumatization, which occurs following the extraction of the maxillary posterior teeth. Pneumatization is characterized by expansion of the sinus in an inferior direction, and although the mean

expansion in a study of 152 subjects was 1.83mm, certain anatomic features of the sinus, such as a superiorly curving sinus floor, resulted in much higher magnitudes of expansion (Sharan and Madjar 2008). It was also noted that extraction of second molars resulted in more expansion than first molars.

Placement of implants into a thin sinus floor often results in inadequate primary stability of the implant, which prevents healing and osseointegration. Dental implants placed into the sinus floor without augmentation can become loose and migrate into the interior of the sinus. Most of these cases resulted in sinusitis with an oral-antral communication, and these required an additional surgical procedure to remove the displaced implant and close the oral-antrum communication. Pathologic displacement and migration of the dental implant remains a significant problem during the prosthodontic restoration of the posterior maxilla with a pneumatized sinus and a thin sinus floor (Manor et al. 2018).

The sinus augmentation surgery was first taught in the Naval Postgraduate Dental School for several years before it was described in the literature (Boyne and James 1980). This lateral window technique was developed at a time when dental implantology was in its infancy, so it was several years before the same authors applied this procedure for the placement of implants in the maxilla where insufficient bone existed to stabilize the implants (Boyne 2004). This study also included histology of the procedure obtained from Rhesus monkeys showing complete encapsulation of the titanium implant in bone within the sinus, and the lack of inflammation surrounding the implants. Briefly, the procedure consists of first elevating a full thickness soft tissue flap over the lateral aspect

of the sinus. Once the bone is visualized, a trap-door window is cut through the bone with a rotating dental burr taking care not to perforate the underlying Schneiderian membrane. The Schneiderian membrane is then elevated and a bone graft material is placed beneath it. The lateral window is then covered with a surgical membrane, and the wound is closed with sutures.

Despite the great success and widespread use of dental implants, forty years of worldwide clinical experience has exposed their limitations and failures. Even in the early development, it was realized that a certain percentage of implants would not become stable abutments for prostheses. Some implants failed to stabilize in their initial integration, but others integrated but then developed inflammation and bone loss. As techniques, materials, and designs improved these failure rates decreased, but failures continued to occur, a condition that become known as periimplantitis (Toth et al. 1985).

Because periimplantitis was causing loss of bone that was supporting the prosthesis, it was initially considered homologous to periodontitis, with the same pathogenic microbiological profile and host susceptibility factors. It is immediately obvious though that the microanatomy of the implant-bone interface in no way resembles the tooth-alveolar bone interface in that implants lack not only Sharpey's fibers and cementum, but also the entire periodontal ligament. Occlusal forces on the tooth are responsible for mechano-transduction of various cellular signaling pathways, such as the β-catenin dependent Wnt pathway, and these are in turn responsible for the homeostasis of the tissue surrounding and supporting the tooth (Men et al. 2020a). Occlusal forces on the titanium implant do not transfer forces to a PDL, so the

homeostasis between bone and metal relies on other mechanisms. It is also noteworthy to mention that the neural crest-derived alveolar bone surrounding teeth has a different origin and cellular expression profile than the jaw bone into which dental implants are placed. The alveolar bone lining tooth sockets is known to be more active than other bone (Hall 2014). The difference in the two disease processes became even more distinct when it was realized that treatment regimens that were generally successful for teeth in periodontitis were not generally useful in the case of dental implants and periimplantitis. These differences led the American Academy of Periodontology to classify periimplantitis as a distinct entity in the "Classification of Periodontal and Peri-Implant Disease and Conditions" in 2017 (Berglundh et al. 2018).

The rise in the use of titanium implants in dentistry was accompanied by a concomitant rise in the use of the same material in orthopedic hip replacement implants. Despite not being located in the oral cavity and not being subject to oral hygiene measures, a similar condition of inflammation and bone loss occasionally developed at the bone titanium interface. It was found that if the implant environment was such that microscopic particles of titanium (1μm – 5μm) were shed, inflammation of the tissue would ensue. This inflammation was often uncontrollable and resulted in loss of the orthopedic implant. Briefly, the small particles of titanium could be phagocytosed by macrophages resulting in a change in their polarity. This immune response to titanium microparticles was later verified in the craniofacial tissues of mice, by surgically implanting particles into mice calvaria.

An alternative to titanium implants is zirconia ceramic. Zirconia has been known as a biocompatible material for decades, but the shear strength was not considered acceptable for the functional demands of occlusal load in dental implants. Since the implant-bone interface has a low modulus of elasticity, i.e., no PDL to absorb and distribute force, the demands for physical strength are higher in the implant material than are required for natural dentine. The changes to zirconia came when it was discovered that by doping the crystal lattice with yttria rather than magnesium, the phase changes within the cubic lattice would actually work to close deformities, and thus prevent propagation of fractures within the material. This property has given this material the strength to be considered for applications in dental implantology.

Although zirconia implants are becoming more common in clinical use they still make up only a tiny fraction of the total implant market. Nevertheless, the top three implant manufacturers have started offering some zirconia alternatives to titanium implants. Marketing claims for superior esthetics and patient acceptability are the driving the clinical use, but there is still a paucity of animal studies to demonstrate the biological function of a loaded implant in animal models, especially when it comes to implants placed into the maxillary sinus. Currently, most implant studies are done on dogs, since the size and scale of the implants are similar to those used in human dentistry. Even though these studies can provide much in the way of valuable preclinical data on biocompatibility, they lack the detail needed for truly understanding the details of the biological reaction to this material (Rodrigues et al. 2009; Wilson Jr et al. 2015).

Because current biomedical research relies on tracking cell populations as well as biochemical processes, it is imperative to use models which allow tags and markers produced intrinsically within the organism. Currently, the only mammalian organism which meets these requirements is the transgenic mouse model, which allows tracking of cellular subsets to elucidate pathways and processes. Although previous murine studies have placed zirconia in non-oral locations, or placed oral implants in larger rodents such as rats, the trans-alveolar placement of zirconia implants into the edentulous maxilla and sinus of transgenic mice has not been attempted due to the difficulty of the microsurgical procedure as well as the non-availability of a suitable zirconia implant in mouse sizes. The purpose of this study, therefore, is to use a transgenic mouse dental implant model previously developed in our lab for titanium implants in mouse mandibles, combined with a zirconia implant produced in our lab, to evaluate the healing around zirconia implants placed in edentulous maxillae combined with sinus augmentation.

Experimental Procedure

Titanium implant fabrication

Titanium implants used for this study 0.6mm titanium dentine pins (STABILOK) as used in previous implant studies (Yi et al. 2019). These implants were shortened to a length of 1.75 mm prior to insertion.

Threaded zirconia implant fabrication

Zirconia implants were fabricated using 1 mm diameter screws composed of yttria-stabilized zirconia ceramic (Kimura-Tec, Shiga, Japan). Since the initial pattern of

these screws was M1 x 2 JIS (Japanese Industrial Standard), It was necessary to machine them to acceptable dimensions to form a dental implant. This was done on a watchmakers' lathe (Sherline Products, Vista, California) using a stereomicroscope (Meiji Techno, Saitama, Japan) under 10x magnification (Fig. 25). Machining was completed using diamond dental burs and polishing to 2000 grit. Finally, implants were sterilized and placed in PBS prior to insertion.

Non-threaded zirconia implant fabrication

Non-threaded (bullet shaped) zirconia implants were fabricated from 0.7 mm zirconia ceramic rod as used in the electronics/ semiconductor industry. These were cut and shaped using diamond dental burs on a watchmakers' lathe (Sherline Products, Vista, California) under a stereomicroscope (Meiji Techno, Saitama, Japan) with 10x magnification (Fig. 25). Implants were completed by polishing to 2000 grit. Finally, implants were sterilized and placed in PBS prior to insertion.

Calcein Green and Alizarin Red: Fluorochrome labeling

CD1 Mice were given injections of fluorophores for the purpose of bone labeling following treatment with dental implants. The two-week mice and the four-week mice were given an intraperitoneal injection of Calcein Green 10mg/ml 10 days before sacrifice. A second label, Alizarin Red 1mg/ml was administered by intraperitoneal injection 2 days before sacrifice, following established protocols (Van Gaalen et al. 2010).

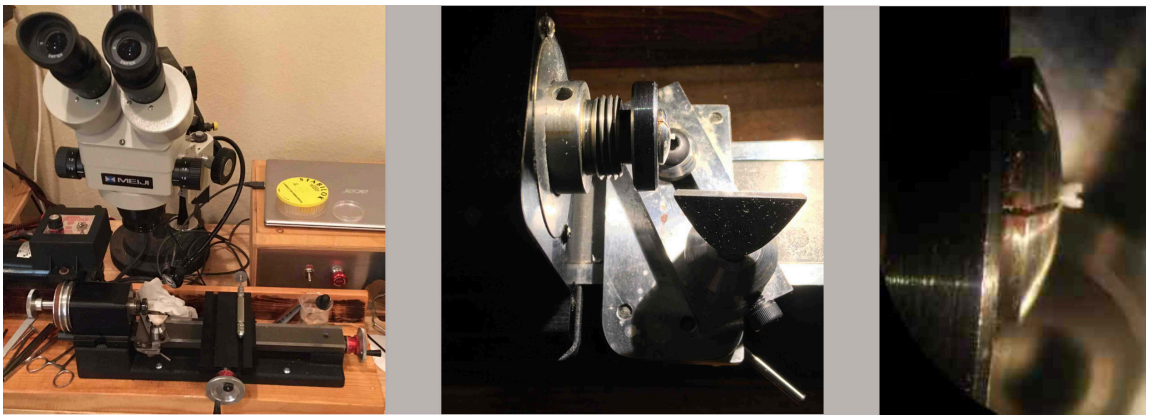

Figure 25 Zirconia implant construction
The second phase of Zirconia implants were produced from yttria-stabilized zirconia screws as described in the materials and methods section. Screws were mounted in a 1.00 mm collet in a watchmakers' lathe. Using a stereomicroscope at 10x, screws were turned at 1000 RPM and wet-ground with a fine diamond dental separating disk mounted on a mandrel held in a pin vise. A graver-style tool rest was used to stabilize the position of the diamond disk during the process. Once the final shaping was accomplished, the implant was polished with a series of abrasive papers up to 4000 grit.

Mice

All protocols for the experimental use of mice were approved by the Institutional Animal Use and Care Committee (IUCAC) of Texas A&M University College of Dentistry. CD1 mice were purchased from Charles River (Wilmington, Massachusetts). The Cdh5-Cre^{ERT2} mice (Eilken et al. 2017) were provided by Dr. Woo-Ping Ge from University of Texas Southwestern Medical Center with an MTA form approved by Cancer Research Limited. The Cdh5-Cre^{ERT2} mice were crossed with Ai47 (JAX 007908) reporter mice. All mice were housed Texas A&M College of Dentistry and complied with Texas A&M University IACUC protocol number 17-0103. For all *in vivo* studies, sex and age matched mice from the same litters were used. No significant differences were noted between male and female mice. All mice used were adults, 5-8 weeks of age. Mice were anesthetized with an intraperitoneal injection of ketamine (100mg/kg) and xylazine (10 mg/kg). Maxillary first molars were extracted with forceps and elevators, and mice were placed on a soft diet during recovery. Implants were placed 2 weeks following extractions.

Tamoxifen Administration

Tamoxifen was diluted in corn oil at a concentration of 20mg/ml and frozen at -20C until needed. This solution was injected intraperitoneally for two consecutive days for induction. The dosage used was 1.5mg/10g based on body weight.

Tissue Clearing

The PEGASOS Method was used for tissue clearing as previously described (Jing et al. 2018). Briefly, the mice were perfused and mandibles were dissected free and

fixed in 4% PFA. The mandibles were then decalcified in 10% EDTA at 37°C for seven days. Decolorization was completed with 25% Quadrol (Sigma-Aldrich 122262) at 37°C for 2 days. Delipidation was then carried out in a graded series of tert-butanol aqueous solutions (Sigma-Aldrich 360538), and dehydration was carried out with tB-PEG solution composed of tert-butanol, PEGMMA500 (Sigma-Aldrich 409529) and Quadrol. For final tissue clearing, samples were placed in a BB-PEG solution containing 72% benzyl benzoate (Sigma-Aldrich 409529), PEGMMA500 and Quadrol. Three-dimensional imaging was performed using a Zeiss LSM780 2-photon microscope (Carl Zeiss AB, Oberkochen, Germany). Three-dimensional image reconstruction was performed with Imaris 9.0 (Oxford Instruments, Concord, MA).

MicroCT

After fixing in 4% paraformaldehyde for 24 hours, specimens were placed in a 12.3 mm tube. μCT imaging was performed at Texas A&M University College of Dentistry on the μCT-35 system (Scanco Medical; Voltage = 70 kV, high resolution 7.0 μm). The files were converted from .ISO to TIF using ImageJ (NIH, Bethesda, MD). For -D reconstruction and quantification, Imaris 9.0 (Bitplane AG, Zurich, Switzerland) was used.

Image acquisition

Fluorescent images of mouse maxilla were obtained using a Zeiss LSM 780 Upright microscope or Zeiss LSM 880 inverted two-photon microscope (Zeiss AB, Oberkochen, Germany). A 488 nm excitation laser was used for GFP, and emissions were captured between 504 nm and 556 nm. For Second Harmonic Generation signals, a

coherent Chameleon Ultra II Ti:sapphire laser was used at 950 nm with a non-descanned detector. A 10x/ 0.3 NA Plan-Neofluor objective (ZEISS AB, Oberkochen, Germany) was used with a working distance of 5.2 mm. Image stacks were acquired at 1024 x 1024 pixel resolution (pixel size 1.19 μm) and *z*-step was set at 2μm. Deconvolution was completed with Autoquant X3 (Media Cybernetics, Rockville, MD, USA). This was done with a blind deconvolution parameter set-up.

3-D Reconstruction of Microscope Images

ImageJ (NIH, Bethesda, MD, USA) was used to merge the individual fluorescent channels. Reconstruction was completed in *x*, *y* and *z* dimensions and quantification was performed with IMARIS 9.0 (Bitplane AG, Zurich, Switzerland). Image stacks were constructed using the "volume rendering" function. Individual images were captures using the "Snapshot" function, and movies were generated using the "animation" function.

Quantitative analysis of blood vessel volume and bone volume

Quantitative analysis was performed on the surface of the implant, and the area between the implant screw threads was defined as the region of interest (ROI) for the purpose of this study.

Bone Volume/Total Volume (BV/TV) quantification

The μCT radiographic images were used for quantification of both the bone volume and the total volume. This was completed using IMARIS 9.0. The bone volume was defined as the calculated volume of bone/ total volume in the ROI.

Statistical Analysis

The numbers of specimens in each quantification is displayed as an N number.

Results

This investigation consisted of 32 implants placed in 20 mice. 16 of these implants were composed of titanium and 16 were fabricated from zirconia. All implants showed initial stability as demonstrated by gentle pressure with a dental explorer at initial placement. Five of the implants were lost prior to the two-week observation period, two of these were zirconia and three of the implants were titanium. The differences between the two groups in terms of implant survival at two weeks was not statistically significant (Appendix B).

Experiment 1

The first experiment consisted of threaded zirconia and titanium implants. Implants were constructed from miniature zirconia screws which were shaped into dental implants using diamond abrasives and a watchmaker's lathe with stereomicroscope magnification (Fig. 25). The final dimensions of the implant were 1.20 mm for the head with a major thread diameter of 1.00 mm (Fig. 26b). The threaded portion of the implant was 2.00 mm in length. This compared roughly to the dimensions of the titanium implants used on this and previous experiments in our lab (Fig. 26c).

The maxillary first molars of these wild type (CD1) mice were extracted under general anesthesia. After a two-week healing period, both zirconia and titanium implants

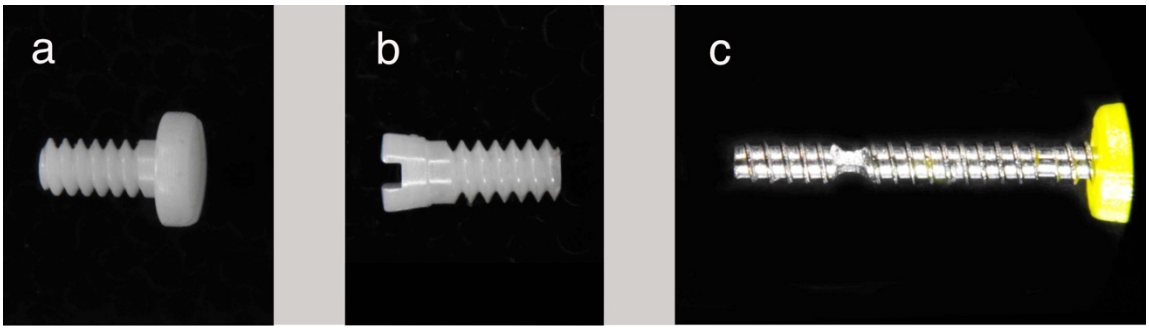

Figure 26 Fabrication of implants used in the mouse
Zirconia implants were fabricated starting with a JIS M1x2 yttria-stabilized screw. A) As delivered the head shape of the screw is too large and inappropriately shaped to serve as a dental implant analog in the mouse model. B) The screw head was reshaped by removing the bulk of the head flange and developing a taper with a minor diameter of approximately 1.2 mm. The reshaped portion was polished to 4000 grit. Implants were then cleaned with sequence of EDTA and 70% ethanol in an ultrasonic cleaner. Following disinfection and cleaning, implants were stored in sterile PBS until use. C) Titanium implants were constructed from titanium dental pins. These were scored at 1.5 mm using a rotary diamond wheel to facilitate separation of the implant portion once it was installed intraorally. These implants were cleaned with a series of 70% ethanol in an ultrasonic cleaner and stored dry until use.

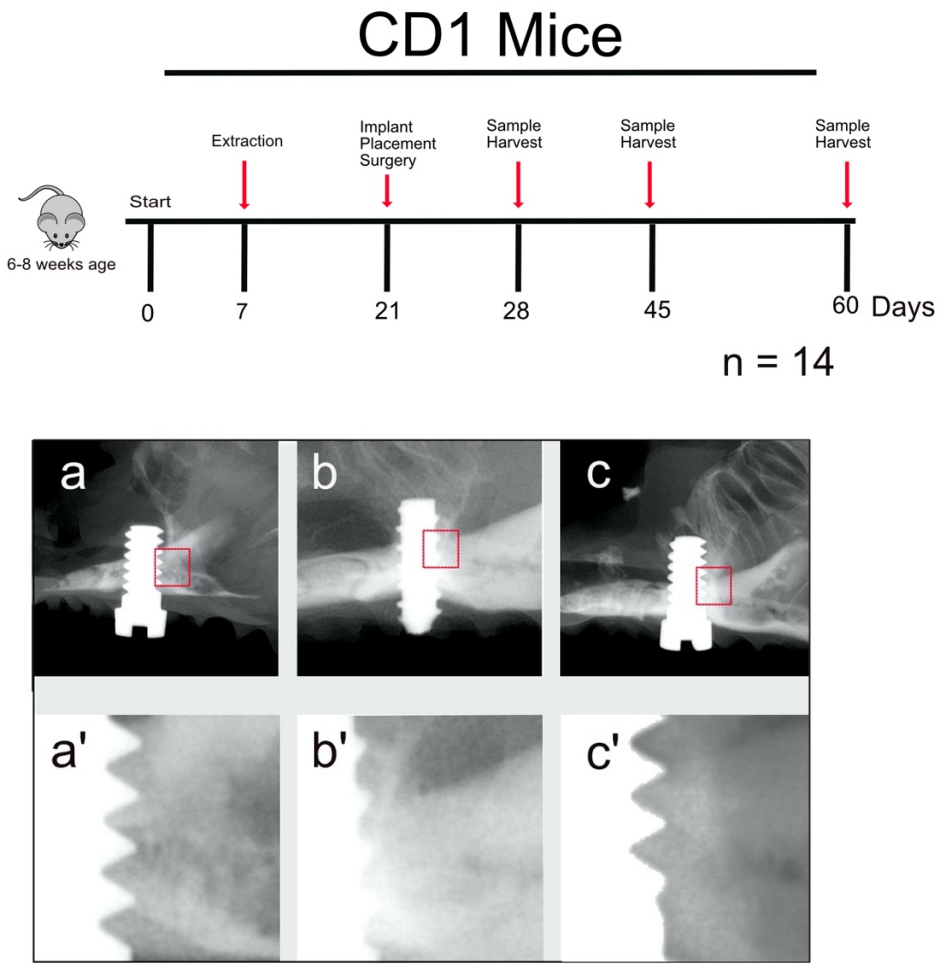

Figure 27 Implants placed in wild-type mouse maxilla after 2 and 4 weeks
These are Plain digital microradiographs demonstrating the osseous integration of the implants in the murine maxilla. The threaded portion of the implant is 1.5mm to 2.0mm in length, and it can be seen that the thickness of the alveolar bone in the first molar region is somewhat less than this dimension, thus all implants enter the soft tissue superior to the maxillary bone. Upon dissection, the bone was seen to cover the superior aspect of the implant (data not shown). The procedure was tolerated well by all mice, and no distress was noted at the post-operative examinations. A) 2-week zirconia implant. B) 2-week titanium implant. C) 4-week zirconia implant.

were placed using a flap approach and osteotomy. This were completed with the use of a surgical microscope. Mice were sacrificed at 1-week, 2-weeks, and 4-weeks. All samples were radiographed using μCT, but the threaded zirconia implants produced so much scattering artifact that they were unusable. The 2-week and 4-week samples were subsequently imaged using plain microradiography which yielded usable data (Fig. 27). Bone density was quantified by mean greyscale values in ImageJ at 10 sites in contact with the implant surface and at 10 sites at 600 μm distant to the implant surface. Measurements were performed on all available microradiograph images, and mean values for each time period were pooled. The results, summarized in Table 6, demonstrate a similar degree of bone density in both the zirconia and the titanium implants. There is a higher degree of bone density at the implant surface than is seen at distant sites.

Experiment 2

To understand the nature of the healing experienced with the first set of implants, a second generation of experiments was performed. These investigations used a transgenic mouse model to evaluate the condition of the vascular healing around the implants. This trial used CDH5-Cre^{ERT2} transgenic mice with yttria-stabilized zirconia, threaded implants as well as threaded titanium implants, as used in the previous experiments. This experiment followed the same extraction, healing and implant timelines described in the timeline with the addition of two injections of tamoxifen (Fig. 28). Stability of the implant was assessed at the time of placement using gentle pressure

Table 6 Bone Density around implants

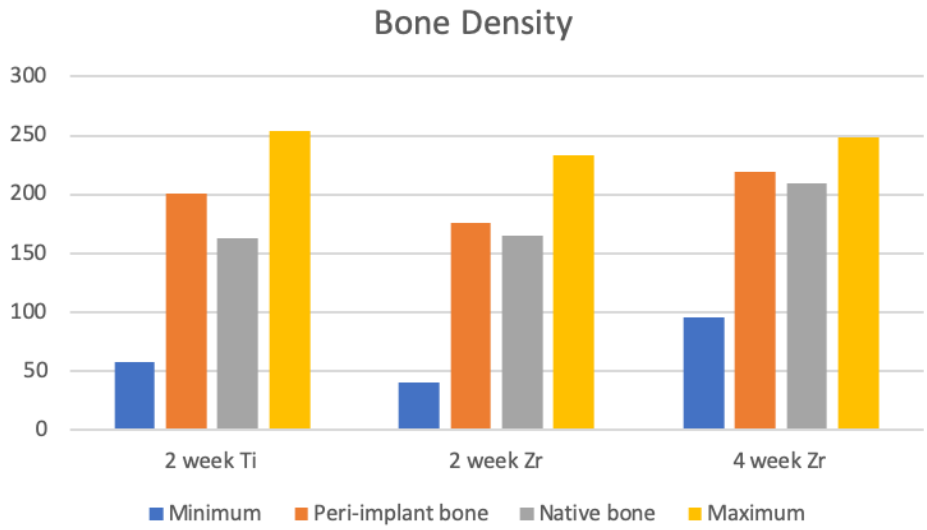

Osseous healing after implant placement was determined radiographically. Based on the average greyscale value of the radiographic images, the minimum (blue) and maximum (yellow) greyscale values for each group are shown in the graph. In all cases the peri-implant bone appears denser than the adjacent bone not associated with the implant. The bone density appears in a similar range in both the zirconia and titanium groups at all timepoints.

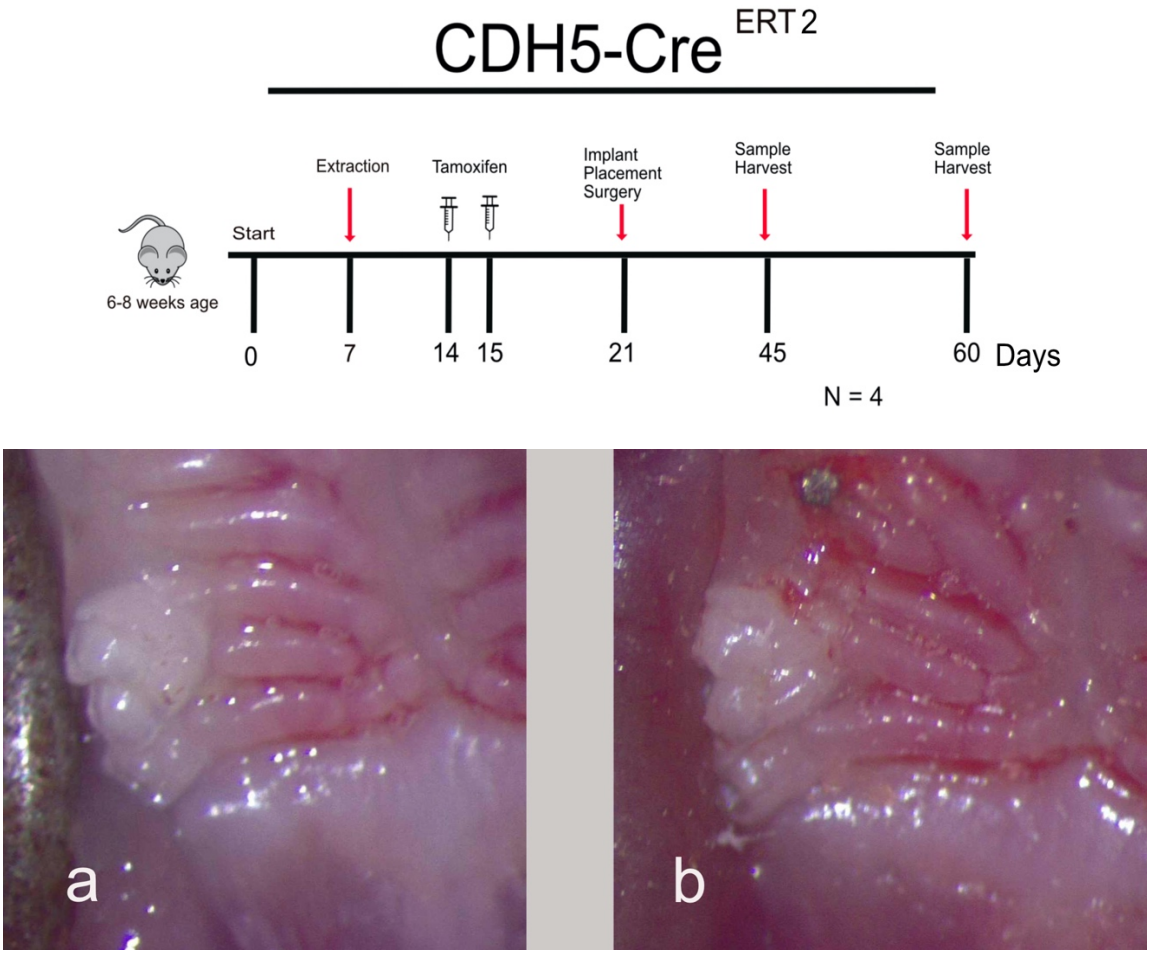

Figure 28 Implant pre-op and at initial placement
This titanium implant was placed following a surgical incision and osteotomy. A) This demonstrates the condition in the oral cavity at the time of surgery. This is one week following extraction of the maxillary first molar, and complete closure of the soft-tissue has occurred. B) The photo shows the titanium implant in place. Gentle pressure with a dental explorer was used to ascertain initial stability. The implant was placed at the level of the soft tissue.

with a dental explorer. At 2 and 4 weeks, samples were harvested and prepared for fluorescent imaging using the PEGASOS technique for tissue clearing. The dissected and cleared hemimaxillae were imaged using two-photon microscopy to evaluate vascularization and second harmonic generation (SHG) to evaluate osseous healing. At two weeks of healing, a high degree of vascularization of the peri-implant surface was noted in both the zirconia and the titanium groups, while at four weeks more osseous healing had taken place (Fig. 29). Previous experiments had shown nearly complete osseous healing around implants in mice at four weeks (data not shown). In general, the imaged showed a higher degree of initial osseous healing in the zirconia implants at the two-week time point, but the osseous healing appeared to be greater in the titanium implants at the four-week timepoint.

To explore this finding quantitatively, the data was evaluated using ImageJ to separate the red and blue channels, and then quantify them separately in order to compare the area occupied by blood vessels in comparison to bone. These values were in turn evaluated against the total area of the section. The samples which had healing for two weeks showed a high degree of vascularization, which tended to decrease by the four-week timepoint. The amount of bone present appeared to increase between the two and four-week time points, (Table 7). The quantification appeared to confirm the visual observation of increased early healing of the zirconia implants at two weeks, but this was surpassed by the healing of the titanium implants at four weeks.

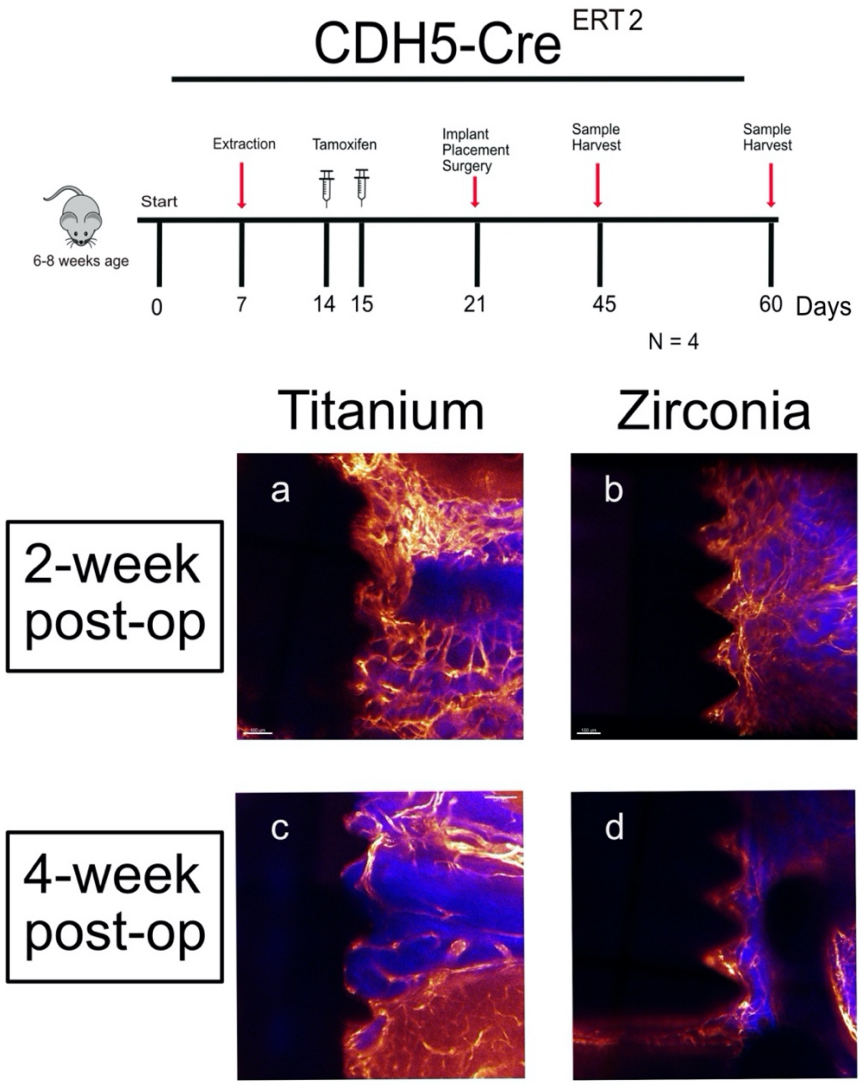

Figure 29 Two-photon images of bone healing around implants
Images were acquired following extraction of maxillary first molars, implant placement, tissue clearing with the PEGASOS technique, then either a 2-week or 4-week healing period. The black area on the left side of each image is the dental implant which is opaque and does not show visibility with this technique. A-B) At the two-week timepoint, sections showed the presence of greater amounts of bone, represented in blue, as imaged with SHG. The red portion of the images shows neovascularization, and invariably new blood vessels were present along the implant surface at this point. At 4-weeks, the titanium implants showed greater amounts of bone. Both materials showed more bone in direct contact with the implant surface and reduction of vasculature.

Table 7 Quantification of results from histology and 2-photon imaging- CDH5-Cre^{ERT2}

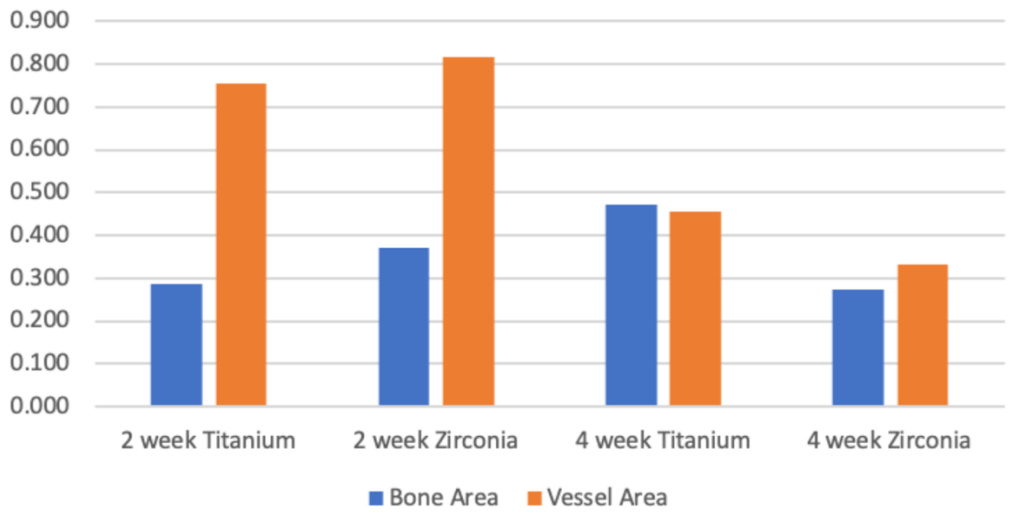

The results of the histology and two-photon imaging were quantified using the image ImageJ program. Initial healing at the 2-week timepoint showed a greater amount of bone surrounding the zirconia implant. Both titanium and zirconia showed a high level of neovascularization during this healing period. At 4-weeks, the healing was virtually complete, and the volume of blood vessels in the peri-implant tissue had decreased in both groups. In our samples, the amount of bone increased around the titanium implant, while it seemed to stay roughly the same in the zirconia implant.

Experiment 3

The third investigation in this series involved the use of Gli1-Cre^{ERT2}; Ai14 transgenic mice. The use of these root-form implants in these mice allowed for tracking of stem cell proliferation during the healing process. Previous studies in our lab have shown that these cells are a critical part of the osseointegration process. In addition, the use of root form implants could allow us to track stem cell proliferation around healing implants placed into the maxillary sinus. The implants from the previous experiments were not suitable due to the high level of radiographic scattering, since μCT radiography would be an essential part of this evaluation. To this end, bullet shaped implants were fabricated as described in the materials and methods. Some of these implants were placed into the maxilla following extraction and healing, and some were placed deeper in the maxilla to elevate the floor of the maxillary sinus, using a murine version of the transcrestal sinus augmentation technique (Summers 1998).

All mice healed uneventfully following surgery. The maxillae containing the implants from these mice were cleared using the PEGASOS technique as previously described. The zirconia material proved to be easy to visualize *in situ* with stereomicroscopy. Following the use of the PEGASOS tissue clearing technique, not only the presence but the exact location of the healed implant could be determined (Fig. 30a & 30b). Using μCT radiography, it is possible to evaluate osseous healing at the various healing intervals. At 2-weeks, bone in close apposition to the root form-implant can be seen. Close inspection of this image reveals, however, a slight gap between the healing bone and the implant surface. Even at this early stage of healing, bone can be

seen developing within the notch on the implant surface, indicating new bone growth (Fig. 30c). At the 4-week evaluation period, bone can be seen in direct contact with the implant surface, and it appears that osseointegration has been achieved at this point (Fig. 30d).

Following radiography, implants were visualized 3-dimensionally via 2-photon microscopy. Reconstructed 3D images allowed visualization of the entire implant surface. With this method of microscopy, the Gli1+ stem cells, as well as their daughter cells, showed a distinct red fluorescence which was recorded in a stacked scan. In addition, second harmonic generation (SHG) was used to visualize the extent of the bone present in the sample (Fig. 31). At 4-weeks, SHG revealed bone in direct contact with the implant surface, confirming our radiographic findings. Also noted was the exuberant response of the Gli1+ stems cells and their progeny in the integrating bone along the implant surface. The bone appears to mature around the implant at this timepoint, so this gives us an indication of the source of the cells providing the osseointegration response.

As implants have become a common clinical procedure in humans, the limitations of the depth of the crestal alveolar bone due to pneumatization of the maxillary sinus have limited the ability to place implants. To overcome this difficulty, the maxillary sinus augmentation surgery was developed (Boyne and James 1980). To test the potential for bone growth around implants placed in the maxillary sinus of mice, several implants were placed deep, beyond the bony confines of the alveolar ridge, using the trans-alveolar sinus augmentation technique (Summers 1998) modified for the dimensions of the mouse oral/nasal cavity.

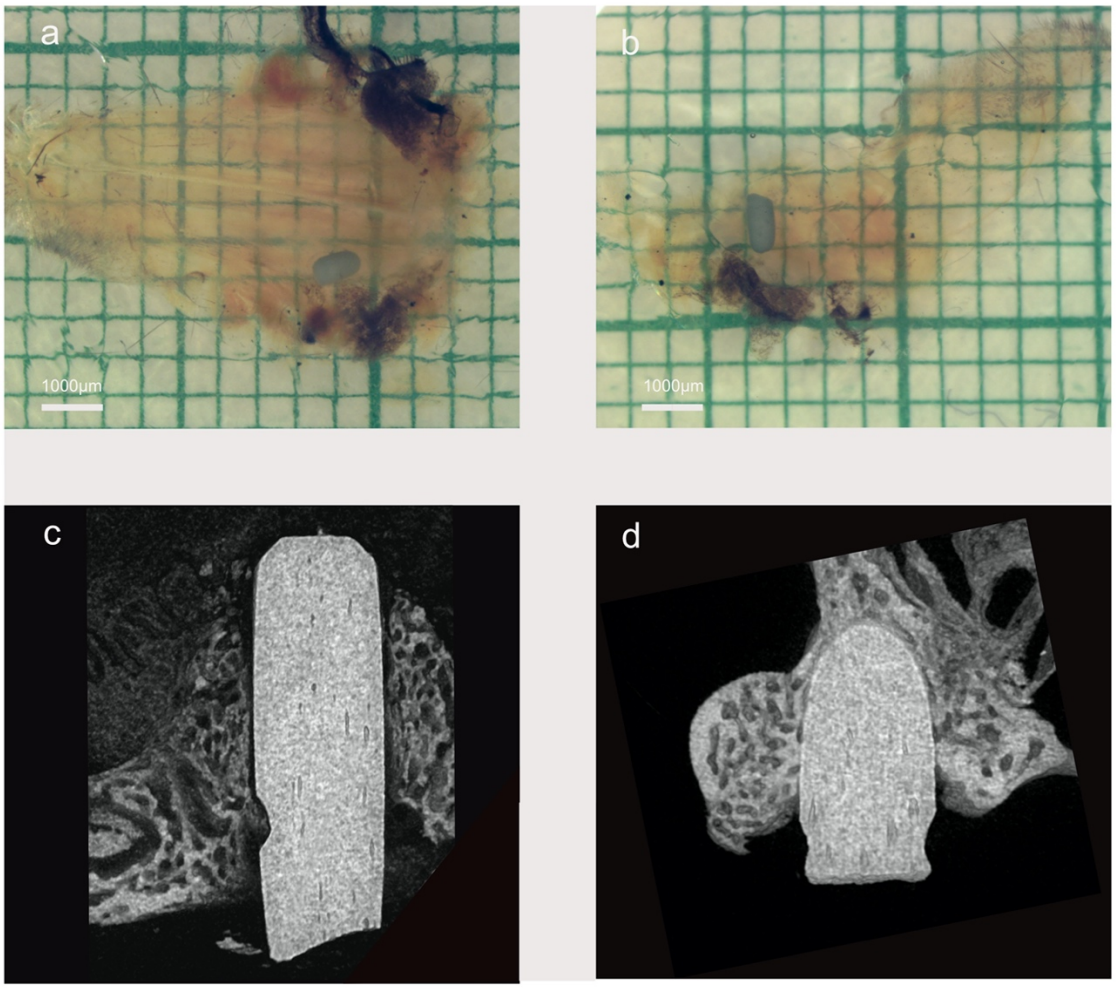

Figure 30 Zirconia implant placement in the maxilla of mice
These implants were placed in the maxillae of adult mice approximately 1 week following extractions of the maxillary first molars. A) Dorsal view of the implant in place following the PEGASOS clearing protocol. B) the same implant as seen in the previous photograph demonstrating the ability of the clearing method to allow visualization of the implant in situ. C) Following 2 weeks of healing, bone can be seen in close apposition to the implant surface, but a gap between the bone and implant is still present, indication a lack of integration at this timepoint. D) At four weeks of healing, the osseous tissue can be seen in direct contact with the implant surface, indicating osseointegration.

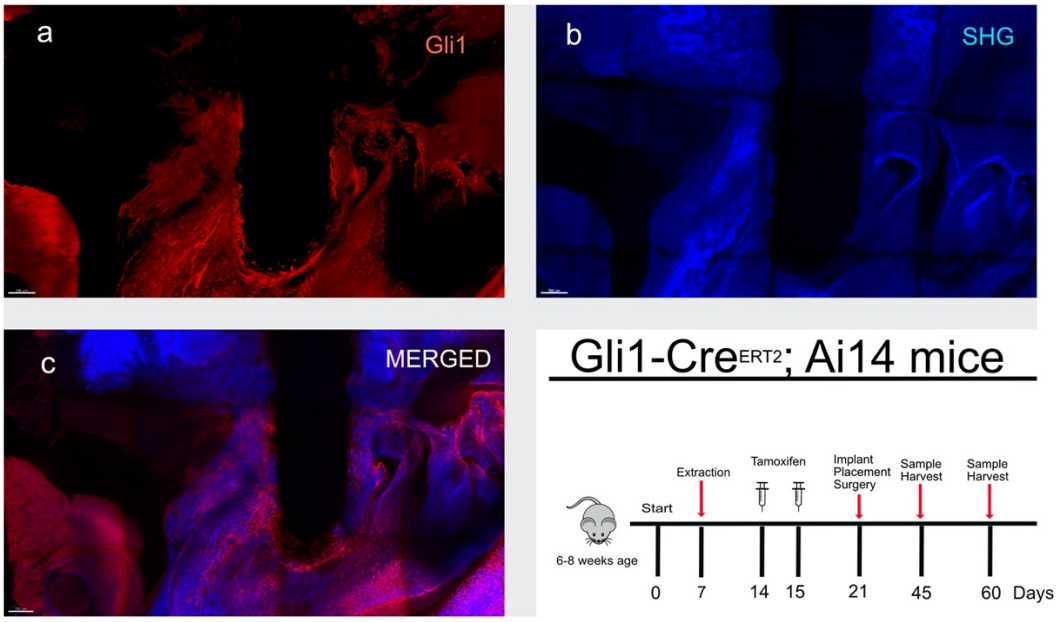

Figure 31 Zirconia implant placement in transgenic mice.
The zirconia implants were placed in to the maxillae of adult mice approximately 2 weeks following extraction of the maxillary first molars and one week following the administration of tamoxifen. This specimen came from a mouse that was allowed 4-weeks of healing following implant placement. These tissues were processed with the PEGASOS protocol and visualized with 2-photon microscopy. A) The red fluorescence demonstrates the presence of Gli1+ stems cells as well as their daughter cells. B) The blue patterns reveal the presence of bone through SHG. Bone can be seen in intimate contact with the implant surface indicating osseointegration. C) The merged image shows that bone has filled in surrounding the implant, and that the cellular components have derived from the proliferation of Gli1+ cells following the placement of the implant.

Other than a slight epistaxis in a single mouse, no other complications were noted in this procedure; all mice healed uneventfully. Either two of four weeks of healing was allowed before mice were sacrificed. At this timepoint, μCT radiography was performed to assess healing. Stacked images were used to reconstruct a 3-dimensional image of the sinus region containing the dental implant. The pre-operative condition of the post-extraction, post-healing alveolar ridge shows a lack of bone bulk (Fig. 32b). Bone was seen to develop along the perimeter of the implant which was protruding up to 1.5 mm into the maxillary sinus, including area previously occupied by the cavity of the maxillary sinus. Bone growth can be seen into the notch on the lateral surface of the implant, indicating this is new bone, not pre-exiting bone (Fig. 32). Healing was impaired surrounding a retained root tip (Fig. 32c). Despite this, osseous healing and integration took place at the apical portion of the dental implant.

Discussion

While the use of dental implants is now well established in dentistry, much of the molecular mechanisms behind the healing phenomena remains to be elucidated. Earlier work in our laboratory has shed light on the early stages of healing of titanium implants in the mandibular bone (Yi et al. 2019), however healing in the edentulous maxilla presents a different set of tissues and conditions. In order to evaluate this in the mouse, it was determined to use zirconia ceramic implants. Although these are new to the clinical marketplace and research is still in the early stages, the use of zirconia eliminates the

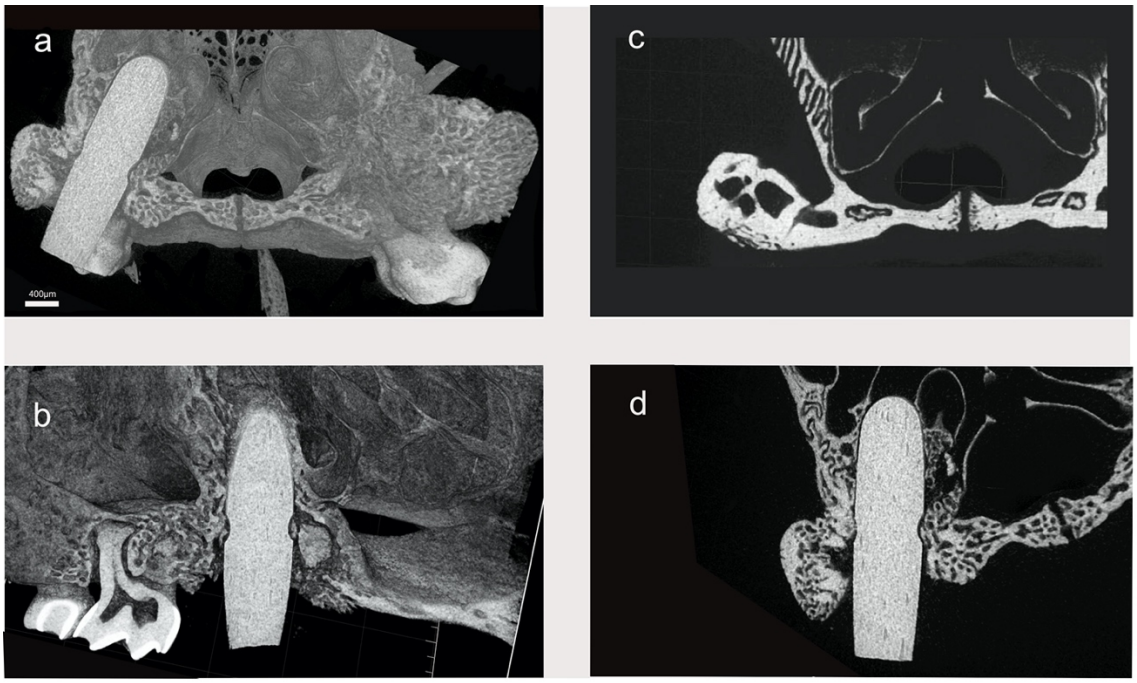

Figure 32 Implant healing in maxillary sinus
Several implants were placed beyond the confines of the maxilla to evaluate the healing and response of the tissues within the respiratory spaces, as well as the utility of this model to replicate clinical maxillary sinus augmentation procedures. These implants were placed in adult mice, and specimens were obtained 4 weeks following implant placement. Imaging was completed with µCT radiography. A, B, D) These radiographs show bone healing around the perimeter of the implant placed into the maxillary sinus. A, D) Bone growth can be seen within the notch on the implant surface indicating new osseous growth. C) This image shows an alveolar ridge following dental extraction and healing, but before implant placement. The lack of bone and atrophy of the ridge following extraction can be seen. B) The deleterious effect of retained root fragments on bone formation can be noted in this image. Despite this, the apical portion of the implant exhibited osseous healing.

possibility of peri-implantitis caused by exfoliating particles of titanium. Nevertheless, titanium implants were placed as a comparison to the zirconia implants. In the first experiment, there was profound healing and integration of the implants into the maxillary bone. There was little radiographic difference between the zirconia and the titanium implants at any time point. It is to be noted that the bone density in contact with the implant was generally higher than the density of the bone a short distance away. This finding illustrates the notion that implant materials, whether they be zirconia or titanium, are not in reality biocompatible. Instead they are causing a certain degree of inflammatory reaction resulting in the host's attempt to wall off this foreign body. At this level of observation, both materials healed well and resulted in osseointegration.

When the same experiment was repeated in CDH5-Cre^{ERT2} transgenic mice, it was possible to follow the healing on a cellular level. In this case, the similar levels of healing were noted, confirming the results in the previous experiment. There were differences that could be noted, however, based on the data available through genetic/molecular markers and three-dimensional fluorescent microscopy. This additional information points to an earlier, advanced healing response in the zirconia implants. Improved clinical healing of zirconia implants is claimed in the human literature (Blaschke and Volz 2006), so this may lend credence to this notion. By 4 weeks, when it has been determined the final healing is complete, the advantage of the zirconia is no longer evident, and in fact, the titanium appears to have surpassed the zirconia. So, it appears from our data, that the advantages of zirconia are in the early stages of healing, but final healing in titanium implants may be superior.

The third experiment tested the ability for implants to not only osseointegrate into the maxilla, but to form bone along the zirconia implant surface placed within the maxillary sinus of the mouse. In these cases, the implant is placed into the respiratory space of the sinus, but remains beneath the Schneiderian membrane. Since there are no bone cells in direct contact with the apical portion of the implant in this circumstance, osteoblasts must differentiate along the implant surface so that bone production can begin. Our investigation followed the Gli1+ stem cells as well as their daughter cells during the bone formation process. It was possible to detect the Gli1+ cells along the implant surface by means of two-photon microscopy, and later confirm that mineralization of bone had occurred by use of μCT radiography.

From our data it is possible to observe that bone formation is occurring in spaces where there was no bone originally present, i.e., along the implant surface within the maxillary sinus. This demonstrates the compatibility of the zirconia material with the investing tissues in this model, and the ability of cells to migrate from the periosteum to form bone along its surface. This investigation also demonstrates the possibility of using the mouse model for investigations in implant/sinus augmentation surgery. Previous animal studies have relied on primates due to their similarity in structure and size to the human condition (Palma et al. 2006; Piccinini et al. 2013). These studies have been able to demonstrate the osteoinductive potential of the Schneiderian membrane as well as the ability of a wide variety of graft materials and growth factors to facilitate healing in this area. In fact, early primate studies were among the first demonstrate the utility of the sinus augmentation, long before it become a routine procedure (Boyne and Jones 2004;

Boyne 2004). Further animal studies not involving primates have involved dogs (Berardinelli et al. 2013), sheep (Berardinelli et al. 2013), goats (Bravetti et al. 1998), mini-pigs (Terheyden et al. 1999), and rabbits (Choi et al. 2012). Studies in rats have shown the ability of the sinus mucosa and periosteum to accelerate osteogenesis through paracrine effects (Sun et al. 2019), but this study was limited in that it did not involve placing implants in the sinus region.

The ability to manipulate genes and introduce cellular markers in mice has made this this model an unparalleled technique in pre-clinical studies. The wide commercial availability of transgenic mouse lines, as well as the ability of investigators to develop their own customized mouse lines, has revolutionized biomedical investigation. Many studies have done comparisons of mouse and human physiology, and many of these differences are well known (Treuting et al. 2011). Nevertheless, the overarching commonalities of mammalian tissues continue to make mouse studies extremely valuable in relation to human medicine. Perhaps the most valuable point, in our type of investigations, is the ability to place DNA containing coding for fluorescent markers within the murine chromosomes. These can then be manipulated to express certain chromophores, and these can be customized for expression in certain cells at specific times, allowing precise inspection of cellular processes. Combined with the innovative PEGASOS tissue clearing technique, 3-D imaging of specifically labelled cells can be obtained. This type of precision cannot be attained as of yet in other mammalian models, making this mouse model invaluable in pre-clinical studies.

Despite the great advantages of the mouse model in biomedical studies, a severe limitation in dental implantology is its small size. Despite this limitation, it has been successfully used in our laboratory in previous investigations. These prior investigations utilized the mandibular placement of implants due to the availability of an adequate amount of investing bone for the placement of implants. The maxilla was considered unsuitable due to a thin alveolar bone and proximity on the nasal cavity and maxillary sinus. While these factors are limiting, these are the same limitations that are often found clinically in the posterior maxilla making this mouse model valuable for transalveolar augmentation studies.

In this investigation it was possible to demonstrate not only that zirconia can used as a dental implant material with osseointegration patterns similar to titanium, but also that the edentulous maxillae of transgenic mice can be utilized as an implant placement model. This study successfully demonstrated the transalveolar placement of dental implants, and have been able to observe the formation of new bone surrounding an implant in an area previously occupied by the maxillary sinus in a condition characteristic of a clinical sinus augmentation. This procedure has allowed the observation of the population of stem cells and their daughter cells during the healing and integration process giving insight into the healing physiology which is not possible in other animal models or clinical studies.

While the current studies involved only small numbers of mice and implants, they have demonstrated the potential for this model. Future investigations could involve improved designs for implants and surgical instrumentation, similar to what is now

available in clinical practice. In addition, a wide variety of transgenic mouse constructions could be implemented to track specific cellular markers.

These can be combined with improved clearing and three-dimensional imaging techniques to give visibility to what was once invisible deep inside the body. It is our thought that this model can be used to improve the clinical techniques of implant dentistry, thus improving the lives of the multitudes of people suffering from edentulism.

CHAPTER V

CONCLUSIONS

The PDL is a unique and marvelous tissue, poised as it is between to distinct skeletal tissues, important for binding them together, but essential for keeping them apart. Destruction of the PDL through periodontitis is a major cause of tooth loss and is responsible for many millions of dollars of healthcare expenditures every year. Much of what is known about periodontitis and the periodontal apparatus comes from human studies, although primate studies have yielded a great deal of knowledge (Magnusson et al. 1985). A great deal also comes from dog studies, since dogs share a similar root size and form. A problem exists, however, in that dogs have a different disease process, different healing rate, and different regenerative potential (Magnusson et al. 1990). In order to truly understand the nature of the PDL, it is necessary to look beyond the common models and consider it in the total context of vertebrate fauna. This evolutionary medicine approach will cause us to consider such questions as why PDL even exists, where and when did it first arise, what factors and forces are required for its maintenance, and what happens to these factors when the PDL is bypassed and connect the tooth directly to the bone through a dental implant.

In our first query, we considered how the PDL first arose by considering its appearance in a non-mammalian line, the marine squamate *Globidens phosphaticus*. Although the PDL is best known in mammals, it occasionally appears in various forms in non-mammalian lines. Its sudden appearance in this reptilian line gives us a chance to

consider the other characters that appeared along with it. This gives us insight into the environment and circumstances into which it arose. In this case, it was found that it appears as the last of a sequence of mammal-like characters, namely an elevated body temperature, the development of specialized teeth and stronger mandible, increased bite force, durophagy and prismatic enamel. The similarity of the reptilian pattern to the pattern that developed in mammals points not only to similar environmental pressures, but also to the activation of conserved biochemical and developmental pathways, where each step in this direction creates an easier pathway for the next step.

As the appearance and development of the PDL in the *G. phosphaticus* is considered, it is immediately apparent that this reptile had teeth that look quite different than any mammalian tooth. By examination of the tooth crowns, we were able to demonstrate through wear patterns that these teeth underwent severe occlusal loading during the life of the animal. Although these loads may be considered extreme for a squamate, they are in the normal range for a mammal. Another noteworthy item, the abundant cementum is quite bizarre, being perforated longitudinally with cellular/vascular channels. Although vascular cementum is known in some mammals such as horses (Mitchell et al. 2003), the appearance is quite different these mammals and the exact homologies are unclear. Nevertheless, it was possible to use histologic examination and SEM to demonstrate the presence of PDL remnants and provide evidence for a mammal-like PDL.

The fossil evidence for a non-mineralized PDL in *G. phosphaticus* is clear, and it appears that this arose as the need for a shock absorbing tissue became necessary with

the introduction of a durophagous diet and increased bite forces. Other reptiles with strong bite forces, such as alligators, depend on the mandibular sutures to dissipate forces and prevent bone and tooth damage. The *G. phosphaticus* has such sutures and it appears that the non-mineralized PDL arose in some fashion as an extension of those sutures. This analysis is based entirely on the fossil evidence, and since fossils only represent a small sample of the species' history, it is impossible to base firm conclusion based entirely on this data. To understand the process, fossil data must be correlated from known samples of extant organisms (Kemp 1999). In our case, it was possible to examine the data from the monitor lizards, perhaps the closest living relative to *G. phosphaticus*. In addition, consideration was made to another distantly related squamate, the iguana, as well as a much more distantly related crocodilian. These were all in turn compared to the North American marsupial mammal, the opossum, being one of the living mammals most distantly related to humans. In all cases it was possible to demonstrate a direct contact of the tooth attachment tissues to the sutures of both the mandible and the maxilla, and it is easy to predict a transfer of tissue-diffusible factors linking the development of these two tissues.

To confirm this hypothesis in a living organism, the transgenic mouse model was chosen. This model allowed the genetic labeling of certain stem cells specific to the craniofacial sutures. Using novel tissue clearing and imaging techniques, it was possible to demonstrate the same unique pattern of Gli1+ stem cells in the PDL of the mice as in the sutures, demonstrating a common developmental origin and function of these cells.

Our hypothesis depends on the increased occlusal loading of mammals and durphagous marine reptiles to be responsible for the non-mineralization of the PDL. Previous experiments in our lab had determined that occlusal function has a direct influence on Wnt-signaling in the PDL. The failure of the PDL to mineralize in mammals appears to be related inhibitors of the β-catenin dependent Wnt signaling pathway. Using a mouse model in which it was possible to configure an inducible knockout to simulate the overproduction of Wnt, an overgrowth of cementum, similar to what was seen in the tooth roots *G. phosphaticus* was observed. This modification of the Wnt pathway also produced a vascular cementum phenotype, reminiscent of the condition in *G. phosphaticus*.

The diseases of the periodontium often result in severe tissue destruction ending with tooth loss and edentulism. The prosthetic replacement of teeth has made great strides, and the use of dental implants in the last four decades has revolutionized dentistry. Although implant dentistry has become routine, some aspects of this emerging field remain open to controversy. Peri-implantitis is a major concern. Although superficially similar to the more common periodontitis, there is increasing evidence that it is due to separation of minute particles of titanium in the peri-implant tissues- particles small enough to be immunogenic and cause disease. Various alternatives have been proposed, of which zirconia ceramic seems most promising.

Another controversy in implant dentistry is the edentulous posterior maxilla. Although sinus augmentation has been available for more than 30 years, there is still little consensus on the proper materials or techniques. The problems of finding answers

to these two problems, immunogenic materials, and sinus augmentation materials, is due to the lack of suitable models for investigation. Up until now, models have been chosen for convenience due to their size and similarity to human structures, rather than their potential for understanding the molecular mechanisms for healing at the cellular and tissue levels. Further implant studies with the mouse model will likely provide answers to these and many other questions in implant dentistry.

Periodontal disease is a serious public health problem throughout the world. Providing a cure will require not only the characteristics of the disease in humans, but a deep understanding of how mammals are built and the place of the periodontal ligament within the overall context of amniote evolution. The body is built from a finite number of cellular building blocks and a finite number of cellular signaling mechanisms. It appears the Wnt system is not only vitally important in the homeostasis of the PDL, but it appears to be responsible for whether the PDL develops like a mammal, or an ankylosis develops like a reptile. The degree and timing of the expression as well as the location determines the outcome. A detailed understanding of this mechanism will be critical to the development of future clinical therapeutics. Likewise, the adaptation of these laboratory techniques to dental implantology will further advance our understanding of craniofacial biology, and lead us to clinically translatable findings.

Understanding the millions of years of evolutionary progress that have resulted in the human dentition will point us, as craniofacial scientists, in the direction required for future investigations.

Peering into the molecular gearwork of our periodontal cells will allow us to eliminate suffering for many generations to come.

REFERENCES

Adell R, Hansson B, Brånemark P, Breine U. 1970. Intra-osseous anchorage of dental prostheses. Scandinavian journal of plastic and reconstructive surgery. 4(1):19-34.

Alaqeel S, Hinton R, Opperman L. 2006. Cellular response to force application at craniofacial sutures. Orthodontics & Craniofacial Research. 9(3):111-122.

An Z, Akily B, Sabalic M, Zong G, Chai Y, Sharpe PT. 2018. Regulation of mesenchymal stem to transit-amplifying cell transition in the continuously growing mouse incisor. Cell reports. 23(10):3102-3111.

Augusta BG. 2019. Anatomy, taxonomy, ontogeny and phylogeny of basal mosasaurians (Squamata, Mosasauria) and their implications to the evolution of Anguimorpha. Universidade de São Paulo.

Badve CA, Mallikarjunappa M, Iyer RS, Ishak GE, Khanna PC. 2013. Craniosynostosis: imaging review and primer on computed tomography. Pediatric radiology. 43(6):728-742.

Bardet N, Suberbiola XP, Iarochene M, Amalik M, Bouya B. 2005. Durophagous Mosasauridae (Squamata) from the Upper Cretaceous phosphates of Morocco, with description of a new species of Globidens. Netherlands Journal of Geosciences. 84(3):167-175.

Bell GL, Barnes KR, Polcyn MJ. 2012. Late Cretaceous mosasauroids (Reptilia, Squamata) of the Big Bend region in Texas, USA. Earth and Environmental Science Transactions of the Royal Society of Edinburgh. 103(3-4):571-581.

Bennett D. 2002. Diet of juvenile Varanus niloticus (Sauria: Varanidae) on the Black Volta River in Ghana. Journal of Herpetology. 36(1):116-117.

Berardinelli P, Valbonetti L, Muttini A, Martelli A, Peli R, Zizzari V, Nardinocchi D, Vulpiani MP, Tetè S, Barboni B. 2013. Role of amniotic fluid mesenchymal cells engineered on MgHA/collagen-based scaffold allotransplanted on an experimental animal study of sinus augmentation. Clinical oral investigations. 17(7):1661-1675.

Berglundh T, Armitage G, Araujo MG, Avila‐Ortiz G, Blanco J, Camargo PM, Chen S, Cochran D, Derks J, Figuero E. 2018. Peri‐implant diseases and conditions: Consensus report of workgroup 4 of the 2017 World Workshop on the

Classification of Periodontal and Peri‐Implant Diseases and Conditions. Journal of periodontology. 89:S313-S318.

Berkovitz BK, Moxham BJ, Newman HN. 1995. The periodontal ligament in health and disease. Bookmantraa. com.

Bertin TJ, Thivichon-Prince B, Leblanc AR, Caldwell MW, Viriot L. 2018. Current perspectives on tooth implantation, attachment, and replacement in Amniota. Frontiers in physiology. 9:1630.

Blaschke C, Volz U. 2006. Soft and hard tissue response to zirconium dioxide dental implants--a clinical study in man. Neuroendocrinology letters. 27(1):69-72.

Bobbio A. 1972. The first endosseous alloplastic implant in the history of man. Bulletin of the history of dentistry. 20(1):1-6.

Boyne P, Jones SD. 2004. Demonstration of the osseoinductive effect of bone morphogenetic protein within endosseous dental implants. Implant Dentistry. 13(2):180-184.

Boyne PJ. 2004. Augmentation of the posterior maxilla by way of sinus grafting procedures: recent research and clinical observations. Oral and Maxillofacial Surgery Clinics. 16(1):19-31.

Boyne PJ, James RA. 1980. Grafting of the maxillary sinus floor with autogenous marrow and bone. J Oral Surg. 38(8):613-616.

Branemark P-I. 1977. Osseointegrated implants in the treatment of the edentulous jaw. Experience from a 10-year period. Scand J Plast Reconstr Surg Suppl. 16.

Brånemark P-I, Breine U, Adell R, Hansson B, Lindström J, Ohlsson Å. 1969. Intra-osseous anchorage of dental prostheses: I. Experimental studies. Scandinavian journal of plastic and reconstructive surgery. 3(2):81-100.

Bravetti P, Membre H, Marchal L, Jankowski R. 1998. Histologic changes in the sinus membrane after maxillary sinus augmentation in goats. Journal of oral and maxillofacial surgery. 56(10):1170-1176.

Callaway JM, Nicholls EL. 1997. Ancient marine reptiles. Academic Press.

Camp CL. 1923. Classification of the lizards. order of the Trustees, American Museum of Natural History.

Carlton RA. 2011. Polarized light microscopy. Pharmaceutical microscopy. Springer. p. 7-64.

Choi Y, Yun JH, Kim CS, Choi SH, Chai JK, Jung UW. 2012. Sinus augmentation using absorbable collagen sponge loaded with Escherichia coli‐expressed recombinant human bone morphogenetic protein 2 in a standardized rabbit sinus model: a radiographic and histologic analysis. Clinical oral implants research. 23(6):682-689.

Clarke SA, Walsh P, Maggs CA, Buchanan F. 2011. Designs from the deep: marine organisms for bone tissue engineering. Biotechnol Adv. 29(6):610-617.

Cope E. 1869. On the reptilian orders Pythonomorpha and Streptosauria. Proceedings of the boston Society of Natural History.

Cuvier G. 1808. Sur le grand animal fossile des carrières de Maestricht. Frères Levrault.

D'amore DC. 2015. Illustrating ontogenetic change in the dentition of the Nile monitor lizard, Varanus niloticus: a case study in the application of geometric morphometric methods for the quantification of shape–size heterodonty. Journal of Anatomy. 226(5):403-419.

De Vries TJ, Andreotta S, Loos BG, Nicu EA. 2017. Genes critical for developing periodontitis: lessons from mouse models. Frontiers in immunology. 8:1395.

Diekwisch TG. 2016. Our periodontal tissue: a masterpiece of evolution. Journal of clinical periodontology. 43(4):320-322.

Eilken HM, Diéguez-Hurtado R, Schmidt I, Nakayama M, Jeong H-W, Arf H, Adams S, Ferrara N, Adams RH. 2017. Pericytes regulate VEGF-induced endothelial sprouting through VEGFR1. Nature communications. 8(1):1-14.

Eke PI, Dye BA, Wei L, Slade GD, Thornton‐Evans GO, Borgnakke WS, Taylor GW, Page RC, Beck JD, Genco RJ. 2015. Update on prevalence of periodontitis in adults in the United States: NHANES 2009 to 2012. Journal of periodontology. 86(5):611-622.

Ford DP, Benson RBJ. 2020. The phylogeny of early amniotes and the affinities of Parareptilia and Varanopidae. Nature Ecology & Evolution. 4(1):57-65.

Frost HM. 1994. Wolff's Law and bone's structural adaptations to mechanical usage: an overview for clinicians. The Angle Orthodontist. 64(3):175-188.

Gignac P, Erickson G. 2016. Ontogenetic bite‐force modeling of Alligator mississippiensis: implications for dietary transitions in a large‐bodied vertebrate and the evolution of crocodylian feeding. Journal of Zoology. 299(4):229-238.

Hall BK. 2014. Bones and Cartilage: Developmental and Evolutionary Skeletal Biology. Academic Press.

Han J, Menicanin D, Gronthos S, Bartold P. 2014. Stem cells, tissue engineering and periodontal regeneration. Australian dental journal. 59:117-130.

Harada N, Tamai Y, Ishikawa TO, Sauer B, Takaku K, Oshima M, Taketo MM. 1999. Intestinal polyposis in mice with a dominant stable mutation of the β - catenin gene. The EMBO journal. 18(21):5931-5942.

Harrel SK, Wilson Jr TG, Pandya M, Diekwisch TG. 2019. Titanium particles generated during ultrasonic scaling of implants. Journal of periodontology. 90(3):241-246.

Hendy J, Warinner C, Bouwman A, Collins MJ, Fiddyment S, Fischer R, Hagan R, Hofman CA, Holst M, Chaves E. 2018. Proteomic evidence of dietary sources in ancient dental calculus. Proceedings of the Royal Society B: Biological Sciences. 285(1883):20180977.

Isson TT, Planavsky NJ, Coogan LA, Stewart EM, Ague JJ, Bolton EW, Zhang S, Mckenzie NR, Kump LR. 2020. Evolution of the Global Carbon Cycle and Climate Regulation on Earth. Global Biogeochemical Cycles. 34(2):e2018GB006061.

James RA. 1979. The support system and pergingival mechanisms surrounding oral implants. Biomaterials, Medical Devices, and Artificial Organs. 7(1):147-153.

Jenkins KM, Shaw JO. 2020. Bite force data suggests relationship between acrodont tooth implantation and strong bite force. PeerJ. 8:e9468.

Jing D, Zhang S, Luo W, Gao X, Men Y, Ma C, Liu X, Yi Y, Bugde A, Zhou BO. 2018. Tissue clearing of both hard and soft tissue organs with the PEGASOS method. Cell research. 28(8):803-818.

Kelly JF, Connole PW, Hiatt WR, Mainous EG, Messer EJ. 1978. Management of War Injuries to the Jaws and Related Structures. NAVAL MEDICAL RESEARCH INST BETHESDA MD.

Kemp TS. 1999. Fossils and evolution. Oxford University Press.

Kielan-Jaworowska Z, Cifelli RL, Luo Z-X. 2005. Mammals from the age of dinosaurs: origins, evolution, and structure. Columbia University Press.

King GM. 1996. Reptiles and herbivory. Springer Science & Business Media.

Kohal RJ, Klaus G. 2004. A zirconia implant-crown system: a case report. International Journal of Periodontics & Restorative Dentistry. 24(2).

Komaki M, Karakida T, Abe M, Oida S, Mimori K, Iwasaki K, Noguchi K, Oda S, Ishikawa I. 2007. Twist negatively regulates osteoblastic differentiation in human periodontal ligament cells. Journal of cellular biochemistry. 100(2):303-314.

Kratochvil FJ, Boyne PJ, Bump R. 1976. Rehabilitation of grossly deficient mandibles with combined subperiosteal implants and bone grafts. The Journal of prosthetic dentistry. 35(4):452-461.

Lafuma F, Corfe IJ, Clavel J, Di-Poï N. 2020. Multiple evolutionary origins and losses of tooth complexity in squamates. bioRxiv.2020.2004.2015.042796.

Lang NP, Salvi GE, Sculean A. 2019. Nonsurgical therapy for teeth and implants—When and why? Periodontology 2000. 79(1):15-21.

Leblanc AR, Apesteguía S, Larsson HC, Caldwell MW. 2020. Unique tooth morphology and prismatic enamel in Late Cretaceous sphenodontians from Argentina. Current Biology.

Leblanc AR, Brink KS, Cullen TM, Reisz RR. 2017a. Evolutionary implications of tooth attachment versus tooth implantation: A case study using dinosaur, crocodilian, and mammal teeth. Journal of Vertebrate Paleontology. 37(5):e1354006.

Leblanc AR, Lamoureux DO, Caldwell MW. 2017b. Mosasaurs and snakes have a periodontal ligament: timing and extent of calcification, not tissue complexity, determines tooth attachment mode in reptiles. Journal of anatomy. 231(6):869-885.

Leblanc AR, Reisz RR. 2013. Periodontal ligament, cementum, and alveolar bone in the oldest herbivorous tetrapods, and their evolutionary significance. PLoS One. 8(9).

Leblanc AR, Reisz RR, Brink KS, Abdala F. 2016. Mineralized periodontia in extinct relatives of mammals shed light on the evolutionary history of mineral homeostasis in periodontal tissue maintenance. Journal of Clinical Periodontology. 43(4):323-332.

Lee MSY. 1997. On snake-like dentition in mosasaurian lizards. Journal of Natural History. 31(2):303-314.

Lee MSY, Caldwell MW. 2000. Adriosaurus and the affinities of mosasaurs, dolichosaurs, and snakes. Journal of Paleontology. 74(5):915-937.

Luan X, Walker C, Dangaria S, Ito Y, Druzinsky R, Jarosius K, Lesot H, Rieppel O. 2009. The mosasaur tooth attachment apparatus as paradigm for the evolution of the gnathostome periodontium. Evolution & development. 11(3):247-259.

Luo Z-X. 2007. Transformation and diversification in early mammal evolution. Nature. 450(7172):1011.

Magnusson I, Claffey N, Bogle G, Garrett S, Egelberg J. 1985. Root resorption following periodontal flap procedures in monkeys. Journal of periodontal research. 20(1):79-85.

Magnusson I, Stenberg W, Batich C, Egelberg J. 1990. Connective tissue repair in circumferential periodontal defects in dogs following use of a biodegradable membrane. Journal of Clinical Periodontology. 17(4):243-248.

Manor Y, Anavi Y, Gershonovitch R, Lorean A, Mijiritsky E. 2018. Complications and Management of Implants Migrated into the Maxillary Sinus. International Journal of Periodontics & Restorative Dentistry. 38(6).

Martin JE, Fox JE. 2007. Stomach contents of Globidens, a shell-crushing mosasaur (Squamata), from the Late Cretaceous Pierre Shale Group, Big Bend area of the Missouri River, central South Dakota. SPECIAL PAPERS-GEOLOGICAL SOCIETY OF AMERICA. 427:167.

Martinelli AG, Soares MB, Schwanke C. 2016. Two New Cynodonts (Therapsida) from the Middle-Early Late Triassic of Brazil and Comments on South American Probainognathians. PLOS ONE. 11(10):e0162945.

Maruyama T, Jeong J, Sheu T-J, Hsu W. 2016. Stem cells of the suture mesenchyme in craniofacial bone development, repair and regeneration. Nature communications. 7(1):1-11.

Mcintosh JE, Anderton X, Flores‐De‐Jacoby L, Carlson DS, Shuler CF, Diekwisch TG. 2002. Caiman periodontium as an intermediate between basal vertebrate ankylosis‐type attachment and mammalian "true" periodontium. Microscopy research and technique. 59(5):449-459.

Men Y, Wang Y, Yi Y, Jing D, Luo W, Chai Y, Ge W-P, Shen B, Stenberg W, Feng JQ et al. 2020a. Gli+ periodontium stem cells are regulated by osteocytes and occlusal force.

Men Y, Wang Y, Yi Y, Jing D, Luo W, Shen B, Stenberg W, Chai Y, Ge W-P, Feng JQ. 2020b. Gli1+ Periodontium Stem Cells Are Regulated by Osteocytes and Occlusal Force. Developmental Cell.

Mitchell S, Kempson S, Dixon P. 2003. Structure of peripheral cementum of normal equine cheek teeth. Journal of veterinary dentistry. 20(4):199-208.

Modesto SP. 2020. Rooting about reptile relationships. Nature Ecology & Evolution. 4(1):10-11.

Morgan H, Szmyd L. 1968. Maxillofacial war injuries. Journal of oral surgery (American Dental Association: 1965). 26(11):727.

Muller J, Reisz RR. 2006. The phylogeny of early eureptiles: comparing parsimony and Bayesian approaches in the investigation of a basal fossil clade. Syst Biol. 55(3):503-511.

Muller WE, Wang X, Chen A, Hu S, Gan L, Schroder HC, Schlossmacher U, Wiens M. 2011. The unique invention of the siliceous sponges: their enzymatically made bio-silica skeleton. Prog Mol Subcell Biol. 52:251-281.

Nagai N, Takeshita N. 1982. Mechanical and biological properties of partially stabilized zirconia ceramic implants. J Dent Res. 25:581-596.

Noble H. 1969. The evolution of the mammalian periodontium. Biology of the Periodontium (ed. by MELCHER, AH and BOWEN, WH), 1-26. Academic Press, New York.

O'neil JR, Roe LJ, Reinhard E, Blake R. 1994. A rapid and precise method of oxygen isotope analysis of biogenic phosphate. Israel Journal of Earth Sciences. 43(3-4):203-212.

Opperman LA. 2000. Cranial sutures as intramembranous bone growth sites. Developmental dynamics: an official publication of the American Association of Anatomists. 219(4):472-485.

Opperman LA, Passarelli RW, Morgan EP, Reintjes M, Ogle RC. 1995. Cranial sutures require tissue interactions with dura mater to resist osseous obliteration in vitro. Journal of Bone and Mineral Research. 10(12):1978-1987.

Osborn J. 1984. From reptile to mammal: evolutionary considerations of the dentition with emphasis on tooth attachment. Symposia of the Zoological Society of London. 52:549-574.

Ozanne CR, Harries PJ. 2002. Role of predation and parasitism in the extinction of the inoceramid bivalves: an evaluation. Lethaia. 35(1):1-19.

Palma VC, Magro‐Filho O, De Oliveria JA, Lundgren S, Salata LA, Sennerby L. 2006. Bone reformation and implant integration following maxillary sinus membrane

elevation: an experimental study in primates. Clinical implant dentistry and related research. 8(1):11-24.

Parsons RW, Thering HR. 1972. An approach to reconstruction of complex lower face injuries. British journal of plastic surgery. 25:23-28.

Peyer B, Zangerl R. 1968. Comparative Odontology. University of Chicago Press.

Piccinini M, Rebaudi A, Sglavo VM, Bucciotti F, Pierfrancesco R. 2013. A new HA/TTCP material for bone augmentation: an in vivo histological pilot study in primates sinus grafting. Implant Dentistry. 22(1):83-90.

Pickrell J. 2019. The making of mammals. Nature. 574(7779):468-472.

Pirelli P, Ragazzoni E, Botti F, Arcuri C, Cocchia D. 1997. A comparative light microscopic study of human midpalatal suture and periodontal ligament. Minerva stomatologica. 46(9):429-433.

Polcyn M, Bell G. 2005. The rare mosasaur genus Globidens from north central Texas (Mosasaurinae: Globidensini). Journal of Vertebrate Paleontology. 25(3):101A-101A.

Polcyn MJ, Jacobs LL, Araújo R, Schulp AS, Mateus O. 2014. Physical drivers of mosasaur evolution. Palaeogeography, Palaeoclimatology, Palaeoecology. 400:17-27.

Polcyn MJ, Jacobs LL, Schulp AS, Mateus O. 2010. The North African mosasaur Globidens phosphaticus from the Maastrichtian of Angola. Historical Biology. 22(1-3):175-185.

Polcyn MJ, Tchernov E, Jacobs LL. 1999. The Cretaceous biogeography of the eastern Mediterranean with a description of a new basal mosasauroid from'Ein Yabrud, Israel. National Science Museum Monographs. 15:259-290.

Pyron RA. 2017. Novel approaches for phylogenetic inference from morphological data and total-evidence dating in squamate reptiles (lizards, snakes, and amphisbaenians). Systematic Biology. 66(1):38-56.

Rasmussen AR, Murphy JC, Ompi M, Gibbons JW, Uetz P. 2011. Marine reptiles. PLOS one. 6(11).

Rodrigues DC, Urban RM, Jacobs JJ, Gilbert JL. 2009. In vivo severe corrosion and hydrogen embrittlement of retrieved modular body titanium alloy hip‐implants. Journal of Biomedical Materials Research Part B: Applied Biomaterials: An Official Journal of The Society for Biomaterials, The Japanese Society for

Biomaterials, and The Australian Society for Biomaterials and the Korean Society for Biomaterials. 88(1):206-219.

Romer AS. 1956. Osteology of the Reptiles.

Sander P. 1999. The microstructure of reptilian tooth enamel: terminology, function, and phylogeny: Muncher Geowissenshaftliche Abhandlungen, v. A38.102.

Schneiderman ED. 1978. The functional meaning of the mammaliam mandible. [Evanston, Illinois]: Northwestern University.

Schoch RR, Sues H-D. 2016. The diapsid origin of turtles. Zoology. 119(3):159-161.

Schwenk K. 2000. Feeding: form, function and evolution in tetrapod vertebrates. Elsevier.

Senarath-Yapa K, Chung MT, Mcardle A, Wong VW, Quarto N, Longaker MT, Wan DC. 2012. Craniosynostosis: molecular pathways and future pharmacologic therapy. Organogenesis. 8(4):103-113.

Sharan A, Madjar D. 2008. Maxillary sinus pneumatization following extractions: a radiographic study. International Journal of Oral & Maxillofacial Implants. 23(1).

Shi Y, He G, Lee W-C, Mckenzie JA, Silva MJ, Long F. 2017. Gli1 identifies osteogenic progenitors for bone formation and fracture repair. Nature communications. 8(1):1-12.

Simões TR, Caldwell MW, Tałanda M, Bernardi M, Palci A, Vernygora O, Bernardini F, Mancini L, Nydam RL. 2018. The origin of squamates revealed by a Middle Triassic lizard from the Italian Alps. Nature. 557(7707):706-709.

Snyder AJ, Leblanc AR, Jun C, Bevitt JJ, Reisz RR. 2020. Thecodont tooth attachment and replacement in bolosaurid parareptiles. PeerJ. 8:e9168.

Strganac C, Jacobs L, Polcyn M, Ferguson K, Mateus O, Gonçalves AO, Morais M-L, Da Silva Tavares T. 2015. Stable oxygen isotope chemostratigraphy and paleotemperature regime of mosasaurs at Bentiaba, Angola. Netherlands Journal of Geosciences. 94(1):137-143.

Sues H-D, Reisz RR. 1998. Origins and early evolution of herbivory in tetrapods. Trends in Ecology & Evolution. 13(4):141-145.

Summers RB. 1998. Sinus floor elevation with osteotomes. Journal of Esthetic and Restorative Dentistry. 10(3):164-171.

Sun R, Xu S, Wang Z. 2019. Rat sinus mucosa- and periosteum-derived exosomes accelerate osteogenesis. J Cell Physiol. 234(12):21947-21961.

Terheyden H, Jepsen S, Möller B, Tucker MM, Rueger DC. 1999. Sinus floor augmentation with simultaneous placement of dental implants using a combination of deproteinized bone xenografts and recombinant human osteogenic protein ‐ 1. A histometric study in miniature pigs. Clinical Oral Implants Research. 10(6):510-521.

Thewissen J. 2014. The walking whales: from land to water in eight million years. Univ of California Press.

Toth RW, Parr GR, Gardner LK. 1985. Soft tissue response to endosseous titanium oral implants. Journal of Prosthetic Dentistry. 54(4):564-567.

Treuting PM, Dintzis SM, Liggitt D, Frevert CW. 2011. Comparative anatomy and histology: a mouse and human atlas (expert consult). Academic Press.

Trevathan W. 2018. Evolutionary medicine. The International Encyclopedia of Biological Anthropology.1-4.

The Reptile Database. 2020. [accessed May 3, 2020]. http://www.reptile-database.org.

Van Gaalen SM, Kruyt MC, Geuze RE, De Bruijn JD, Alblas J, Dhert WJ. 2010. Use of fluorochrome labels in in vivo bone tissue engineering research. Tissue engineering Part B: Reviews. 16(2):209-217.

Weinmann JP, Sicher H. 1955. Bone and bones. Fundamentals of bone biology. Bone and bones Fundamentals of bone biology. (2nd ed).

Wilson Jr TG, Valderrama P, Burbano M, Blansett J, Levine R, Kessler H, Rodrigues DC. 2015. Foreign bodies associated with peri ‐ implantitis human biopsies. Journal of periodontology. 86(1):9-15.

Wu Y, Yuan X, Perez KC, Hyman S, Wang L, Pellegrini G, Salmon B, Bellido T, Helms JA. 2019. Aberrantly elevated Wnt signaling is responsible for cementum overgrowth and dental ankylosis. Bone. 122:176-183.

Xie X, Wang J, Wang K, Li C, Zhang S, Jing D, Xu C, Wang X, Zhao H, Feng J. 2019. Axin2+-Mesenchymal PDL Cells, Instead of K14+ Epithelial Cells, Play a Key Role in Rapid Cementum Growth. Journal of dental research. 98(11):1262-1270.

Yi Y, Men Y, Jing D, Luo W, Zhang S, Feng JQ, Liu J, Ge WP, Wang J, Zhao H. 2019. 3 ‐ dimensional visualization of implant ‐ tissue interface with the polyethylene

glycol associated solvent system tissue clearing method. Cell proliferation. 52(3):e12578.

Zaher H, Rieppel O. 1999. Tooth implantation and replacement in squamates, with special reference to mosasaur lizards and snakes. American Museum of Natural History.

Zhao H, Feng J, Ho T-V, Grimes W, Urata M, Chai Y. 2015. The suture provides a niche for mesenchymal stem cells of craniofacial bones. Nature cell biology. 17(4):386-396.

APPENDIX A

IMPLANT DATA

Table 8 Bone Density values for implants

	Min	Implant	Bone	Max	Min
2wkTi	58	200.87	162.65	254	58
2wkZr	40	176.26	164.87	233	40
4wk Zr	96	218.74	209	248	96

Based on pixel intensity on CT images.

Table 9 2-photon histology results

	Total Area	Bone Area	Bone Percent	Vessels	Vessels Percent
2 week Titanium	1171528	334365	0.285	882536	0.75332045
2 week Zirconia	2859982	1064763	0.372	2340262	0.818278577
4 week Titanium	5285262	2498010	0.472636929	2402341	0.454535839
4 week Zirconia	2400872	655626	0.273078282	799591	0.333041911

APPENDIX B

STATISTICAL ANALYSIS

Table 10 Implant survival at 2-week timepoint

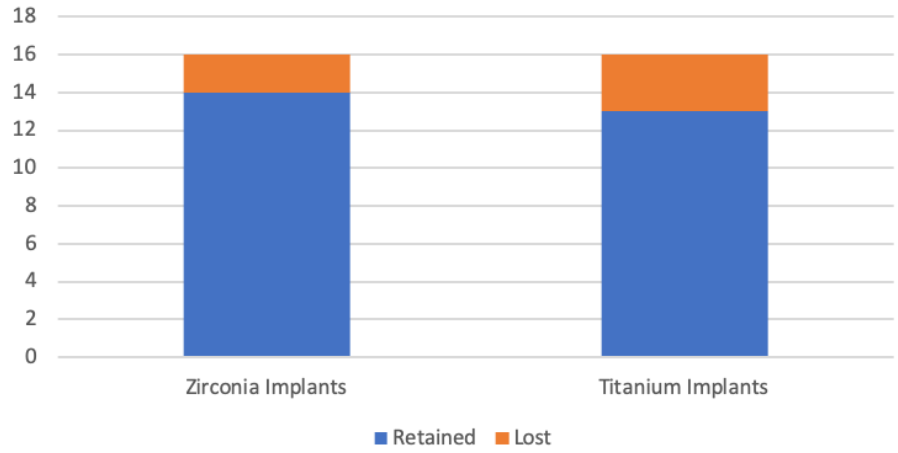

	Retained	Lost
Zirconia Implants	14	2
Titanium Implants	13	3

The proportion of implants that were retained did not differ by material, zirconia vs. titanium, χ^2 (1, N = 32) = 0.237, p> .05. Analysis was not completed at the 4-week timepoint due to a smaller number of samples at that time. In addition, all implant loss occurred during the initial healing period, i.e., the first two weeks. No additional implants were lost between the 2-week and the 4-week interval.